

1      **The Role of Biomechanical Stress in Extracellular Vesicle Formation, Composition and**  
2      **Activity**

3  
4                    Will Thompson <sup>a</sup> and Eleftherios Terry Papoutsakis <sup>a</sup>

5  
6                    <sup>a</sup> Department of Chemical and Biomolecular Engineering, University of Delaware, 590 Avenue  
7                    1743, Newark, DE 19713, USA

8  
9                    Corresponding author: Eleftherios Terry Papoutsakis: [epaps@udel.edu](mailto:epaps@udel.edu), Tel: +1-302-831-8376,  
10                    ORCID # 0000-0002-1077-1277

11  
12  
13  
14  
15  
16  
17  
18  
19  
20  
21  
22  
23  
24  
25  
26  
27  
28  
29  
30  
31  
32  
33  
34  
35  
36  
37  
38  
39  
40  
41  
42  
43  
44  
45  
46  
47  
48  
49  
50  
51

52 **Abstract:**

53 Extracellular vesicles (EVs) are cornerstones of intercellular communication with exciting  
54 fundamental, clinical, and more broadly biotechnological applications. However, variability in EV  
55 composition, which results from the culture conditions used to generate the EVs, poses  
56 significant fundamental and applied challenges and a hurdle for scalable bioprocessing. Thus,  
57 an understanding of the relationship between EV production (and for clinical applications,  
58 manufacturing) and EV composition is increasingly recognized as important and necessary.  
59 While chemical stimulation and culture conditions such as cell density are known to influence  
60 EV biology, the impact of biomechanical forces on the generation, properties, and biological  
61 activity of EVs remains poorly understood. Given the omnipresence of these forces in EV  
62 preparation and in biomanufacturing, expanding the understanding of their impact on EV  
63 composition—and thus, activity—is vital. Although several publications have examined EV  
64 preparation and bioprocessing and briefly discussed biomechanical stresses as variables of  
65 interest, this review represents the first comprehensive evaluation of the impact of such stresses  
66 on EV production, composition and biological activity. We review how EV biogenesis, cargo,  
67 efficacy, and uptake are uniquely affected by various types, magnitudes, and durations of  
68 biomechanical forces, identifying trends that emerge both generically and for individual cell  
69 types. We also describe implications for scalable bioprocessing, evaluating processes inherent  
70 in common EV production and isolation methods, and propose a path forward for rigorous EV  
71 quality control.

72 **Keywords:**

73 Extracellular vesicles, exosomes, microparticles, cellular communication, biomechanical force,  
74 shear, tension, compression, cyclic stretch, bioprocessing

75 **Abbreviations:**

76 ABCA1, ATP binding cassette transporter A1; ABP, actin binding protein; ADP, adenosine  
77 diphosphate; Ago2, Argonaute 2; Akt, protein kinase B; ALG-2, apoptosis-linked gene 2; ALIX,  
78 ALG-2-interacting protein X; ARF6, ADP-ribosylation factor 6; ASK1, apoptosis signal-regulating  
79 kinase 1; AT1R, angiotensin II type 1 receptor; ATF4, activating transcription factor 4; ATP,  
80 adenosine triphosphate; BAX, BCL-2-associated X protein; BCL, B-cell lymphoma 2; BEC,  
81 bronchial epithelial cell; CD, cluster of differentiation; C/EBP, cytosine-cytosine-adenosine-  
82 adenosine-thymidine-enhancer-binding protein; CHO, Chinese Hamster Ovary; CHOP, C/EBP  
83 homologous protein; DOK2, docking protein 2; ECMO, extracorporeal membrane oxygenation;  
84 eNOS, endothelial nitric oxide synthase; ER, endoplasmic reticulum; ERK, extracellular signal-  
85 regulated kinase; ESCRT, Endosomal Sorting Complex Required for Transport; EV,  
86 extracellular vesicle; EZH2, enhancer of zeste 2 polycomb repressive complex 2 subunit; GMP,  
87 good manufacturing practice; GPIb, glycoprotein Ib; GPIIb-IIIa, glycoprotein IIb-IIIa; GRK6, G  
88 protein-coupled receptor kinase; GRP78, glucose-regulating protein 78; GTP, guanosine  
89 triphosphate; HEK, human embryonic kidney; hnRNP, heterogeneous nuclear  
90 ribonucleoprotein; HSPC, hematopoietic stem and progenitor cell; HUVEC, human umbilical  
91 vein endothelial cells; ICAM-1, intercellular adhesion molecule 1; IGF2, insulin-like growth factor  
92 2; IL, interleukin; KLF2, Krüppel-like Factor 2; KO, knockout; LAMP1, lysosomal-associated  
93 membrane protein 1; LC3, microtubule-associated protein light chain 3; lincRNA, long intergenic  
94 non-coding RNA; LVAD, left ventricular assist device; MAPK, mitogen-activated protein kinase;  
95 MGP, matrix Gla protein; miRNA, microRNA; Mk, megakaryocyte; M-MDSC, mononuclear  
96 myeloid-derived suppressor cell; MSC, mesenchymal stem cell; MVB, multivesicular body;  
97 NADPH, nicotinamide adenine dinucleotide phosphate; NF-κB, nuclear factor kappa-B; NO,  
98 nitric oxide; Notch2, neurogenic locus notch homolog protein 2; NOX4, NADPH oxidase 4;  
99 NPP1, nucleotide pyrophosphatase/phosphodiesterase-1; NTA, nanoparticle tracking analysis;  
100 NRP1, neuropilin 1; OMV, outer membrane vesicle; p53, tumor protein p53; PCR, polymerase  
101  
102

103 chain reaction; PD-L1, protein death-ligand 1; PECAM-1, platelet endothelial cell adhesion  
104 molecule 1; PI3K, phosphoinositide 3-kinase; PKC, protein kinase C; PLT, platelet; PS,  
105 phosphatidylserine; RAB, Ras-associated binding protein; RANKL, receptor activator of nuclear  
106 factor kappa-B ligand; RhoA, Ras homolog family member A; RNA, ribonucleic acid; RBP, RNA  
107 binding protein; ROCK, Rho-associated protein kinase; SAVR, surgical aortic valve  
108 replacement; sICAM-1, soluble intercellular adhesion molecule 1; siRNA, small interfering RNA;  
109 SIRT1, sirtuin 1; SkMC, skeletal muscle cell; SMC, smooth muscle cell; SNARE, soluble N-  
110 ethylmaleimide-sensitive factor attachment protein receptor; SOCS1, suppressor of cytokine  
111 signaling 1; Src, proto-oncogene tyrosine-protein kinase Src; TAZ, tafazzin; TF, tissue factor;  
112 TFAP2A, transcription factor activating enhancer binding protein 2 alpha; TGF, transforming  
113 growth factor; THBS1, thrombospondin-1; TIPA, transcription-independent p53-induced  
114 apoptosis; TNAP, tissue-nonspecific alkaline phosphatase; TRPV4, transient receptor potential  
115 vanilloid 4; TSG101, tumor susceptibility gene 101 (protein); UCHL1, ubiquitin C-terminal  
116 hydrolase L1; VCAM-1, vascular cell adhesion molecule 1; VEC, vascular endothelial cell; vWF,  
117 von Willebrand factor; WT, wild type; YAP, yes-associated protein

118	<b>Table of Contents:</b>
119	1. Extracellular vesicles: exosomes, microparticles, and their emerging clinical applications
120	2. Biomechanical forces in defined flows and bioreactors
121	2.1. Lab-scale isolation of defined biomechanical forces
122	2.2. Complex forces in cell culture bioreactors
123	3. Impacts of biomechanical forces on EV biogenesis and release
124	3.1. Mesenchymal stem cells
125	3.2. Fibroblasts
126	3.3. Bone and cartilage tissue
127	3.4. Bronchial epithelial cells
128	3.5. Endothelial cells
129	3.6. Smooth muscle cells
130	3.7. Platelets and megakaryocytes
131	3.8. Skeletal muscle cells
132	3.9. Tumor cells
133	3.10. Other mammalian cells
134	3.11. Non-mammalian cells
135	3.12. General themes and trends
136	4. Impacts of biomechanical forces on EV cargo and composition
137	4.1. Mesenchymal stem cells
138	4.2. Fibroblasts
139	4.3. Bone and cartilage tissue
140	4.4. Bronchial epithelial cells
141	4.5. Endothelial cells
142	4.6. Smooth muscle cells
143	4.7. Platelets and megakaryocytes
144	4.8. Skeletal muscle cells
145	4.9. Tumor cells
146	4.10. Other mammalian cells
147	4.11. General themes and trends
148	5. Impact of biomechanical forces on EV uptake and cargo delivery
149	5.1. Impact of biomechanical forces on cell-EV collision and adhesion
150	5.2. Impact of biomechanical forces on EV internalization
151	5.3. Examples from published research
152	6. Do biomechanical forces affect and complicate EV isolation and purification?
153	7. Considerations for the scale-up of EV production
154	7.1. EV production in stirred/aerated tank bioreactors
155	7.2. Mixing characteristics for scalable EV production
156	7.3. Shear sensitivity and EV product quality
157	8. Future directions
158	
159	
160	
161	
162	
163	
164	
165	
166	
167	

168 **1. Extracellular vesicles: exosomes, microparticles and their emerging clinical**  
169 **applications**

170 Once maligned as the rubbish bins of the cell, extracellular vesicles (EVs) have recently been  
171 heralded as integral to intercellular communication (Hopkin, 2016; Ratajczak et al., 2006).  
172 Distinct from apoptotic bodies, these vesicles enclose nucleic acid, protein, and lipid cargo in a  
173 lipid bilayer membrane and are traditionally subdivided into two major categories: exosomes  
174 and microparticles (Ratajczak and Ratajczak, 2020). The smaller exosomes are produced via  
175 inward budding of multivesicular bodies (MVBs) and released into the extracellular space  
176 following the exocytosis of those same bodies. The larger microparticles, on the other hand,  
177 form directly from outward budding of the plasma membrane. Still, overlapping  
178 exosome/microparticle size distributions and challenges in biogenesis-based isolation have  
179 resulted in inconsistent sample categorization (Thery et al., 2018). This review therefore  
180 generously applies the term “EVs” in place of paper-specific nomenclature, except where  
181 exosome- or microparticle-enriched samples display different phenotypes. EVs bind—often  
182 specifically—to target cells and are subsequently internalized via endocytosis or membrane  
183 fusion, with successful cargo delivery commonly affecting cellular phenotypic change. The  
184 biogenesis, release, and uptake of EVs are illustrated in **Figure 1**.

185  
186 The clinical implications of industrial-scale EV production are exciting and seemingly endless  
187 (Wiklander et al., 2019). Endogenous EV cargo is often capable of inducing specific desirable  
188 phenotypes in target cells. Exosomes from mesenchymal stem cells (MSCs) have been a prime  
189 focus, first used in humans as a successful therapy for graft-versus-host disease (Kordelas et  
190 al., 2014) and more recently evaluated as a treatment for severe COVID-19 (Sengupta et al.,  
191 2020). Megakaryocyte-derived microparticles, which uniquely target hematopoietic stem and  
192 progenitor cells (HSPCs) to promote *de novo* megakaryopoiesis, have been proposed as an  
193 alternative to platelet transfusions (Escobar et al., 2020; Jiang et al., 2014; Kao et al., 2022).  
194 EVs from endothelial progenitor cells have been shown to promote angiogenesis in endothelial  
195 cells (Deregibus et al., 2007), protect against lung and kidney injury (Cantaluppi et al., 2012; Wu  
196 et al., 2018), and ameliorate the effects of sepsis in murine models (Zhou et al., 2018). Absent  
197 significant endogenous cargo, however, EV membranes can still be harnessed as vehicles for  
198 drug delivery, transporting exogenous cargo to specific target cells while evading the immune  
199 system (Herrmann et al., 2021). In clinical settings, EVs can be used as a diagnostic tool:  
200 tumor-derived EVs, which promote tumor metastasis, could serve as valuable biomarkers for  
201 the progression of cancer (Becker et al., 2016). Even in biopharmaceutical manufacturing, EVs  
202 are omnipresent, facilitating massive and underappreciated intercellular communication among  
203 cultured Chinese Hamster Ovary (CHO) cells (Belliveau and Papoutsakis, 2022).

204  
205 EV bioprocessing must enable the large-scale production of EVs with consistent purity,  
206 glycosylation patterns, and protein, lipid, and nucleic acid contents. Variation in these factors  
207 would likely impact EV efficacy, inhibiting the possibility of clinical applications for lack of  
208 material consistency. Although some progress has been made, the field still largely lacks  
209 rigorous correlations between specific bioprocessing procedures and EV quality control.  
210 Because biomechanical stresses are omnipresent in EV bioprocessing, an understanding of  
211 those stresses—both how they arise and their impact on EV biology—is essential. While several  
212 reviews (Colao et al., 2018; Grangier et al., 2021; Kao and Papoutsakis, 2019; Lee et al., 2021;  
213 Patel et al., 2018) have broadly discussed EV bioprocessing and briefly examined  
214 biomechanical stresses as relevant factors, this review represents the first comprehensive  
215 evaluation of the impact of biomechanical forces—such as those encountered during  
216 biomanufacturing and production generally—on EV generation, properties, and biological  
217 activity. It also examines the potential impact of biomechanical forces on EV separation,  
218 enrichment, and purification, as well as the ability of EVs to recognize target cells and deliver

219 cargo. The scope of this review is largely and necessarily confined to EVs from “natural”—as  
220 opposed to genetically engineered—cells, since research into the effects of biomechanical  
221 forces on the biology of EVs from genetically engineered cells is relatively scarce.

## 223 **2. Biomechanical forces in defined flows and bioreactors**

224 Cells and EVs are primarily exposed to and influenced by three types of mechanical forces—  
225 shear, tension, and compression—exerted by a variety of sources, both *in vivo* and *in vitro*  
226 (Shah et al., 2014; Wang and Li, 2010). Shear stress is defined as the parallel force on a “body”  
227 (here: cell or EV) induced by differing velocity of an adjacent body or fluid (Papaioannou and  
228 Stefanidis, 2005). Most often associated with the effects of fluid flow, the application of shear  
229 can be steady, pulsatile, or oscillatory (Shah et al., 2014). In pulsatile flow, the magnitude of  
230 shear varies regularly with time, while in oscillatory flow, the *direction* of shear varies with time  
231 (though the magnitude may also change) (Shah et al., 2014). Physiologically, shear stress—  
232 typically observed in blood vessels—is implicated in the biology of vascular endothelial cells  
233 (VECs), platelets (PLTs), and megakaryocytes (Mks) (Ballermann et al., 1998; Jiang et al.,  
234 2014; Shah et al., 2014). Interstitial fluid flow can likewise expose chondrocytes and  
235 osteocytes—in cartilage and bone, respectively—to shear stress (Wang and Li, 2010;  
236 Wittkowske et al., 2016). In contrast with shear stress, tensile and compressive stresses are  
237 exerted *perpendicularly* to their targets (Shah et al., 2014). However, compression acts in the  
238 direction of the target, imposing a “squeeze,” while tension pulls away from the target, resulting  
239 in a “stretch” (Shah et al., 2014). Tension and compression are often paired, and—in the case of  
240 suspension cells—commonly result from “elongational” or “extensional” flows, which occur at  
241 flow field constrictions or in areas of accelerating/ decelerating flow (Chisti, 2001; Foster et al.,  
242 2021; Petry and Salzig, 2021). In physiological settings, tension is almost always cyclic; it  
243 applies mostly to fibroblasts in ligaments and tendons and is also important in bone and  
244 cartilage biology (Wada et al., 2017; Wang and Li, 2010). Frequently, tensile stress has been  
245 found to impact cellular phenotype more substantially than shear stress of the same magnitude  
246 (Foster et al., 2021; Gregoriades et al., 2000). Compression is widespread in the cartilage and  
247 is likewise an essential mediator of intercellular communication during proliferation, as cells are  
248 increasingly pressed together (Shah et al., 2014; Wada et al., 2017). Both tension and  
249 compression are applied to VECs and smooth muscle cells (SMCs) as a result of blood  
250 pressure, and to bronchial epithelial cells as a result of ventilation (Wada et al., 2017; Wang and  
251 Li, 2010). **Figure 2** illustrates the three basic biomechanical forces, methods for their lab-scale  
252 application, and their common manifestations in culture/bioreactors.

253 Generally, cells react differently to each of the three types of stresses. In fibroblasts, for  
254 instance, tension and compression of equal magnitude differentially regulate intracellular protein  
255 and RNA content (He et al., 2004). Erythrocyte membrane tension is on average far greater  
256 under shear than under tensile stress (Faghih and Sharp, 2018). VECs can likewise distinguish  
257 between shear and tension by virtue of plasma membrane characteristics such as lipid order,  
258 fluidity, cholesterol content, and receptor activation (Yamamoto and Ando, 2015).

### 261 ***2.1. Lab-scale isolation of defined biomechanical forces***

262 Lab-scale experiments can effectively apply defined biomechanical forces. Microfluidic devices  
263 can isolate the impacts of shear via controlled, laminar flow over a stationary sample of  
264 adherent cells, avoiding complications at gas-liquid interfaces and any cell-cell or cell-to-hard  
265 surface collisions (Czermak et al., 2009; Papoutsakis, 1991). Various viscometers (e.g., cone-  
266 and-plate, cone-and cone, coaxial cylindrical) can likewise modulate shear while minimizing  
267 other mechanical stressors (Papoutsakis, 1991; Thomas, 1993). Isolation of tensile stress on  
268 adherent cells is often achieved via static or cyclic “stretch,” which is induced by extending the  
269 length of (i.e., stretching) a flexible (silicone) substrate on which the cells are attached. This

stretching is accomplished by pulling a vacuum (e.g., the “Flexcell” system pictured in **Figure 2**) (Yu et al., 2016). The tension in such a system can be applied across any number of axes (e.g., uniaxial stretch, biaxial stretch, etc.) and is usually quantified by the “percent strain/elongation” (e.g., 5%, 10%, 15%) of the flexible substrate (Yu et al., 2016). Extracellular matrix stiffness also exerts tension on cells by promoting integrin clustering and subsequent cytoskeletal reinforcement (Paszek et al., 2005). There are notable parallels between this phenomenon and the tension exerted on cells as a result of microcarrier contact angle (Tsai et al., 2020). Elongational flow can be applied to suspension cells by use of microfluidic devices incorporating constrictions or cross-flow geometries (Foster et al., 2021). Optical tweezers have also been used to apply tension or compression on a single-cell basis (Foster et al., 2021). Even hydrostatic pressure and various osmotic treatments can be employed as models of tension and compression (Le Roux et al., 2019; Wang and Li, 2010).

## 2.2. Complex forces in cell culture bioreactors

The situation becomes murkier, however, for most practical applications, including agitated bioreactors employed in cell culture biomanufacturing. Mechanical stresses can no longer be individually isolated and analyzed because the use of impellers, baffles, probes, and direct gassing for oxygenation generate complex combinations of shear, tensile, and compressive forces (Cherry and Kwon, 1990; Czermak et al., 2009; Foster et al., 2021; Papoutsakis, 1991). Bubble entrainment and breakup at the bulk gas-liquid interface have been well-documented as inducing both shear and tension (Foster et al., 2021; Gregoriades et al., 2000; Papoutsakis, 1991), as have turbulent eddies (Cherry and Kwon, 1990; Faghih and Sharp, 2018; Papoutsakis, 1991; Petry and Salzig, 2021). The relative influence of such complex biomechanical forces in determining biological outcomes in cultures will vary with vessel geometry and culture properties, as discussed in more detail later in this review. As a further complication, complex biomechanical forces in agitated and aerated bioreactors of any scale are often categorized broadly as “shear stress,” confounding precise correlations between mechanical stressors and biological phenotypes (including EV generation and characteristics) (Chisti, 2001; Foster et al., 2021; Thomas, 1993).

Turbulent flow is the counterpart of laminar flow, and typically occurs in agitated systems such as stirred and aerated bioreactors. In turbulent flow, flow characteristics vary with time and space (Papoutsakis, 1991). In turbulent flows such as in bioreactors, energy is dissipated through a cascade of eddies which decrease in size and, after reaching some minimum length scale (where they are referred to as “Kolmogorov eddies”), are converted to heat (Thomas, 1993). These eddies begin imposing significant stress on cells (or on cells attached to small beads, known as microcarriers) when the eddy length scale—the size of the smallest eddies in the cascade—is less than or roughly equal to cell/microcarrier size (Croughan et al., 1987; Papoutsakis, 1991; Thomas, 1993). The size of Kolmogorov eddies in agitated bioreactors is typically higher than the size of mammalian cells (which, when in free suspension, and thus rounded, range in diameter from 7 to 15  $\mu\text{m}$ ), meaning that freely suspended cells in bioreactors do not experience damaging biomechanical forces from turbulent eddies (Kunas and Papoutsakis, 1990). This is in contrast to cells attached to microcarriers (which are much larger than cells, typically over 150  $\mu\text{m}$  in diameter) (Cherry and Papoutsakis, 1988; Cherry and Papoutsakis, 1989; Papoutsakis, 1991; Thomas, 1993). Bubble breakup at the free liquid surface of agitated and aerated bioreactors is responsible for detrimental biomechanical effects on freely suspended cells (Kunas and Papoutsakis, 1990; Michaels et al., 1996; Papoutsakis, 1991).

The challenge in current EV research lies in isolating the impact of various stressors on EV biogenesis, composition, and uptake and subsequently applying these findings, in a meaningful

321 way, to scale up EV production. While some notable progress has been made in the former  
322 endeavor, the latter effort remains nearly nonexistent, complicated by the complexity of forces  
323 encountered in large-scale culture. If EVs are to have any significant industrial or clinical impact,  
324 however, correlations and empirical relationships between mechanical stress and EV product  
325 quantity/quality must be established, likely with computational aid. The difficulty of this endeavor  
326 is exacerbated by the fact that the susceptibility of cells to mechanical stress varies with cell  
327 type, age, and the culture environment (Chisti, 2001).

### 329 **3. Impact of biomechanical forces on EV biogenesis and release**

330 EV biogenesis and release is highly dependent on mechanical stress. However, the  
331 mechanisms underlying this dependence vary and almost always informed by the physiological  
332 relevance of the stress levels, which must be determined on a cell-by-cell basis. Indeed, some  
333 EV production processes—such as microparticle release from endothelial cells—are actually  
334 inhibited by higher shear. Below, we first summarize what is generally known about the  
335 mechanisms involved in EV biogenesis and release and then what is known about these  
336 processes under various conditions of biomechanical stress. The goal is to identify broad  
337 themes and to suggest avenues for future investigation.

339 Exosomes are formed through both ESCRT-dependent and ESCRT-independent pathways,  
340 where ESCRT stands for Endosomal Sorting Complex Required for Transport (van Niel et al.,  
341 2018). In the ESCRT-dependent pathway, ubiquitinated MVB membrane cargo congregates in  
342 tetraspanin-rich “microdomains” on the MVB membrane (van Niel et al., 2018). The ESCRT-0,  
343 ESCRT-I, and ESCRT-II complexes subsequently recruit cytosolic cargo, RNA, and associated  
344 binding proteins (van Niel et al., 2018). Finally, ESCRT-III serves to “pinch off” the  
345 microdomains, which become intraluminal vesicles via “inward budding” of the MVB membrane  
346 (van Niel et al., 2018). The ESCRT-independent pathway is similar but distinct: both membrane  
347 and cytosolic cargo congregate on the MVB membrane, likely due to regulatory behavior of  
348 tetraspanins (especially CD9, CD63, and CD81); the subsequent conversion of sphingomyelin  
349 to ceramide results in negative membrane curvature and promotes the “pinching off” of  
350 intraluminal vesicles (Anand et al., 2019; Trajkovic et al., 2008; van Niel et al., 2018).  
351 Nevertheless, ESCRT-III is once again required for inward budding of the MVB membrane (van  
352 Niel et al., 2018). During both types of exosome biogenesis, interactions between the proteins  
353 syndecan and syntenin serve to recruit ALIX, which works in tandem with fellow endosomal  
354 protein TSG101 to assist ESCRT function (Anand et al., 2019; Baietti et al., 2012; van Niel et  
355 al., 2018). Once intraluminal vesicles have been created, their parent MVBs may be transported  
356 to lysosomes (often, by way of autophagosomes) for degradation; the MVBs that escape this  
357 fate (likely due to their enrichment in cholesterol) bind to the plasma membrane via actin,  
358 SNARE proteins, and synaptotagmin family members, subsequently releasing intraluminal  
359 vesicles as exosomes (Mathieu et al., 2019; van Niel et al., 2018). Distinct RAB GTPases drive  
360 the intracellular transport of MVBs along microtubules, variously directing said MVBs to either  
361 lysosomes or the plasma membrane (Mathieu et al., 2019; van Niel et al., 2018).

362 Unlike exosomes, microparticle biogenesis is initiated by the congregation of membrane cargo  
363 and ceramide in tetraspanin-rich microdomains on the *plasma* membrane (Raposo and  
364 Stoorvogel, 2013; van Niel et al., 2018). Much as in the case of ESCRT-dependent exosome  
365 biogenesis, ESCRT complexes serve to recruit microparticle cargo from the cytoplasm (van Niel  
366 et al., 2018). Again, as before, ESCRT-III plays a particularly vital role in the outward blebbing  
367 by which microparticles are eventually released (van Niel et al., 2018). This blebbing is  
368 characterized by an influx of  $\text{Ca}^{2+}$  ions and the protein ARF6 (van Niel et al., 2018). Subsequent  
369 actin- and myosin-driven contractions of the plasma membrane accompany disruption of

371 phosphatidylserine (PS) equilibrium, which—through a process known as “lipid flipping”—spurs  
372 local reorganization of the actin cytoskeleton (van Niel et al., 2018).

### 374 **3.1. Mesenchymal stem cells**

375 The substantial impact of mechanical stress on MSC biology has been well-established. For  
376 instance, cyclic stretch of 10% promotes MSC chondrogenesis, while relatively high shear  
377 stress—in the range of to 5 to 25 dyn/cm<sup>2</sup>—will induce osteoblast differentiation (Kang et al.,  
378 2022; Vining and Mooney, 2017). However, despite relatively widespread research into MSC  
379 EVs, the relationship between mechanical agitation and MSC EV production is only just  
380 emerging. To date, controlled *in vitro* experiments have found low (0.001 and 0.0001 dyn/cm<sup>2</sup>)  
381 shear stress (Kang et al., 2022), physiological (8%) cyclic stretch (Xiao et al., 2021), and (1.5  
382 g/cm<sup>2</sup>) compression to promote MSC EV production. For the noted shear stresses, EV yield  
383 (i.e., overall EV quantity) increased by 6.5- and 6.7-fold after 24 h (Kang et al., 2022); the  
384 stretch-induced increase in EVs was not quantified (Xiao et al., 2021) and the compressive  
385 stress resulted in a 4-fold increase in EV yield after 24 h, with similar results observed *in vivo*  
386 using a murine model (Huang et al., 2022). MSC EV production was also boosted by nearly 4-  
387 fold in the 48 h following brief application of a custom microfluidic device designed to gently  
388 “squeeze” the cells (Hao et al., 2023). These effects of mechanical stress have also been  
389 confirmed in more complex spheroid (Cha et al., 2018; Min Lim et al., 2022), scaffold-based  
390 (Guo et al., 2021), and microcarrier-based (Adlerz et al., 2019; de Almeida Fuzeta et al., 2020;  
391 Gazeau et al., 2020; Haraszti et al., 2018) cultures, but often cannot be directly attributed to  
392 shear, tension, or compression, as differences between control and experimental culture  
393 architecture create numerous confounding variables. In one study of spheroid culture, however,  
394 the impact of culture architecture was controlled, and EV production under complex mechanical  
395 stress increased by as much as 9-fold (Cha et al., 2018). Indeed, among common mechanical  
396 stresses, only 20% static stretch (imposed for 72 h via the Flexcell system) failed to appreciably  
397 increase MSC EV yield (Yu, Wenting et al., 2021). Comparable results have been observed for  
398 MSCs grown on stiff hydrogel substrates, which exert continual (not cyclic) tension; MSCs in  
399 these conditions produced 2- and 10-fold *more* EVs than MSCs grown on soft hydrogel  
400 substrates and rigid plastic substrates, respectively (Lenzini et al., 2021). This was the result of  
401 tension-induced development of dense actin “mesh” which served to stabilize the cytoskeleton  
402 and inhibited MVB transport to the plasma membrane; such transport is required for MVB  
403 exocytosis and subsequent exosome release (Lenzini et al., 2021). It appears that this  
404 phenomenon may be unique to the static/continual application of tension on parent MSCs,  
405 because, as noted, MSC EV release is increased under cyclic stretch.

406 Notably, expected EV production sometimes differs remarkably between MSC subtypes. For  
407 instance, shear stress is far more effective at promoting EV production in MSCs derived from  
408 dental pulp than in those derived from adipose tissue (Guo et al., 2021). Under average shear of  
409 0.5 to 5 dyn/cm<sup>2</sup>, EV production by dental pulp-derived MSCs increased by 24-fold after 48 h,  
410 while EVs production by adipose tissue increased by only 2-fold in the same conditions. In fact,  
411 for the latter MSC subtype, EV release appeared to decrease under higher shear (5 to 30  
412 dyn/cm<sup>2</sup>), suggesting the existence of cell-specific optimal shear levels for EV production,  
413 beyond which additional mechanical stress negatively impacts EV yield (Guo et al., 2021).

414 The reasons for mechanical stress-induced increases in MSC EV generation need additional  
415 investigation. Low shear stress (0.001 to 0.0001 dyn/cm<sup>2</sup>) has been linked to plasma membrane  
416 ion channel activation, with a subsequent influx of intracellular Ca<sup>2+</sup> promoting EV release (Kang  
417 et al., 2022). Moreover, the impact of Ca<sup>2+</sup> is likely mediated by upregulation of proteins related  
418 to cytoskeleton remodeling, including β-catenin, phosphorylated extracellular signal-regulated  
419 kinases 1 and 2 (ERK 1/2), and calpain (Kang et al., 2022). Involvement of caspase-3 was

422 explicitly ruled out (Kang et al., 2022), a largely predictable outcome at lower shear stresses  
423 due to the absence of shear-induced apoptosis (in which caspase-3 is implicated). The  
424 accumulation of the Yes-Associated Protein (YAP) in MSC nuclei was additionally found to be  
425 required for increased MSC EV production under shear (Guo et al., 2021). YAP likely mediates  
426 the EV release process via activation of the canonical Wnt signaling pathway, which is itself  
427 responsible for the accumulation of  $\beta$ -catenin in the cytoplasm (Guo et al., 2021). MSC EV  
428 release under compression is dependent on RAB27b (but not RAB27a) (Huang et al., 2022),  
429 while EV production by the aforementioned “squeezed” MSCs is thought to depend on plasma  
430 membrane permeabilization and the corresponding formation of transient nanopores through  
431 which  $\text{Ca}^{2+}$  can enter the cell(s) (Hao et al., 2023).

432

### 433 **3.2. Fibroblasts**

434 The impact of mechanical stress on fibroblast EV biogenesis and release—not extensively  
435 studied to this point—varies widely as a function of cell source and stimulation method, perhaps  
436 a testament to the diversity of fibroblast types. Fibroblast-like periodontal ligament cells released  
437 roughly 30-fold more EVs under 20% cyclic stretch (at 0.17 Hz for 24 h) than under static  
438 conditions, but EV yield from both gingival and dental pulp fibroblasts remained unchanged,  
439 possibly because these latter two cell types do not experience cyclic stretching *in vivo* (Wang, Z.  
440 et al., 2019). Similarly, aortic fibroblasts exposed to slightly less acute cyclic stretch of 12% (at 1  
441 Hz for 18 h) experienced only a 1.3-fold boost in EV production (Akerman et al., 2019). Static  
442 stretch of 15% also increased EV production—by 2.5-fold after 24 h—in cultures of hallux  
443 valgus (bunion) fibroblasts (Xie et al., 2020). Interestingly, however, periodontal ligament  
444 fibroblasts exposed to 1 g/cm<sup>2</sup> compression (for 4 h) displayed a 2-fold decrease in EV release  
445 relative to unstressed control cultures (Zhao et al., 2021), though a separate study observed a  
446 1.3-fold increase in EV yield from the same fibroblasts following 24 h exposure to the same  
447 stress (Zhang et al., 2022). Whether this discrepancy is attributable to the nature of the  
448 compressive force, the unique characteristics of the parent fibroblasts in question, or variation in  
449 experimental methods (e.g., EV isolation and quantification) remains unclear. In every case, the  
450 mechanisms informing fibroblast EV production under mechanical stress have not been  
451 investigated. Moreover, published research is limited in scope, examining only exosome-  
452 enriched EV samples. The impact of mechanical stress on the release of larger fibroblast EVs is  
453 therefore unknown.

454

### 455 **3.3. Bone and cartilage tissue**

456 Bone and cartilage are highly responsive to mechanical loading. Bone integrity depends on  
457 physical exercise, with loss of bone tissue occurring in response to underuse and/or  
458 microgravity environments (Morrell et al., 2018). While tension and compression remain  
459 unevaluated for their role in EV production by bone and cartilage tissue, shear stress promotes  
460 EV production in both tissue types (Liu, Q. et al., 2022; Morrell et al., 2018). Shear stress of 35  
461 dyn/cm<sup>2</sup> applied in two 10 min intervals boosted EV production by 22-fold in osteocyte-like MLO-  
462 Y4 cells, a result of transient intracellular influxes of  $\text{Ca}^{2+}$  that trigger simultaneous actomyosin  
463 contractions (Morrell et al., 2018). Similarly, cultures of rat condylar chondrocytes exposed to  
464 shear stresses of 4, 8, and 16 dyn/cm<sup>2</sup> produced 1.3, 1.7, and 2.5 times as many EVs as control  
465 cultures (Liu, Q. et al., 2022). Additional study into the impact of tension and compression on EV  
466 production by bone and cartilage tissue must be a priority.

467

### 468 **3.4. Bronchial epithelial cells**

469 The bronchial epithelium is exposed to cyclic tension and compression during natural  
470 ventilation; this stress reaches pathological levels during mechanical ventilation (Wang et al.,  
471 2022) and asthmatic episodes, with constricted airways amplifying compressive forces in the  
472 latter case (Mitchel et al., 2016; Mwase et al., 2022; Park et al., 2012). The impacts of these

473 stresses on EV production by bronchial epithelial cells (BECs) is not yet well-understood. In the  
474 most comprehensive study to date, BEC EV yield was increased by 2-fold following 10% cyclic  
475 stretch (at 0.67 Hz for 24 h), but remained unchanged following 5% static stretch over the same  
476 period (Najrana et al., 2020). Both of the aforementioned stretch protocols were developed to  
477 mimic the *in vivo* forces exerted during fetal lung development (Najrana et al., 2020). BEC EV  
478 production was likewise boosted by nearly 2-fold under even higher (supraphysiological) levels  
479 of cyclic tension (i.e., 20% cyclic stretch at 1 Hz for 24 h), a direct result of endoplasmic  
480 reticulum (ER) stress mediated by apoptosis signal-regulating kinase 1 (ASK1) (Tang et al.,  
481 2022). A similar increase in BEC EV yield—incurred via the same mechanism—was observed *in*  
482 *vivo* for a murine model of mechanical ventilation-induced pulmonary fibrosis (Tang et al.,  
483 2022). BEC EV yield also appeared to increase following the application of supraphysiological  
484 levels of compression (at 30 cm H<sub>2</sub>O for 3 h), but this increase was not quantified (Mwase et al.,  
485 2022).

486

### 487 **3.5. Endothelial cells**

488 The impact of shear stress on vascular endothelial cells (VECs) has been well-reviewed (Feng,  
489 S. et al., 2022). Unlike most other cell types, cultured VECs have repeatedly yielded *more*  
490 microparticle-enriched EVs as shear magnitude decreases (Kim et al., 2015; Ramkhelawon et  
491 al., 2008; Vion et al., 2013b). For physiological levels of shear stress between 1.5 and 2  
492 dyn/cm<sup>2</sup>, VEC-derived EV production was consistently about 1.3-fold *lower*—relative to static  
493 conditions—after 24 h (Ramkhelawon et al., 2008; Vion et al., 2013b). Under supraphysiological  
494 shear levels of 15 to 20 dyn/cm<sup>2</sup>, EV production dropped even further: by 3- to 4-fold (relative to  
495 static conditions) after 24 to 36 h (Kim et al., 2015; Ramkhelawon et al., 2008; Vion et al.,  
496 2013b). These findings have been confirmed *in vivo* for low and oscillatory shear, and manifest  
497 most substantially in atheroprone or otherwise diseased individuals (Boulanger et al., 2007;  
498 Jenkins et al., 2013; Kim et al., 2015; Navasiolava et al., 2010; Silva et al., 2021; Tremblay et  
499 al., 2017; Vion et al., 2013b). Still, this makes physiological sense, as higher shear in blood  
500 vessels is atheroprotective, while lesser, oscillatory, or retrograde shear is associated with the  
501 turbulent flow patterns caused by vessel blockage and atherosclerosis (Rautou et al., 2011).  
502 Whereas excess shear is an unwelcome stressor for most cell types, VECs—normally exposed  
503 to high shear *in vivo*—may experience static (i.e., subphysiological) conditions as “more  
504 stressful” and release EVs as a result. Indeed, endothelial microparticles produced via various  
505 chemical stressors transport apoptotic agent caspase-3 away from parent cells, preserving local  
506 viability of the endothelium; a similar role has been suggested for microparticles forged under  
507 shear (Abid Hussein et al., 2007; Rautou et al., 2011). However, one recent study found VECs  
508 to produce roughly thrice as many EVs after 24 h exposed to both supraphysiological (20  
509 dyn/cm<sup>2</sup>) and turbulent oscillatory ( $\pm 5$  dyn/cm<sup>2</sup>) shear stress (Chung et al., 2022). HUVEC-like  
510 cells seeded on microcarriers have also produced increasing EV yields with increased rotational  
511 agitation, though the yields were correlated with Kolmogorov eddy length scale, not shear stress  
512 (Gazeau et al., 2020). Moreover, even under very low average and maximum shear rates (0.015  
513 dyn/cm<sup>2</sup> and 1.3 dyn/cm<sup>2</sup>, respectively), VECs seeded on scaffolds in flow-perfusion bioreactors  
514 were found to boost EV production by 100- and 10,000-fold after 24 and 36 h, respectively  
515 (though much of this yield increase may be due to shear-independent factors such as improved  
516 nutrient availability, oxygenation, and waste removal) (Patel et al., 2019). The observed  
517 discrepancy in VEC EV production as a function of shear stress may be due to the recent  
518 ascent of nanoparticle tracking analysis (NTA) as the primary method of EV quantification. The  
519 earlier papers described above all employed flow cytometry, which is limited in its ability to  
520 count exosome-scale particles (Kim et al., 2015; Ramkhelawon et al., 2008; Vion et al., 2013b).  
521 Moreover, the differential centrifugation techniques in these papers preclude any significant  
522 inclusion of exosome-scale particles, which generally require ultracentrifugation at 100,000 g to  
523 precipitate. This suggests distinct and possibly opposing roles for endothelial exosomes and

524 microparticles in the presence of shear stress, with higher exosome levels under physiological  
525 conditions and higher microparticle levels following exposure to subphysiological magnitudes (or  
526 absence) of shear. Still, more investigation is necessary, and oscillatory shear, despite its  
527 pathogenic associations, appears to promote exosome and microparticle formation alike  
528 (though the content of EVs produced under oscillatory shear is distinct, as discussed in section  
529 4.5) (Chung et al., 2022). Low CD63 (an exosome marker) levels in VEC-derived EV samples  
530 from the flow-perfusion bioreactors suggest that the release of uniquely small microparticles  
531 (i.e., plasma membrane-derived particles), rather than exosomes, may be responsible for the  
532 NTA-detected uptick in EV biogenesis under shear (Patel et al., 2019).

533  
534 In the lungs, tensile and compressive forces imposed by ventilation may be more influential than  
535 shear in modulating VEC phenotypes. Even absent ventilation, blood pressure imposes  
536 significant tensile stress on VEC cells in a cyclic manner. Three papers have quantified the  
537 impact of cyclic stretching on microparticle-enriched EV production from VECs (Jia et al., 2017;  
538 Letsiou et al., 2015; Vion et al., 2013a). Supraphysiological levels of cyclic stretching (i.e., 15%  
539 to 18%) have increased in EV production by 2- to 3-fold after 4 to 6 h, 1.5- to 4-fold after 24 h,  
540 and up to 13-fold after 48 h (Jia et al., 2017; Letsiou et al., 2015; Vion et al., 2013a). To the  
541 contrary, physiological levels of cyclic stretching (i.e., 5%) have not appreciably increased EV  
542 yields relative to static conditions (Vion et al., 2013a), though one paper notes an increase of  
543 roughly 2-fold that remains consistent from 4 to 24 h (Letsiou et al., 2015). These trends have  
544 been confirmed in murine models (Letsiou et al., 2015). Notably, only microparticle-enriched  
545 samples have been evaluated in the context of cyclic stretch; the impact of cyclic stretch on  
546 VEC exosome production remains unknown.

547  
548 Mechanisms underlying mechanical stress-induced variation in VEC microparticle release have  
549 been proposed. Static conditions induce apoptotic processes in VECs, and subsequent  
550 microparticle release is dependent on caspase activation (Vion et al., 2013b). Under  
551 physiological levels of shear stress, however, microparticle release is caspase-independent,  
552 mediated instead by the activity of ERK 1/2 and Rho kinase (ROCK) (Vion et al., 2013b).  
553 Mitochondrial dysfunction and ABCA1-mediated phosphatidylserine (PS) exposure serve as  
554 additional mechanisms promoting microparticle release in these conditions (Kim et al., 2015;  
555 Vion et al., 2013b). Under high levels of shear, activation of sirtuin 1 (SIRT1) raises nitric oxide  
556 (NO) levels; the joint action of SIRT1 and NO serves to increase mitochondrial biogenesis in  
557 VECs, and NO additionally attenuates ABCA1 expression (Kim et al., 2015; Vion et al., 2013b).  
558 Notably, calpain activity is not associated with VEC microparticle release in any instance (Vion  
559 et al., 2013b). To date, no explanation has been offered regarding the increase in exosome-  
560 scale EVs derived from VECs under shear. The increase in VEC microparticles under cyclic  
561 stretch, meanwhile, is mediated by non-apoptotic caspase action, but not ROCK or calpain  
562 activity (Vion et al., 2013a). ER stress has also been implicated in this phenomenon (Jia et al.,  
563 2017).

564

### 565 **3.6. Smooth muscle cells**

566 Smooth muscle cells (SMCs) in the blood vessels, protected from shear by the endothelial  
567 lining, are nonetheless exposed to significant tensile stress imposed by blood pressure. SMC  
568 EV production as a function of tension is not well-characterized. In one study, murine aortic  
569 SMCs exposed to supraphysiological (18%) cyclic stretch (at 1 Hz) experienced 2- and 3-fold  
570 increases in microparticle-enriched EV yield after 24 and 48 h, respectively (Jia et al., 2017).  
571 This stretch-mediated increase in EV production was further found to depend on ER stress, and,  
572 in particular, the up-regulation of ER stress proteins GRP78, ATF4, and CHOP (Jia et al., 2017).  
573 A second study, however, observed no change in the production of exosome-enriched EVs

574 following 12% cyclic stretch (at 1 Hz) for 24 h (Akerman et al., 2019). The reason for this  
575 discrepancy is unclear, but may involve differences in mechanical loading or EV isolation.  
576

### 577 **3.7. Platelets and megakaryocytes**

578 Supraphysiological levels of shear stress (variously >60 or  $\geq$ 100 dyn/cm<sup>2</sup>) (Haga et al., 2003;  
579 Holme et al., 1997) have been found to significantly boost human platelet EV production *in vitro*  
580 (Chen et al., 2010; Haga et al., 2003; Holme et al., 1997; Leytin et al., 2004; Miyazaki et al.,  
581 1996; Reininger et al., 2006; Roka-Moia et al., 2021; Sakariassen et al., 1998). Where  
582 quantified (using flow cytometry), EV yields under shear stress of 100 to 108 dyn/cm<sup>2</sup> have  
583 increased by between 3.1- and 14.5-fold after 1 to 5 min (relative to yields in static conditions)  
584 (Chen et al., 2010; Haga et al., 2003; Miyazaki et al., 1996; Reininger et al., 2006). One study  
585 further suggests that EV undercounting may disguise even higher “true” EV yields—of up to 55-  
586 fold—in these conditions, as platelets present in the samples may “mask” the presence of EVs  
587 during flow cytometry (Reininger et al., 2006). On the other hand, lower, physiological shear  
588 levels (1.4 to 60 dyn/cm<sup>2</sup>) (Haga et al., 2003; Holme et al., 1997) have repeatedly failed to  
589 significantly elevate EV production, though most studies nonetheless note small production  
590 increases of between 1.1- and 2.7-fold after 1 to 5 min, relative to EV production in static  
591 conditions (Chen et al., 2010; Haga et al., 2003; Holme et al., 1997; Leytin et al., 2004; Miyazaki  
592 et al., 1996; Reininger et al., 2006; Roka-Moia et al., 2021; Sakariassen et al., 1998; Shai et al.,  
593 2012). These conclusions are supported by a significant body of research examining shear-  
594 induced platelet EV production *in vivo*. With noted exceptions (Rigamonti et al., 2020),  
595 increases in circulating platelet-derived EVs have been observed in response to a variety of  
596 physical exercises, including strenuous treadmill (Maruyama et al., 2012) and cycling exercise  
597 (Chaar et al., 2011; Wilhelm et al., 2016) and moderate cycling exercise (Sosdorf et al., 2010,  
598 2011). Whether such EV increases can be primarily attributed to increased shear in the blood  
599 vessels is disputed, however (Wilhelm et al., 2017). Platelets sampled from subjects engaged in  
600 strenuous physical exertion (graded exercise on a bicycle ergometer until exhaustion) and  
601 subsequently sheared *in vitro* have also demonstrated increased capacity for EV production  
602 under supraphysiological (but not physiological) shear levels (Chen et al., 2010). Elevated  
603 platelet EV production has also been confirmed *in vitro* and *in vivo* for cardiopulmonary bypass  
604 systems—such as left ventricular assist devices (LVADs) and extracorporeal membrane  
605 oxygenation (ECMO)—that induce supraphysiological levels of shear or other mechanical stress  
606 (Diehl et al., 2010; Meyer et al., 2020; Sun et al., 2022). Interestingly, platelets exposed to an  
607 artificial stenosis produced EVs more efficiently (i.e., produced more EVs per unit time) than  
608 platelets exposed to constant shear of the same magnitude exerted by the stenosis (Holme et  
609 al., 1997; Sakariassen et al., 1998). This suggests that sudden changes in the magnitude of  
610 shear may be more important in platelet EV biology than the shear levels themselves. Notably,  
611 however, all of the platelet research described to this point was conducted exclusively on  
612 microparticle-enriched EV samples. The role of shear in modulating platelet-derived exosome  
613 release remains unclear. Only one study has evaluated the role of shear in exosome-scale EV  
614 production, reporting that platelet exosome yield is unaffected by variation in shear stress  
615 induced by surgical aortic valve replacement (SAVR) (Weber et al., 2020). This stands in  
616 significant contrast to the stress-induced production of larger EVs, and requires controlled *in*  
617 validation, especially as the shear in question was broadly defined and, by nature,  
618 transiently applied.  
619

620 The mechanisms by which supraphysiological levels of shear promote platelet EV release have  
621 been extensively investigated. In particular, the binding of platelet glycoprotein Ib (GPIb) to von  
622 Willebrand factor (vWF) is significantly implicated in this process (Goto et al., 2003; Miyazaki et  
623 al., 1996; Pontiggia et al., 2006; Reininger et al., 2006). Under high shear, platelet membranes  
624 form “tethers” following their GPIb-mediated binding to immobilized or platelet-expressed vWF

625 (Reininger et al., 2006). These tethers act as a mechanism by which the shear-exposed  
626 platelets maintain contact with bound vWF, even as they are increasingly dragged downstream  
627 (Reininger et al., 2006). Eventually, the tethers detach from their parent platelets, fragmenting  
628 into numerous EVs that remain bound—at least temporarily—to vWF (Reininger et al., 2006).  
629 This process is mediated by an influx of intracellular  $\text{Ca}^{2+}$ , which activates platelet calpain, itself  
630 required for the degradation of actin binding protein (ABP) (Miyazaki et al., 1996). Binding of  
631 platelet glycoprotein IIb-IIIa (GPIIb-IIIa) to vWF—a process that further strengthens the bonds  
632 established by the adhesion of GPIb to vWF—has likewise been suggested to have a minor  
633 (Goto et al., 2003; Miyazaki et al., 1996; Pontiggia et al., 2006) or even significant (Haga et al.,  
634 2003) role in shear-induced platelet EV release, though data conflict (Reininger et al., 2006).  
635 For longer shearing timeframes (i.e., >2 min), EV production may operate independently from  
636 the binding of GPIb and vWF, and be mediated instead by activation of protein kinase C (PKC)  
637 (Miyazaki et al., 1996). In other words, PKC seemingly works to extend—but not initiate—  
638 platelet EV release (Miyazaki et al., 1996). EV release under supraphysiological levels of shear  
639 has additionally been shown to depend on stress-induced increases in cytokine levels (i.e., IL-6,  
640 erythropoietin, and thrombopoietin levels) (Nomura et al., 2000).

641 Importantly, the bulk of the aforementioned literature concerning platelets was published prior to  
642 2009, when the field lacked differentiation between platelet- and Mk-derived EVs (Flaumenhaft  
643 et al., 2009; Stone et al., 2022). In 2009, a large fraction of so-called “platelet-derived EVs” were  
644 recognized as originating from Mks (Flaumenhaft et al., 2009). Renewed research into the  
645 distinctions between platelet and Mk EV production under mechanical stress must therefore be  
646 a priority. Mks, themselves platelet progenitors, are exposed to shear stress as they protrude  
647 through the endothelial lining of sinusoidal blood vessels and subsequently encounter blood  
648 flow (Junt et al., 2007). Mks have experienced a boost in EV production—by 47-fold—following  
649 2 h of exposure to physiological ( $2.5 \text{ dyn/cm}^2$ ) shear (Jiang et al., 2014). Shorter exposure (for  
650 0.5 h) was associated with lesser production (a 24- to 27-fold increase over static conditions).  
651 This shear-induced Mk EV release is dependent on a non-lethal subset of apoptotic processes  
652 mediated by activation of caspase-9 and caspase-3 (Jiang et al., 2014; Luff et al., 2018). The  
653 binding of p53 to BAX is up-regulated in Mks under shear, and subsequent cytochrome c  
654 release from the mitochondria—likely caused by insertion of BAX into the mitochondrial  
655 membrane—activates the caspase cascade (Luff et al., 2018). As with platelets, mechanical  
656 stress-related Mk EV research has been conducted almost exclusively on microparticle-  
657 enriched samples; relatively little is known about exosome-scale EVs derived from Mks.  
658 Moreover, tensile and compressive stress have not been investigated for any potential role in  
659 EV release from platelets/Mks, though these stressors are not commonly experienced by such  
660 cell types (with the exception of Mks migrating through the endothelial lining of sinusoidal blood  
661 vessels). Additionally, given the propensity of suspension cells—such as platelets and Mks—to  
662 rotate in response to shear, we remind the reader that shear stress will be experienced  
663 differently by suspension and adherent cells.

664  
665 **3.8. Skeletal muscle cells**  
666 Although data are somewhat sparse, skeletal muscle cells (SkMCs) *in vitro* have thus far  
667 demonstrated increased EV production *only* in response to tension. This is likely due to the  
668 significant involvement of tension in skeletal muscle function—and the relative physiological  
669 irrelevance of other forms of mechanical stress, such as shear. Although mild shear stress ( $6 \text{ dyn/cm}^2$ )  
670 (Takafuji et al., 2021) and general mechanical overload (induced by electric pulse  
671 stimulation) (Vechetti et al., 2021) demonstrated no impact on SkMC EV yield *in vitro*, 25%  
672 cyclic stretch (at 1 Hz for 48 h) resulted in an 11-fold increase in EV yield (Guo et al., 2021).  
673 This increase is dependent on YAP, which accumulates in the nuclei of SkMCs in response to  
674 mechanical stretch, likely activating the canonical Wnt signaling pathway (Guo et al., 2021). In

676 another study, sustained, low-strain cyclic stretch (of 15% at 1 Hz for 24 h) and brief, high-strain  
677 cyclic stretch (of 12-22% at 1 Hz for 24 h, with 50 min of rest for every 10 min stretching)  
678 boosted SkMC EV yield by 2.5- and 4.2-fold, respectively (Mullen et al., 2022). More complex  
679 forms of mechanical stress—resulting from physical exercise in humans (Rigamonti et al., 2020)  
680 and synergist ablation in a murine model (Vechetti et al., 2021)—have also promoted SkMC EV  
681 generation *in vivo*. We note that the described research involving SkMC EVs has focused  
682 exclusively on exosomes or exosome-enriched samples; the interrelationships between  
683 mechanical stress and SkMC microparticle production have yet to be investigated.  
684

### 685 **3.9. Tumor cells**

686 Relative to healthy surrounding tissue, the tumor microenvironment is characterized by high  
687 levels of mechanical stress, primarily incurred by elevated interstitial fluid flow rates and  
688 increased hydrostatic and compression-induced pressure (Feng, T. et al., 2022; Stylianopoulos  
689 et al., 2013). By nature, tumor growth serves to continually modify interstitial fluid flow, creating  
690 blockages and increasing pressure in the surrounding microenvironment (Koomullil et al., 2021).  
691 This phenomenon renders tumor-derived EV production rates uniquely time-dependent, with  
692 higher such rates likely to occur in late-stage tumors (Koomullil et al., 2021). Additionally,  
693 circulating tumor cells encounter significant mechanical stress during transport through the  
694 vasculature, with membrane deformation likely common in narrow capillaries (Wan et al., 2022).  
695 Without exception, application of shear, tension, and compression on tumor cells has served to  
696 increase exosome-scale EV production (Koomullil et al., 2021; Wang, K. et al., 2019; Wang, Y.  
697 et al., 2020). Shear of 10 dyn/cm<sup>2</sup> applied for 1 h resulted in a 2-fold increase in HeLa cell-  
698 derived EVs and a 2.5-fold increase in EVs from MDA-MB-231 (human triple negative breast  
699 cancer) cells (Wang, K. et al., 2019). Uniaxial cyclic stretch of 10% (applied at 0.3 Hz for 48 h)  
700 had a similar impact on exosome production, with EV production in MCF-7 (human estrogen  
701 receptor positive breast cancer), MDA-MB-231, and 4T1.2 (murine triple negative breast cancer)  
702 cells increasing by 1.2-fold (insignificant), 6-fold, and between 1.9- and 2.4-fold, respectively  
703 (Koomullil et al., 2021; Wang, Y. et al., 2020). Compression of HeLa cells has likewise promoted  
704 EV release, with a peak production increase of 4.7-fold observed following the application of  
705 0.23 kPa press stress (1 h) (Wang, K. et al., 2019). Increased substrate stiffness, which induces  
706 tension on parent cells, has also been well-established as increasing tumor EV yields from  
707 breast (Patwardhan et al., 2021; Wu et al., 2023), liver (Wu et al., 2023), pancreatic (Wu et al.,  
708 2023), and prostate cancer (Liu, Z. et al., 2022) cell lines. Where quantified, tumor EV yields in  
709 stiff substrates have increased by 3- to 7-fold relative to EV yields from soft substrates (Liu, Z. et  
710 al., 2022; Wu et al., 2023). Similar findings have been observed for cancer-associated  
711 fibroblasts grown on stiff substrates (Xiao et al., 2022). More complex mechanical forces  
712 induced by turbulent agitation in a bioreactor have also been correlated with increased EV  
713 production in HeLa cells (Grangier et al., 2020). Notably, malignant parent cells have  
714 demonstrated higher EV yields than non-malignant cells in response to similar substrate  
715 stiffness, suggesting oncogenic mutations may uniquely increase cellular sensitivity to  
716 biomechanical force (Wu et al., 2023). The mechanism underlying increased EV production in  
717 tumor cells under mechanical stress is not well understood, except in the case of substrate  
718 stiffness, where increased EV yields have been linked to phosphorylation of focal adhesion  
719 kinases and subsequent activation of Akt, which boosts GTP-RAB8 levels. YAP/TAZ action also  
720 plays a key role in increased breast cancer EV production in stiff substrates. Additionally, EV  
721 production by MDA-MB-231 and 4T1.2 cells under long-term (48 h) cyclic stretch can be  
722 explained almost entirely by increased cellular proliferation, suggesting EV release in these  
723 conditions remains constant on a per-cell basis (Wang, Y. et al., 2020). Mechanical stress may  
724 also modulate the size of secreted EVs. In one case, the tension-mediated action of myosin II  
725 served to decrease the average size of exosome-enriched EVs derived from Ewing's sarcoma  
726 cells (Villasante et al., 2016), though this phenomenon was not observed in other models that

727 increased stiffness of the extracellular matrix in order to induce tension (Liu, Z. et al., 2022; Wu  
728 et al., 2023). In contrast with most other cell types, tumor cells have been well-characterized  
729 with respect to exosome production under mechanical stress; after all, almost all the research  
730 described above involves exosomes or exosome-enriched samples. However, the role of  
731 mechanical stress in the biogenesis/release of larger (microparticle-scale) EVs remains to be  
732 investigated.

### 733 **3.10. Other mammalian cells**

734 The impact of mechanical stress on EV generation has been briefly examined in several  
735 additional cell types. For instance, human urinary podocytes have been found to increase EV  
736 production by 3.8-fold following the application of 10% cyclic stretch (at 0.5 Hz and for 24 h)  
737 (Burger et al., 2014). This magnitude of cyclic stretch mimics pathological levels of  
738 intraglomerular stress experienced *in vivo* (Burger et al., 2014). EV yields from HEK293T cells  
739 overexpressing angiotensin II type 1 receptor (AT1R) were increased by 2-fold following osmotic  
740 stretch (i.e., application of 143 mOsm/kg hypotonicity for 30 min) (Pironti et al., 2015). This  
741 research is particularly notable due to the genetic engineering of the parent cells. Similarly, a  
742 murine model of cardiac pressure overload—induced by surgical transverse aortic constriction—  
743 boosted serum EV yields by 2-fold after 1 day and 3-fold after 7 days; most such EVs were  
744 derived from cardiomyocytes (Pironti et al., 2015). Neonatal rat cardiomyocyte EV yield also  
745 increased by 2-fold following 24 h application of 20% static stretch *in vitro* (Yuan et al., 2018).  
746 However, for Schwann cells—the glial cells of the peripheral nervous system—no EV yield  
747 differentials were observed following the application of complex mechanical force (induced by  
748 the magnetic stimulation of co-cultured nanoparticles) (Xia et al., 2020).

749 Publications relating biomechanical stress to the biogenesis of leukocyte-derived EVs are  
750 limited. In one study of note, stirred-tank bioreactors increased EV yields from THP-1  
751 (immortalized human monocyte) cells by 10-fold (Grangier et al., 2020). In another instance, a  
752 novel seesaw-motion bioreactor boosted daily EV production from natural killer cells by almost  
753 2-fold relative to static culture (Wu et al., 2022). Beyond these two cases, however, the impact  
754 of mechanical stress on the biogenesis of leukocyte- and erythrocyte-derived EVs has only  
755 been examined in the context of physical exercise. In such studies, mechanical stress cannot be  
756 effectively isolated as an independent variable and results understandably conflict (Chaar et al.,  
757 2011; Sosdorff et al., 2011). However, atomic force microscopy has indicated an increase in  
758 EV-like particles on the membranes of erythrocytes cultured on tilting shakers, a phenomenon  
759 possibly linked to faster cellular aging under sustained biomechanical stress (Dinarelli et al.,  
760 2022).

### 761 **3.11. Non-mammalian cells**

762 Though clinical relevance and unique susceptibility to mechanical stress (Chalmers and Ma,  
763 2015; Thomas, 1993) have made mammalian cells the prime targets of research involving  
764 stress-induced EV production, EVs derived from non-mammalian sources will likely exhibit  
765 characteristics similar to those observed in their mammalian counterparts. For instance,  
766 preliminary research suggests mechanical stress serves to increase ciliary EV production in  
767 *Caenorhabditis elegans* (Wang, J. et al., 2020). The yield of outer membrane vesicle (OMV)  
768 derived from *Acinetobacter baumannii* bacteria is likewise boosted by more than 5-fold following  
769 agitation with a high speed dispersator (Li et al., 2020). OMVs produced under these stress  
770 conditions were nearly 1.5 times larger, less polydisperse, and more negatively charged, and  
771 possessed distinct proteomic profiles and increased (by 3-fold) lipopolysaccharide content (Li et  
772 al., 2020).

### 773 **3.12. General themes and trends**

778 Clearly, the reasons for the summarized correlations between mechanical stress and EV  
779 biogenesis are complex, depending heavily on both parent cell type and the nature of the  
780 applied stress. Nevertheless, recurring themes have begun to emerge. In the majority of cases,  
781 EV release increases following exposure of parent cells to mechanical stress. However, we  
782 have found five exceptions to this rule. The first occurs when the applied stress is not reflective  
783 of pathological conditions experienced *in vivo* by the cell type in question. For instance,  
784 microparticle production is not increased in VECs under high shear, since shear is required for  
785 normal VEC physiology. The second exception occurs when the stress is not physiologically  
786 relevant. For instance, shear stress applied to SkMCs and cyclic stretch applied to both gingival  
787 and dental pulp fibroblasts fails to appreciably alter EV release, as the mechanical stresses in  
788 question are not natively experienced by the respective cell types. The third exception occurs  
789 when EV yields “plateau” (and in some cases, subsequently decrease) at high stresses or after  
790 long periods of stress exposure. For several samples, including adipose-derived MSCs under  
791 shear (Guo et al., 2021) and HeLa tumor cells under compression (Wang, K. et al., 2019), EV  
792 yields began decreasing when exposed to the highest tested mechanical stress levels,  
793 suggesting the existence of “optimal” stress levels beyond which maximum EV yields diminish.  
794 Similarly, periodontal ligament cell EV production plateaued after 36 h of cyclic stretch,  
795 suggesting cells’ EV production machinery may adapt to chronic mechanical stress (Wang, Z. et  
796 al., 2019). The fourth exception occurs when the applied mechanical stress results in high levels  
797 of apoptosis, preventing the active release of EVs; such an exception has been proposed as the  
798 reason for decreased fibroblast EV production under compression (Zhao et al., 2021). Finally,  
799 and perhaps most importantly, the fifth exception occurs when exosomes yields are unaffected  
800 by mechanical stress, even as microparticle yields (which may not be measured) increase. This  
801 phenomenon has been observed in exosomes from platelets (Weber et al., 2020) and SMCs  
802 (Akerman et al., 2019).

803  
804 Given differential exosome and microparticle yields in parent cells exposed to mechanical  
805 stress, it grows increasingly prudent to analyze the production of both EV subtypes in a single  
806 study. Still, to date, such research is rare. Indeed, among many cell types, the entire relevant  
807 body of literature has been limited to an evaluation of *either* exosome or microparticle  
808 production (but not both). For instance, studies of stress-induced changes in MSC, fibroblast,  
809 and tumor cell EV production are limited almost exclusively to exosomes, while the impact of  
810 mechanical stress on platelet and Mk EVs has primarily been studied in the context of  
811 microparticles. In addition, many cell types—including erythrocytes and leukocytes—have  
812 largely been ignored in the context of mechanical stress-induced EV production.

813  
814 The reasons for EV production (or the lack thereof) under mechanical stress are numerous and  
815 vary on a cell-by-cell basis, though common trends nonetheless emerge. For very high stress  
816 levels, unique, non-apoptotic caspase action appears responsible for the bulk of EV release (Hill  
817 et al., 2022; Jiang et al., 2014; Vion et al., 2013a; Vion et al., 2013b). Both ROCK-dependent  
818 and ROCK-independent pathways have been proposed as an intermediate mechanism (Hill et  
819 al., 2022). Mitochondrial dysfunction appears to wield significant influence in this process; for  
820 both megakaryocytic and endothelial cells, said dysfunction—induced by p53 and the absence  
821 of sirtuin 1 (SIRT1), respectively—is correlated with pathological levels of shear (which differ  
822 with cell type) and linked to a decrease in microparticle-enriched EV samples (Kim et al., 2015;  
823 Luff et al., 2018). In cases of less severe mechanical stress, alternative pathways have been  
824 proposed. An influx in intracellular  $Ca^{2+}$  levels, for instance, is required for stress-induced EV  
825 production by MSCs (Kang et al., 2022), osteocytes (Morrell et al., 2018), and platelets  
826 (Miyazaki et al., 1996). As noted, high  $Ca^{2+}$  levels serve to activate various proteins involved in  
827 cytoskeletal remodeling, including PKC and calpain (Kang et al., 2022; Miyazaki et al., 1996),  
828 and even induce actomyosin contractions along the plasma membrane, with notable examples

829 in blood cells and osteocytes (Morrell et al., 2018; Zwaal and Schroit, 1997). Though not yet  
830 directly linked to increased (exosome-scale) EV production, intracellular  $\text{Ca}^{2+}$  levels are also  
831 elevated in VECs under shear stress, likely a result of ATP release at the caveolae (Yamamoto  
832 et al., 2011). High  $\text{Ca}^{2+}$  levels additionally promote PS externalization—an important step in  
833 membrane budding—via simultaneous activation of scramblase and inhibition of  
834 translocase/floppase coordination (Zwaal and Schroit, 1997). Exosomes in particular may also  
835 be released from the locations of  $\text{Ca}^{2+}$  channels in the plasma membrane, since ESCRT  
836 machinery linked to MVBs often migrates to the channels, complexing with proteins ALIX,  
837 syntenin, and TSG101 as a means of repairing the membrane (Ambattu et al., 2020; Jimenez et  
838 al., 2014; Scheffer et al., 2014). Endoplasmic reticulum (ER) stress has also been linked with  
839 increased EV production by SMCs, VECs, and BECs exposed to supraphysiological cyclic  
840 stretch (Jia et al., 2017; Tang et al., 2022). There is likely significant interplay between the  
841 distinct mechanisms discussed above. For instance, excess  $\text{Ca}^{2+}$  induces mitochondrial  
842 dysfunction independently of the noted p53/SIRT1 pathways (Smith et al., 2012), and the  
843 cytochrome c released as a result may bind to the ER, causing the release even more cytosolic  
844  $\text{Ca}^{2+}$  and introducing a positive feedback loop (Boehning et al., 2003). Shear-induced ATP  
845 release from the mitochondria can trigger an additional influx of extracellular  $\text{Ca}^{2+}$  into the cell  
846 (Yamamoto et al., 2018).

847  
848 YAP was heavily implicated in up-regulated EV release by MSCs and SkMCs under shear and  
849 cyclic stretch, respectively (Guo et al., 2021), and by breast cancer cells grown on stiff  
850 substrates (Patwardhan et al., 2021). Such findings are of particular note due to the widespread  
851 applicability of the observed YAP-dependent mechanism. The application of external force to  
852 cell membranes has been observed to stretch the pores of the nuclear membrane and  
853 subsequently increase nuclear import of YAP (Elosegui-Artola et al., 2017), suggesting that YAP  
854 mediation of EV release in response to biomechanical stress proceeds via transcriptional  
855 regulation.

856  
857 Simple membrane mechanics, not yet discussed in detail, may also weigh heavily on EV  
858 release under stress. For any cell type, increased exosome release during the application of  
859 tensile stress (e.g., cyclic stretch) may be attributed to accelerated exocytosis, which serves to  
860 ease plasma membrane tension by extending the membrane surface (Apodaca, 2002; Le Roux  
861 et al., 2019). Of course, the opposite is likely true for microparticles: membrane budding is  
862 synonymous with membrane loss, which serves to increase tension. Absent other factors,  
863 membrane mechanics would therefore suggest that microparticle release decreases under  
864 tension and increases under compression. Supporting this conclusion is the finding that actin  
865 polymerization induced by cytoskeletal tension has been linked to decreased microparticle  
866 release (Flaumenhaft et al., 2009; Headland et al., 2014; Mo et al., 2018). **Figure 3** illustrates  
867 the various mechanisms informing differential EV biogenesis and release in response to  
868 biomechanical stress.

869  
870 For any cell type, extremely high levels of mechanical stress force the plasma membrane to  
871 rupture entirely, resulting in free-floating membrane fragments. Often intentionally produced via  
872 the extrusion of cells through microchannels, these fragments spontaneously reassemble into  
873 empty vessels resembling EVs (Jo, Wonju et al., 2014; Jo, W. et al., 2014; Wen et al., 2022).  
874 However, the unique biogenesis of these vessels, which relies on “brute force” and entails the  
875 absence of usual cargo-sorting mechanisms, suggests they ought not be classified as EVs for  
876 the purposes of this discussion. Similarly, we forgo an analysis of acoustic stimulation, which,  
877 while somewhat “mechanical” in nature, is not particularly relevant to EV behavior *in vivo* or  
878 during biomanufacturing. Acoustic stimulation has been found to boost exosome production (via

879  $\text{Ca}^{2+}$ -mediated ESCRT pathway activation) (Ambattu et al., 2020) and promote nanoparticle and  
880 macromolecule uptake (Ramesan et al., 2018) in a variety of cell types.

881  
882 **4. Impact of biomechanical forces on EV cargo and composition**  
883 Both the magnitude and duration of biomechanical force influence EV cargo loading by parent  
884 cells. As a result, EVs produced under such force possess different cargo—and, as a result,  
885 promote different cellular phenotypes—than their statically-derived siblings. While miRNAs and  
886 surface/intracellular proteins have received the most attention for their role in modulating EV  
887 bioactivity, any EV cargo—from lipids to additional nucleic acids—may have a role to play. EV  
888 cargo loading is modulated by a bevy of distinct mechanisms (Chen et al., 2021; Corrado et al.,  
889 2021; Fabbiano et al., 2020; Groot and Lee, 2020; Mir and Goettsch, 2020). Below, we  
890 summarize first the known mechanisms underlying EV cargo loading (by parent cells) and then  
891 the published research on biomechanical stress-mediated cargo loading, identifying overarching  
892 themes and directions for future inquiry.

893  
894 While numerous individual proteins involved in EV loading have been identified, the full,  
895 complex cascade of involved mechanisms is not well understood (Groot and Lee, 2020). Protein  
896 sorting in exosomes usually begins with ubiquitination (or similar post-translational modification)  
897 of MVB membrane proteins; subsequent loading occurs via action of the ESCRT complexes  
898 and associated proteins, such as ALIX and TSG101 (Chen et al., 2021). Tetraspanins  
899 (especially CD9, CD63, and CD81) and lipid rafts also have roles in this protein loading process,  
900 and notably serve as dominant protein loading mechanisms during ESCRT-independent  
901 exosome biogenesis (Chen et al., 2021). Though less is known about protein loading into  
902 microparticles, similar mechanisms—with confirmed involvement of ESCRT complexes—have  
903 been proposed (Mir and Goettsch, 2020; van Niel et al., 2018). For both exosomes and  
904 microparticles, RNA loading is mediated by a large number of RNA binding proteins (RBPs), of  
905 which notable examples include Argonaute 2 (Ago2) and several heterogeneous nuclear  
906 ribonucleoproteins (hnRNPs) (Chen et al., 2021; Corrado et al., 2021; Fabbiano et al., 2020;  
907 Groot and Lee, 2020). Recent work has also hinted at the possible involvement of ESCRT-  
908 associated proteins (including ALIX), tetraspanins and lipid rafts (Corrado et al., 2021). Very  
909 little is known about the processes involved in the loading of lipid cargo (Chen et al., 2021).

910  
911 **4.1. Mesenchymal stem cells**  
912 With few exceptions, the application of mechanical stress to MSCs promotes the release of EVs  
913 with “therapeutic” (clinically desirable) cargo and bioactivity. Total MSC EV protein levels  
914 increased significantly under low (0.001 and 0.0001  $\text{dyn/cm}^2$ ) shear (by 6.7- and 6.5-fold after  
915 24 h), 10% static stretch (after 24 h), and complex agitation of MSC spheroid culture (by 5.6-fold  
916 after 7 days), with the two noted shear conditions resulting in the up-regulation of CD105 and  
917 CD44 (traditional MSC markers) and down-regulation of CD81, CD63, and CD9 (traditional EV  
918 markers) (Cha et al., 2018; Kang et al., 2022; Vangapandu et al., 2019). To the contrary, MSC  
919 EVs produced under 1.5  $\text{g/cm}^2$  compression (24 h) were enriched in CD81 and CD63, as well  
920 as in annexin A3, annexin A6, and endocytic/phagocytic proteins generally (Huang et al., 2022).  
921 Proteomic analysis of EVs from shear-exposed, dental pulp-derived MSCs found similarly  
922 differential expression of nearly half the loaded proteins (relative to control EVs) after 48 h (Guo  
923 et al., 2021). Despite its apparent lack of influence over EV yield, static stretch was also found  
924 to significantly impact miRNA loading in MSC EVs (Vangapandu et al., 2019; Yu, Wenting et al.,  
925 2021). Under 10% static stretch (24 h), total tRNA levels increased, while total miRNA and  
926 lincRNA levels—as well as levels of individual miRNAs responsible for inhibiting wound  
927 healing—decreased (Vangapandu et al., 2019). Under slightly increased 20% static stretch (72  
928 h), 565 types of EV-loaded miRNA were differentially expressed, with 16 and 9 miRNAs up- and  
929 down-regulated, respectively, by a substantial margin (i.e., more than 2-fold) (Yu, Wenting et al.,

930 2021). Relative to MSC EVs derived from (low-tension) soft hydrogel substrates, EVs from stiff  
931 substrates were loaded with similar levels of mRNA, miRNA, and mitochondrial DNA associated  
932 with alleviation of lung injury; similar levels of ribosomal RNA were also observed (Lenzini et al.,  
933 2021). An increased EV size distribution was noted following production under 10% static  
934 stretch (24 h), a trend perhaps related to the corresponding increase in EV protein cargo  
935 (Vangapandu et al., 2019), while EV samples produced via the “squeezing” action of a custom  
936 microfluidic device included a relatively higher proportion of small (i.e., 40-80 nm) specimens  
937 (Hao et al., 2023). No size differences were observed in EVs derived from soft and stiff  
938 substrates, however (Lenzini et al., 2021).

939 The desirable bioactivity of MSC EVs—particularly as it relates to bone and neuron health—is  
940 nearly always increased as a result of mechanical stress-induced EV biogenesis, even as the  
941 identities of the specific cargo responsible for the EV bioactivity remain unknown. For instance,  
942 MSC EVs produced under 8% cyclic stretch (48 h) inhibited RANKL-mediated osteoclast  
943 differentiation by attenuating the nuclear factor kappa-B (NF- $\kappa$ B) signaling pathway, and were  
944 uniquely capable of reversing osteoporosis in a murine model (Xiao et al., 2021). Likewise, EVs  
945 produced under 20% static stretch demonstrated faster initial uptake by target MSCs and  
946 subsequently increased the osteogenic differentiation of these MSCs both *in vitro* and *in vivo*  
947 (Yu, Wenting et al., 2021). Separately, MSC exosomes from agitated, microcarrier-based  
948 culture were more efficiently taken up by neurons and were uniquely capable of rescuing them  
949 from 6-hydroxydopamine-induced apoptosis (notably, this latter behavior is not observed in  
950 MSC microparticles produced in agitated cultures) (Haraszti et al., 2018; Jarmalavičiūtė et al.,  
951 2015). Similarly, MSC EVs released under physiological shear promoted relatively more robust  
952 axonal sprouting in primary rat neurons (Guo et al., 2021). Under 10% static stretch, MSCs  
953 released EVs with improved ability to promote fibroblast migration in a scratch wound assay  
954 (Vangapandu et al., 2019). Interestingly, MSC EVs derived under 1.5 g/cm<sup>2</sup> compression  
955 promoted higher levels of osteoclast differentiation in target murine macrophages, likely via  
956 annexin A3-mediated EV uptake and subsequent ERK activation (Huang et al., 2022). Although  
957 this phenotype is associated with clinical undesirability, it is not unexpected; compression—as  
958 opposed to shear and tension—is a well-known promoter of osteoclast activity in bone tissue  
959 (Wang et al., 2018). We have found only three studies in which MSC EVs derived under  
960 mechanical stress do not possess enhanced bioactivity: EVs produced under very low shear  
961 (0.001 and 0.0001 dyn/cm<sup>2</sup>) were not significantly more effective than their statically-derived  
962 counterparts in reducing cisplatin-induced acute kidney injury *in vitro* and *in vivo* (Kang et al.,  
963 2022), while EVs produced via “squeezing” in a custom microfluidic device were likewise  
964 comparable to control EVs in their capacity to promote corneal epithelial wound healing (Hao et  
965 al., 2023). Likewise, EVs produced using soft and stiff hydrogel substrates were similarly  
966 efficacious in alleviating acute lung injury (Lenzini et al., 2021).

#### 967 4.2. Fibroblasts

968 Fibroblast EVs play a vital role in inflammation and wound healing, the nature of which is  
969 determined by mechanical stress-induced cargo loading. Levels of transforming growth factor  
970  $\beta$ 1 (TGF- $\beta$ 1)—a fibrosis promoter—were elevated in EVs from hallux valgus fibroblasts under  
971 15% static stretch (Xie et al., 2020). Moreover, these EVs displayed significant differential  
972 expression of 24 miRNAs; miRNAs linked to increased pathological angiogenesis (e.g., miR-  
973 1246) were up-regulated, while miRNAs associated with inhibition of angiogenesis (e.g., miR-  
974 133a-3p and miR-203-3p) were down-regulated (Xie et al., 2020). More efficiently taken up by  
975 target VECs, these stretch-derived hallux valgus EVs were likely responsible for increased  
976 proliferation, migration, and angiogenesis of the VECs *in vitro*, probably via ERK 1/2 activation  
977 mediated by the described miRNA cargo (Xie et al., 2020). The miRNA and lincRNA profiles of

other fibroblast EVs exposed to static stretch were similarly distinct (Blum et al., 2018). Interestingly, EVs derived from aortic fibroblasts under 12% cyclic stretch were enriched in miR-133a, suggesting these EVs may prevent pathological cardiovascular remodeling (Akerman et al., 2019). Whether this particular enrichment is due to cell type or the nature of the applied stress is unclear, though cell type is clearly a factor in differential fibroblast responses to mechanical stress. Even among ostensibly similar dermal fibroblasts, for instance, tension-derived EVs from high-scarring individuals possess different characteristics than similar EVs from low-scarring individuals (Blum et al., 2018). EVs from compressed (1 g/cm<sup>2</sup>) periodontal ligament fibroblasts are differentially loaded with at least eight cytokines, including immune regulator sICAM-1 (Zhang et al., 2022), and are additionally enriched in YAP (Zhao et al., 2021). Notably, while compressed fibroblasts are enriched in both activated and inactivated (phosphorylated) YAP, they selectively load activated YAP into EVs (Zhao et al., 2021). As a result, the EVs loaded under compression affect higher levels of inflammatory M1 polarization in target THP-1 macrophages (Zhao et al., 2021). However, periodontal ligament cell EVs produced under 20% cyclic stretch work to suppress the activation of inflammasomes in macrophages via inhibition of the NF-κB pathway (this phenotype was not evaluated in EVs produced under static conditions) (Wang, Z. et al., 2019).

#### 4.3. Bone and cartilage tissue

Mechanical loading has a significant impact on the balance of osteogenesis (bone formation) and osteoclastogenesis (bone resorption), with shear stress and cyclic stretch promoting bone formation and compression inhibiting it (Wang et al., 2018). Similarly, EVs produced by bone tissue under shear stress or cyclic stretch exhibit osteogenic phenotypes, while compressive stress results in EVs with osteoclastic potential. Specifically, EVs from osteocyte-like MLO-Y4 cells under 8% cyclic stretch were more effective in promoting the miR-181b-5p-mediated proliferation and osteogenic differentiation of periodontal ligament stem cells (Lv et al., 2020). Levels of miR-181b-5p were 5-fold higher in EVs from stretched culture, and, in total, 206 miRNAs were differentially expressed between the experimental and control EVs (Lv et al., 2020). Additionally, higher levels of proteins associated with the regulation of bone metabolism—RANKL, sclerostin, and osteoprotegerin—were observed in EV samples from MLO-Y4 cells exposed to 35 dyn/cm<sup>2</sup> shear stress, though levels of enrichment in individual EVs is unclear, as EVs were not quantified (Morrell et al., 2018). Under 1 g/cm<sup>2</sup> compression, however, osteoclast-derived EVs were relatively more effective at inhibiting the osteogenesis of target periodontal ligament stem cells, a likely result of their enrichment in miR-133a-3p, miR-203a-3p, miR-106a-5p, and miR-331-3p, which down-regulate bone formation, and their lack of miR-223-5p and miR-181-5p, which promote bone remodeling (Wang et al., 2021).

In the only study to date on chondrocyte-derived EVs produced under shear stress, shear of 16 dyn/cm<sup>2</sup> resulted in EVs with increased levels of tissue-nonspecific alkaline phosphatase (TNAP) and nucleotide pyrophosphatase/phosphodiesterase-1 (NPP1) and decreased levels of matrix Gla protein (MGP) (Liu, Q. et al., 2022). TNAP and NPP1 catalyze reactions necessary for the formation of calcified nodules, while MGP decreases mineralization (Liu, Q. et al., 2022). Therefore, as expected, EVs produced under shear promoted far higher levels of calcification in target chondrocytes than control EVs (Liu, Q. et al., 2022). This finding was confirmed *in vivo* for rats with temporomandibular joint osteoarthritis, which involves aberrant mechanical stress akin to the aforementioned shear stress applied *in vitro* (Liu, Q. et al., 2022). Similarly, chondrocyte-derived EVs produced under cyclic tension (i.e., 10% cyclic stretch at 1 Hz for 24 h) promoted more extensive osteogenic differentiation of chondrocytes, likely due to relatively higher levels of pro-osteogenic cargo (such as miR-199a-5p) and lower levels of anti-osteogenic cargo (such as miR-186-5p and miR-339-5p) (Shi et al., 2022). However, cyclic tension has also been linked to EV samples with greater capacity for miR-9-5p delivery to osteoblasts, whether by higher

1032 overall EV production or enhanced miR-9-5p loading (Li, B. et al., 2023). Since osteoblast  
1033 differentiation is inhibited by miR-9-5p (Li, B. et al., 2023), we suggest that the bioactivity of EVs  
1034 derived from chondrocytes under cyclic tension is somewhat complex, with potential for both  
1035 pro- and anti-osteogenic phenotypes.

#### 1036 **4.4. Bronchial epithelial cells**

1038 The nature of BEC EV cargo is heavily influenced by mechanical stress, but the details of this  
1039 relationship require additional investigation. Following supraphysiological levels of compression  
1040 (at 30 cm H<sub>2</sub>O), BEC EV samples were enriched in tissue factor (Mitchel et al., 2016; Park et al.,  
1041 2012) and tenascin C (Mwase et al., 2022), both of which inform the pathogenesis of asthma.  
1042 Whether the aforementioned proteins were up-regulated in individual EVs is unclear, however,  
1043 as protein levels were not normalized to EV counts. Surprisingly, BEC EVs produced under  
1044 supraphysiological levels of cyclic stretch (20% cyclic stretch at 0.5 Hz for 6 h) exerted an anti-  
1045 inflammatory phenotype, more effectively promoting M2 macrophage polarization via the miR-  
1046 21a-5p-mediated downregulation of the Notch2/SOCS1 signaling axis (Wang et al., 2022).  
1047 Levels of miR-21a-5p were increased by almost 150-fold in EVs from the stretched BECs  
1048 (Wang et al., 2022). However, a second study reported significantly higher levels of fibrosis-  
1049 related mRNA cargo in BEC EVs produced under similar levels of cyclic tension (20% cyclic  
1050 stretch at 1 Hz for 24 h) (Tang et al., 2022). As a result, these EVs were more effective at  
1051 activating lung fibroblasts *in vitro*; similar bioactivity was observed for BEC EVs produced *in vivo*  
1052 using a murine model of mechanical ventilation-induced pulmonary fibrosis (Tang et al., 2022).  
1053 The BEC EV miRNA profiles produced under physiological (10% cyclic and 5% static) stretch  
1054 levels were similarly diverse, with 9 miRNAs differentially loaded under cyclic stretch and 33  
1055 miRNAs differentially loaded under static stretch (Najrana et al., 2020). In both cases, these  
1056 miRNAs were often implicated in lung development, proliferation, and cell cycle regulation  
1057 (Najrana et al., 2020). Taken together, the current literature therefore suggests a pathology-  
1058 inducing role for BEC EVs produced under compression, but a more complex function—both  
1059 anti-inflammatory and pro-fibrotic—for similar EVs produced under supraphysiological levels of  
1060 cyclic stretch. Meanwhile, the impact of physiological levels of cyclic stretch on EV cargo and  
1061 bioactivity needs further investigation. We expect to dramatically refine these conclusions as  
1062 new research comes to light.

#### 1063 **4.5. Endothelial cells**

1065 The impact of mechanical stress on VEC EV cargo has been studied extensively. In general, the  
1066 cargo of VEC EVs exacerbates the pathology induced by the stress (or lack thereof) to which  
1067 the parent cells were exposed. Expression of adhesion molecules ICAM-1 and VCAM-1 and  
1068 exposure of PS were down-regulated on VEC EVs produced under physiological levels of  
1069 shear, suggesting that subphysiological (or absent) flow promotes the formation of EVs with  
1070 abnormally enhanced thrombotic properties (Ramkhelawon et al., 2008). Physiological (high)  
1071 shear also results in significant, selective up-regulation of miR-143 and miR-145 cargo via  
1072 action of the flow-sensitive protein Krüppel-like Factor 2 (KLF2) (Hergenreider et al., 2012; Jae  
1073 et al., 2015). VEC EV enrichment in miR-143 under shear has additionally been shown to  
1074 depend on RAB7a and RAB27b (but not RAB27a) (Jae et al., 2015). Examination of EV cargo  
1075 selected by KLF2-transduced parent cells suggests that physiological shear will additionally  
1076 promote the down-regulation of inflammation-associated miR-155 (He, S. et al., 2018). Notably,  
1077 EVs forged under physiological shear reduced atherosclerotic lesion formation in mouse aortas  
1078 and were more effective at preventing SMC de-differentiation (Hergenreider et al., 2012),  
1079 confirming the known role of the miR-143/145 cluster in ameliorating pathological phenotypes in  
1080 SMCs (Deng et al., 2015). EVs from KLF2-transduced cells, meanwhile, decreased  
1081 proinflammatory M1 macrophage markers and increased anti-inflammatory M2 macrophage  
1082 markers both *in vivo* and *in vitro* (He, S. et al., 2018).

1083  
1084 Recent miRNA sequencing suggests exosome-enriched EVs derived from VECs also  
1085 experience dramatically different miRNA cargo sorting following exposure to physiological  
1086 laminar or subphysiological oscillatory shear (Chung et al., 2022). Both miRNA sequencing and  
1087 subsequent PCR confirmed the up-regulation of 9 miRNAs (including miR-92a-3p, expressed at  
1088 a particularly high level) and down-regulation of 4 miRNAs (including miR-143-3p and miR-145-  
1089 5p) under oscillatory shear (Chung et al., 2022). In general, the differentially-expressed miRNAs  
1090 were related to genes involving vascularization/angiogenesis, cell migration, and inflammatory  
1091 responses (Chung et al., 2022). Indeed, the EVs formed under oscillatory shear were more  
1092 effective in promoting angiogenesis, HUVEC apoptosis, and expression of pro-inflammatory  
1093 adhesion molecules (ICAM-1, VCAM-1, and E-selectin) and genes *in vivo* and *in vitro*. It seems  
1094 that exosome-enriched EVs promote the same phenotypes as the shear stress under which  
1095 they were derived; for instance, EVs produced under oscillatory shear *abolish* shear-induced  
1096 activation of phosphoinositide 3-kinase (PI3K), protein kinase B (Akt), endothelial nitric oxide  
1097 synthase (eNOS), and ERK 1/2, while EVs produced under physiological shear uniquely  
1098 activate these same molecules, even in static culture conditions (Chung et al., 2022). Similar  
1099 bioactivity has been observed in exosomes derived from endothelial progenitor cells exposed to  
1100 (3.5 dyn/cm<sup>2</sup>) oscillatory shear stress (Li, L. et al., 2023). Specifically, these exosomes were  
1101 found to inhibit angiogenesis of endothelial progenitor cells *in vitro* and *in vivo*, promoting  
1102 endothelial-to-mesenchymal transition and accelerating pathological vascular remodeling via  
1103 delivery of circular RNA (circ-1199) cargo (the levels of which were enriched relative to those in  
1104 exosomes from static culture) (Li, L. et al., 2023).  
1105

1106 Numerous proteomic analyses have been performed on microparticle-enriched EVs derived  
1107 from VECs exposed to physiological (i.e., 5%) and supraphysiological (i.e., 15% to 18%) levels  
1108 of cyclic stretch, with EVs from each condition possessing highly unique protein cargo profiles  
1109 (Letsiou et al., 2015; Zhuang et al., 2020a; Zhuang et al., 2020b). Up-regulated EV proteins  
1110 under supraphysiological levels of stretch included antioxidants and cytoskeletal linkers—  
1111 including moesin, an actin-binding linker—as well as proteins involved in neutrophil  
1112 transmigration, actin cytoskeleton regulation, and VEC barrier function (Letsiou et al., 2015).  
1113 Proteins involved in acute lung injury (such as UCHL1) and associated with cardiovascular,  
1114 inflammatory, and lung diseases (such as glutathione S-transferase P1) were also unique to  
1115 EVs produced in this condition (Letsiou et al., 2015). CD151—necessary for Src activation in  
1116 VECs and subsequent inhibition of VEC apoptosis—was notably down-regulated in EVs from  
1117 highly-stretched culture (Zhuang et al., 2020a). Moreover, relative to EVs produced under  
1118 physiological stretch, both statically-derived EVs and EVs from highly-stretched culture appear  
1119 to be enriched in adhesion molecules ICAM-1 and VCAM-1 (Zhuang et al., 2020a; Zhuang et  
1120 al., 2020b). We also point out that no efforts have been made to document differences in RNA  
1121 loading among VEC EVs produced under cyclic stretch. In one unique study, the impact of  
1122 traumatic brain injury on brain microvascular endothelial cells was modeled with a one-time  
1123 (non-cyclic) biaxial stretch—lasting 1 s—of either 12% or 22% (Andrews et al., 2016). EV  
1124 samples from stretch-exposed cells were similarly enriched in ICAM-1, PECAM-1, and occludin  
1125 (a tight junction protein); however, it remains unclear whether this enrichment was the result of  
1126 higher total EV yields or protein up-regulation on a per-EV basis (Andrews et al., 2016).  
1127 Nevertheless, these findings suggest a role for EVs in trafficking disassembled tight junction  
1128 proteins and various inflammatory molecules away from the brain following traumatic injury  
1129 (Andrews et al., 2016).  
1130

1131 The behavior of VEC microparticles produced under cyclic stretch reflects their contents. VEC  
1132 microparticles derived under physiological stretch decrease inflammatory leukocyte-VEC  
1133 adhesion—a result of decreased ICAM-1 enrichment—relative to microparticles produced in

static culture (Zhuang et al., 2020b). On the other hand, VEC microparticles derived from highly-stretched parent cells promote anoikis (“to remove from home;” refers to programmed cell death induced upon cell detachment from the extracellular matrix) and apoptosis in target VECs via Src inhibition (Jia et al., 2017; Zhuang et al., 2020a). These microparticles are about 2.3-fold as efficient (compared to particles from physiologically-stretched parent cells) at binding to target VECs, likely due to their relative enrichment in adhesion molecules ICAM-1 and VCAM-1 (Zhuang et al., 2020a). However, they simultaneously increase Src activation in target SMCs, suggesting that the mechanism for Src stimulation may be largely dependent on cell type (Zhuang et al., 2020a). VEC microparticles produced under supraphysiological levels of stretch have also been reported to uniquely promote lung inflammation and injury in mice, probably as a result of mitogen-activated protein kinase (MAPK) activation (Letsiou et al., 2015). Notably, nothing is known about exosomes derived from cyclically-stretched VECs.

#### **4.6. Smooth muscle cells**

As noted previously, the SMCs comprising the blood vessels experience significant tensile stress as a result of blood pressure, yet are only exposed to shear in cases where VEC damage allows direct contact with blood flow. SMC EVs derived under conditions of supraphysiological tension (15-18% cyclic stretch) promote abnormal phenotypes in target VECs (Jia et al., 2017; Wang, L. et al., 2017). Specifically, these EV samples are enriched (by 5-fold) in miR-27a, which down-regulates G protein-coupled receptor kinase (GRK6) and promotes excessive VEC proliferation (Wang, L. et al., 2017). Notably, EVs produced under physiological tension (5% cyclic stretch) did not display these characteristics. SMC EVs derived under supraphysiological levels of tension have also been shown to promote the expression of inflammatory molecules (VCAM-1, ICAM-1, IL-6, and IL-1 $\beta$ ) on target VEC cells and induce subsequent anoikis (Jia et al., 2017). Similarly, shear stress—which only affects SMCs *in vivo* following disruption of the VEC barrier—has been found to promote the formation of uniquely procoagulant EVs from SMCs (Stampfuss et al., 2006). Specifically, increasing shear stress on parent SMCs from 0.1 to 15 dyn/cm<sup>2</sup> resulted in a log-linear increase in tissue factor (TF) enrichment and corresponding procoagulant activity in EV samples (Stampfuss et al., 2006). Clearly, non-physiological levels of mechanical stress promote the formation of SMC EVs with cargo capable of producing various related pathologies in target cells. It should additionally be noted that all of the described research was performed on microparticle-enriched samples. The impact of mechanical stress on SMC-derived exosomes remains unknown.

#### **4.7. Platelets and megakaryocytes**

As with VEC EV cargo, the cargo of platelet EVs exacerbates the pathology induced by the shear stress (or lack thereof) to which the parent cells were exposed. Supraphysiological levels of shear promote *in vitro* formation of uniquely procoagulant platelet EVs, though increased shear is correlated with increased procoagulant behavior even in physiological shear regimes (Chen et al., 2010; Reininger et al., 2006). Increased procoagulant activity of platelet MPs has likewise been observed *in vivo* following moderate physical exercise (90 min. on a bicycle ergometer) (Sosdorf et al., 2010, 2011). Moreover, platelets sampled from individuals engaged in strenuous physical exertion (graded exercise on a bicycle ergometer until exhaustion) and subsequently exposed to supraphysiological levels of shear *in vitro* possessed more procoagulant properties than platelets from resting individuals (Chen et al., 2010). This phenomenon is likely driven by a variety of selectively-loaded EV cargo. Shear stress promotes the formation of platelet EVs enriched in both coagulation factors—including factor V/Va (FV/Va), factor VIII (FVIII), and tissue factor (TF)—and exposed PS (the negative charge of which promotes the binding of coagulation factors) (Chen et al., 2010). Interestingly, however, EVs derived *in vitro* under supraphysiological levels of shear also display increased annexin V binding (relative to EVs produced via calcium ionophore) (Nomura et al., 2000), a generally

1185 anticoagulant phenomenon perhaps mediated by the presence of excess PS binding sites.  
1186 Platelets may also use EVs as a vehicle in which to dispose of excess adhesion molecules  
1187 responsible for pathological aggregation under excess shear stress. Levels of GPIb-IX-V, GPIIb-  
1188 IIIa, and P-selectin on the surfaces of platelet EVs were all up-regulated in a shear-dependent  
1189 manner for continuous *in vitro* stress of up to 70 dyn/cm<sup>2</sup> (Roka-Moia et al., 2021). Levels of  
1190 GPIb-IX-V and GPIIb-IIIa in parent platelets were simultaneously down-regulated, and  
1191 concentrations of all three molecules were higher on EV surfaces than on parent platelet  
1192 surfaces, suggesting selective loading (Roka-Moia et al., 2021). The shear-induced clustering  
1193 of adhesion molecules in lipid rafts is suggested as a possible mechanism for such loading  
1194 (Roka-Moia et al., 2021). Notably, pulsatile shear was relatively ineffective in enriching platelet  
1195 EVs in the aforementioned adhesion molecules; a minor increase in the per-EV level of GPIIb-  
1196 IIIa was observed, but failed to increase with shear magnitude (Roka-Moia et al., 2021). A  
1197 comparative proteomic analysis of platelet EVs produced *in vitro* via physiological shear stress  
1198 or thrombin stimulation found 26 differentially-expressed proteins, 15 of which were involved in  
1199 platelet activation and 21 of which were involved in cellular assembly, organization, and  
1200 morphology (Shai et al., 2012). The shear-induced up-regulation of integrin  $\alpha$ 6 and down-  
1201 regulation of DOK2—both pro-angiogenic proteins that modulate platelet activation and  
1202 endothelial cell function—were confirmed via western blotting (Shai et al., 2012).  
1203

1204 Almost nothing is known about mechanical stress-induced variation in Mk EV cargo, although  
1205 the ability of Mk-derived microparticles from static cultures to promote megakaryopoiesis is  
1206 dependent on transcription-independent p53-induced apoptosis (TIPA) in parent Mks, a process  
1207 which is notably up-regulated in Mks under shear (Luff et al., 2018). Given that the described  
1208 Mk microparticle bioactivity (the promotion of megakaryopoiesis) is largely informed by the  
1209 action of miR-486-5p and miR-22-3p (Kao et al., 2022), shear stress may prove a powerful tool  
1210 with which to regulate the miRNA cargo of Mk EVs. The impact of tension and compression on  
1211 platelet/Mk EV cargo has not been evaluated, likely due to the relative physiological irrelevance  
1212 of such stresses.  
1213

#### 1214 **4.8. Skeletal muscle cells**

1215 SkMC-derived EVs produced under mechanical stress are enriched in cargo that promotes  
1216 “healthy” phenotypes *in vivo*, likely reflecting the protective effects of physical exercise on  
1217 overall health. Levels of 18 different miRNAs are increased by at least 1.25-fold in SkMC EVs  
1218 produced under 6 dyn/cm<sup>2</sup> shear, with increases in miR-155-5p and miR-196a-5p likely  
1219 informing an anti-osteoclastic phenotype (Takafuji et al., 2021). Specifically, EVs produced  
1220 under shear more effectively suppressed RANKL-mediated osteoclast formation and  
1221 mitochondrial biogenesis (Takafuji et al., 2021). Similarly, EVs from SkMCs exposed to brief,  
1222 high-strain cyclic stretch (of 12-22% at 1 Hz for 24 h, with 50 min of rest for every 10 min  
1223 stretching) had reduced levels of 35 different miRNAs relative to EVs from low-strain or static  
1224 cultures (Mullen et al., 2022). No change in total protein content among EV samples was  
1225 observed in either of the noted studies (Mullen et al., 2022; Takafuji et al., 2021). SkMC EVs  
1226 produced under 25% cyclic stretch (at 1 Hz for 48 h) were particularly enriched in miR-1 (by 12-  
1227 fold after 24 h), with correspondingly diminished miR-1 levels observed in parent SkMCs  
1228 (Vechetti et al., 2021). This result was confirmed *in vivo* following resistance exercise in humans  
1229 and synergist ablation in a murine model (Vechetti et al., 2021). These miR-1-enriched EVs  
1230 were preferentially taken up by epididymal white adipose tissue, promoting lipolysis by targeting  
1231 *TFAP2A*, a repressor of  $\beta$ -adrenergic receptor expression (Vechetti et al., 2021). The  
1232 preferential uptake (by the adipose tissue) of EVs produced under cyclic stretch is likely due to  
1233 surface receptor changes on either the EVs or the target cells (Vechetti et al., 2021). Stress-  
1234 induced SkMC EVs may likewise be instrumental in informing myoblast phenotypes, as EVs  
1235 produced under sustained, low-strain cyclic stretch (of 15% at 1 Hz for 24 h) were relatively

1236 more effective at promoting myoblast proliferation and possessed a unique ability to mediate  
1237 myogenic differentiation (Mullen et al., 2022).

#### 1239 **4.9. Tumor cells**

1240 In general, higher levels of mechanical stress tend to bolster the carcinogenic and  
1241 immunosuppressive functions of tumor cell EVs. This suggests that elevated mechanical stress  
1242 associated with tumor growth (Stylianopoulos et al., 2013) may be a required trigger for the EV-  
1243 mediated survival and metastasis of cancer. Under 10 dyn/cm<sup>2</sup> shear stress, HeLa and MDA-  
1244 MB-231 cells load EVs with high levels of autophagosomes and autophagic vesicles as a  
1245 means of preventing autophagic tumor cell death (Wang, K. et al., 2019). Notably, this EV  
1246 loading is independent of autophagosome levels, occurring only when high shear promotes an  
1247 influx of intracellular Ca<sup>2+</sup> and the subsequent fusion of autophagic vesicles with MVBs (the  
1248 organelles responsible for exosome biogenesis) (Wang, K. et al., 2019). Lysosome marker  
1249 LAMP1 and autophagosome marker LC3-II are up-regulated by 15- and 3-fold, respectively, in  
1250 EVs produced under shear (Wang, K. et al., 2019). Moreover, insulin-like growth factor 2 (IGF2)  
1251 is up-regulated in EV samples derived from HepG2 (human liver cancer) cells under low (1.4  
1252 dyn/cm<sup>2</sup>) shear, and is responsible for an increase in PI3K/Akt-mediated activation of cancer-  
1253 associated fibroblasts (Feng, T. et al., 2022).

1254  
1255 Tumor-derived EVs produced under tension have similarly pronounced roles in carcinogenesis  
1256 and immunosuppression. 4T1.2 cells under uniaxial 10% cyclic stretch produced EV samples  
1257 relatively enriched in protein death-ligand 1 (PD-L1) and depleted of CD54; both proteins are  
1258 associated with immunosuppression/evasion and metastasis (Wang, Y. et al., 2020). The PD-L1  
1259 enrichment appears to be more significant than the CD54 depletion, however, as the EVs  
1260 produced under tension promoted more aggressive tumor growth in murine models, and were  
1261 more efficiently taken up by immunosuppressive M-MDSCs (myeloid-derived suppressor cells)  
1262 and recruited macrophages (though the reason for this is not investigated) (Wang, Y. et al.,  
1263 2020). MCF-7 (but not MDA-MB-231 or 4T1.2) cells under the same cyclic tension produced EV  
1264 samples higher in CD63 but lower in CD81; in this context, the function of these proteins is  
1265 unclear, but may be related to cargo loading generally (Wang, Y. et al., 2020). EVs from Hepa1-  
1266 6 (murine liver cancer) cells grown on stiff (as opposed to soft) substrates promoted more tumor  
1267 growth among target Hepa1-6 cells *in vivo*, likely via Notch signaling (Wu et al., 2023). Similarly,  
1268 EVs from LNCaP (prostate cancer) cells grown on stiff substrates were differentially enriched in  
1269 miRNAs implicated in cancer progression, and, likely as a result, were relatively more effective  
1270 in promoting the *in vitro* migration of LNCaP cells (Liu, Z. et al., 2022). MCF-7 and MDA-MB-231  
1271 (breast cancer) EVs grown on stiff hydrogel substrates were loaded with relatively higher levels  
1272 of the protein thrombospondin-1 (THBS1, associated with cancer metastasis) (Patwardhan et  
1273 al., 2021), while Ewing's sarcoma (SK-N-MC) EVs grown in a more complex tumor model with a  
1274 similarly stiff extracellular matrix were loaded with relatively higher levels of mRNA implicated in  
1275 EZH2-mediated tumor growth and cancer progression (Villasante et al., 2016). Given the  
1276 continuous variation of mechanical stress levels in the tumor microenvironment (Koomullil et al.,  
1277 2021), we suggest that the identity of EV cargo, like EV production, is a uniquely time-  
1278 dependent variable in the context of tumor cells *in vivo*. We also note, once again, that although  
1279 tumor-derived exosomes are well-studied, relatively little is known about the loading of tumor  
1280 microparticles under mechanical stress.

#### 1281 **4.10. Other mammalian cells**

1282 As was the case with mechanical stress-induced changes in EV biogenesis, stress-induced  
1283 differences in EV cargo loading have been observed among a variety of additional, less-studied  
1284 cell types. EVs released by both AT1R-expressing HEK293T cells under osmotic stretch and  
1285 mice with induced cardiac pressure overload were enriched in AT1R cargo (by roughly 18-fold

1287 and over 100-fold, respectively) relative to EVs from unstressed HEK293T cells and control  
1288 mice (Pironti et al., 2015). As a result of this enhanced AT1R loading—mediated by  $\beta$ -arrestin  
1289 2—EVs from stressed cells/mice increased ERK 1/2 phosphorylation in WT HEK293T cells and  
1290 reconstituted blood pressure in AT1R KO mice (Pironti et al., 2015). This instance of  
1291 biomechanical force-mediated cargo loading by cells engineered to overexpress said cargo is  
1292 unique in the literature and invites future investigation into the yet-unknown impacts of genetic  
1293 engineering on EV biology under biomechanical force. In another murine model of cardiac  
1294 pressure overload, serum samples from afflicted mice contained higher levels of miR-378, a  
1295 fibrosis inhibitor (Yuan et al., 2018). This suggests that supraphysiological levels of  
1296 biomechanical stress promote the formation of cardiomyocyte-derived EVs with higher levels of  
1297 anti-fibrotic cargo, though this finding may also be a result of higher EV yields overall, as miR-  
1298 378 levels were not characterized on a per-EV basis (Yuan et al., 2018). *In vitro*, however,  
1299 opposing factors were also at play: relative to EVs from static culture, neonatal rat  
1300 cardiomyocyte EVs exposed to 24 h of biaxial, 15% cyclic stretch were larger and contained  
1301 more than twice as much miR-494-3p, a known *promoter* of fibrosis (Tang et al., 2023). As a  
1302 result, these EVs were *more* effective in activating cardiac fibroblasts, a process mediated by  
1303 the miR-494-3p-induced inhibition of PTEN and subsequent activation of Akt, Smad, and ERK  
1304 signaling pathways (Tang et al., 2023). In another study, Schwann cells co-cultured with  
1305 magnetically-stimulated nanoparticles produced EVs with relatively higher miRNA levels (as a  
1306 fraction of the total RNA cargo) (Xia et al., 2020). Of the 20 miRNAs differentially expressed  
1307 between EVs from stimulated and unstimulated cultures, the five most up-regulated miRNAs in  
1308 the former EVs were all predicted to target the neuropilin 1 gene (*NRP1*) (Xia et al., 2020).  
1309 Indeed, this action was verified for the most significantly up-regulated miRNA—miR-23b-3p—  
1310 and it was further determined that the EVs derived from stimulated culture enhanced axonal  
1311 elongation *in vitro* and axonal regeneration *in vivo* due largely to the miR-23b-3p-mediated  
1312 inhibition of *NRP1* (Xia et al., 2020).  
1313

#### 1314 **4.11. General themes and trends**

1315 Clearly, type and quantity of mechanical stress are inextricably linked with the quality and  
1316 quantity of EV cargo. In nearly every case, significant differences exist in the RNA and  
1317 proteomic profiles of EVs produced under mechanical stress, even as EV size and morphology  
1318 remain generally consistent. **Figure 4** illustrates the nature of these differences—and their  
1319 clinical implications—in four cell types. In some cases, stress-induced EV production promotes  
1320 the loading of cargo that exerts pro-survival phenotypes in target cells (e.g., EVs from  
1321 mechanically-stressed MSCs promote desirable phenotypes in a variety of target cells, including  
1322 neurons and fibroblasts; EVs from mechanically-stressed VECs promote positive outcomes;  
1323 EVs from mechanically-stressed tumors drive subsequent tumor growth) or in the broader  
1324 organism (e.g., EVs from mechanically-stressed skeletal muscle trigger bone growth and  
1325 adipose tissue lipolysis). However, in other instances, significant mechanical stress serves to  
1326 induce pathological outcomes (e.g., EVs from mechanically-stressed platelets and SMCs  
1327 possess procoagulant and inflammatory properties). The mechanism by which mechanical  
1328 stress influences this loading is somewhat unclear, but depends to a large extent on the  
1329 physiological relevance of the stress in question. That is, with some notable exceptions,  
1330 “healthy” cells exposed to physiological levels of mechanical stress load EVs with pro-survival  
1331 cargo, which, upon delivery to target cells, assists in maintaining a “healthy” homeostasis.  
1332 Meanwhile, “unhealthy” cells exposed to non-physiological (i.e., pathological) levels of  
1333 mechanical stress selectively load EVs with inflammatory, apoptotic, or otherwise damaging  
1334 cargo, perhaps intending to rid themselves of dangerous proteins and RNAs. However, uptake  
1335 of these harmful EVs by target cells establishes a pathological phenotype as the new local  
1336 homeostasis. Still, exceptions to this rule exist; for instance, BEC EVs produced under  
1337 supraphysiological cyclic stretch exerted an anti-inflammatory phenotype in target macrophages

(Wang et al., 2022). As in the prior section of this review, investigations into EV cargo are limited by bodies of literature that exclusively examine either exosomes or microparticles (but not both) from a given cell type. We expect that in many cases, exosomes and microparticles from the same cell type may possess distinct cargo loading processes, perhaps even affecting opposing phenotypes in target cells as a means of maintaining homeostasis in response to stressful conditions. Nevertheless, this topic has strangely not yet been evaluated in the context of mechanical stimulation. Moreover, the diverse impact of mechanical stress on EV cargo suggests that common metrics for EV quantity—such as total protein content or surface receptor concentration—are inappropriate for comparing EV yields from static and agitated cultures. Finally, we again note that the impact of mechanical stress on EV cargo remains to be investigated in a wide variety of cell types, including erythrocytes, leukocytes, and, notably, megakaryocytes.

Notably, there is evidence that some EVs can ameliorate the impacts of mechanical stress on various non-parent cell types. For instance, exosome-enriched EVs from human MSCs were shown to attenuate cyclic stretch-induced oxidative stress and apoptosis in chondrocytes via miR-100-5p-mediated down-regulation of NADPH oxidase 4 (NOX4) (Li et al., 2021). In a second study, similar EV samples from murine MSCs reduced compression-induced apoptosis of nucleus pulposus cells (which generate energy through anaerobic glycolysis), alleviating mitochondrial damage and inhibiting oxidative stress (Hu et al., 2021). Adipose-derived EVs have likewise demonstrated a protective effect on murine pulmonary endothelial cells exposed to supraphysiological cyclic stretch, lowering intracellular  $\text{Ca}^{2+}$  levels by inhibiting transient receptor potential vanilloid 4 (TRPV4) (Yu et al., 2020). In each of the three described studies, the EVs in question were derived from static cultures; effects of similar EVs from mechanically-stressed cultures have not been investigated. Collectively, such findings complicate EV biomanufacturing. After all, if certain EVs serve to modulate cellular sensitivity to mechanical stress, we suspect that local EV concentration—a time-dependent variable—inform subsequent EV biogenesis and loading in stressed cultures. In other words, the response of an EV parent cell to mechanical stress may be modulated by the quantity and cargo of already-released EVs near the cell surface. This transient nature of EV quality is illustrated in **Figure 5**.

## **5. Impact of biomechanical forces on EV uptake and cargo delivery**

The impact of biomechanical force on EV uptake and delivery, a subject of relatively less study, remains just as integral to a full understanding of EV behavior. EV uptake occurs in three steps: collision, adhesion, and internalization. First, a cell-EV collision must provide the necessary membrane contact for subsequent binding. Thereafter, cell-EV adhesion proceeds via the coupling of appropriate membrane proteins. Finally, endocytosis (for smaller EVs) or membrane fusion (for larger EVs) facilitates EV internalization. Both *in vivo* and *in vitro*, biomechanical forces influence each of these three steps. **Figure 6** summarizes the impacts of biomechanical force on EV uptake by target cells.

### ***5.1. Impact of biomechanical forces on cell-EV collision and adhesion***

By its nature, biomechanical force-induced fluid mixing will increase cell-EV collision probability. However, the strong flow inherent in many forms of shear will also naturally decrease the residence time of EVs or other particles on or near the target cell membrane, inhibiting adhesion and preventing uptake (Chen, Y.Y. et al., 2020; Karami et al., 2022). Moreover, as discussed previously, EV biogenesis is nearly always accelerated under mechanical stress. Often, such increased biogenesis correlates with increased delivery to other cells in culture or *in vivo* by increasing EV concentration and facilitating faster EV motion, thereby enhancing the likelihood of cell-EV contact (Koomullil et al., 2021). Specific cellular protein receptors required for EV

1388 binding may also be up- or down-regulated by mechanical stress of any kind on a case-by-case  
1389 basis, subsequently mediating cell-EV adhesion (Chappell et al., 1998; Letsiou et al., 2015).  
1390

### 1391 **5.2. Impact of biomechanical forces on EV internalization**

1392 The same processes responsible for small EV (i.e., exosome) release and uptake—namely,  
1393 exocytosis and endocytosis—also help mediate mechanical stress on the plasma membrane.  
1394 Importantly, these processes are also a major mechanism by which biomechanical forces  
1395 regulate EV internalization. Membrane fusion—which facilitates the internalization of  
1396 predominantly larger EVs—may serve a similar function, though published research in this  
1397 regard is scarce.

1398 During the application of tensile stress, exocytosis and endocytosis are often up-regulated and  
1399 down-regulated, respectively, as a means of easing membrane tension (Apodaca, 2002; Le  
1400 Roux et al., 2019). In particular, tension blocks the polymerization of clathrin (Kaksonen and  
1401 Roux, 2018) and results in the compensatory disassembly of caveolae (Sinha et al., 2011). Both  
1402 clathrin- and caveolin-mediated endocytosis are heavily implicated in (primarily small) EV  
1403 internalization (Ratajczak and Ratajczak, 2020). In some cases, however, endocytotic rates may  
1404 increase during tension to compensate for excess exocytosis (Apodaca, 2002). This allows an  
1405 equilibrium membrane tension to be sustained and may make endocytosis relatively more  
1406 common in cells that have been well-adapted to cyclic stretch or other tensile force (as opposed  
1407 to naïve cells). Similarly, endocytosis rates generally increase under compression, as the  
1408 plasma membrane suddenly develops an excess of invaginations which must be reduced  
1409 (Apodaca, 2002; Le Roux et al., 2019). Mechanical force broadly can also trigger rearrangement  
1410 of actin in the cytoskeleton, recruiting it to form stress fibers as a means to stabilize the cell in  
1411 response to chronic stress (Bhowmick et al., 2012; Han et al., 2012). Such a phenomenon  
1412 results in lessened actin availability for modulation of plasma membrane deformation during  
1413 endocytosis (Bhowmick et al., 2012; Han et al., 2012).

1414  
1415 Shear stress increases the disorder and fluidity of the plasma membrane, though its generalized  
1416 impact on exocytosis and/or endocytosis is less apparent (Le Roux et al., 2019). Actin  
1417 recruitment to stress fibers will again down-regulate endocytosis (Bhowmick et al., 2012; Han et  
1418 al., 2012). In one study of HUVECs and HepG2 cells, however, shear stress was shown to  
1419 enhance caveolin-dependent (but not clathrin-dependent) endocytosis (He, Z. et al., 2018). In  
1420 another study, clathrin- and dynamin-dependent endocytosis were enhanced in kidney proximal  
1421 tubule cells exposed to shear (though caveolin-dependent endocytosis does not occur in this  
1422 cell type) (Raghavan et al., 2014).

1423  
1424 Cell cycle phase—itself modulated by mechanical stress—may also play an unappreciated role  
1425 in the internalization of bound EVs. Generally speaking, endocytosis is almost completely  
1426 inhibited during early mitosis (Fielding and Royle, 2013). In one study, however, prostate cancer  
1427 cells in the G<sub>2</sub>/M phase of the cell cycle were relatively *more* likely to take up their own EVs  
1428 (Lazaro-Ibanez et al., 2017). Given that tumor cell cycle arrest in those same phases has been  
1429 observed following shear application *in vitro* (Chang et al., 2008; Lee et al., 2018), shear-  
1430 mediated cell cycle regulation presents as an additional possible mechanism governing EV  
1431 internalization, though the impacts of shear on cycle phase distribution differ with cell type  
1432 (Lakhotia et al., 1992; Lin et al., 2000).

1433  
1434 The role of the membrane fusion internalization pathway—and its susceptibility to mechanical  
1435 stress—is not well-understood. Given the importance of this particular internalization pathway to  
1436 EV-induced phenotypic change in target cells (Ratajczak and Ratajczak, 2020), this is a topic in  
1437 need of immediate attention. The ability of fused EVs to extend the plasma membrane suggests

1439 that membrane fusion, unlike endocytosis, may be up-regulated under tension as a mechanism  
1440 of stress alleviation.

### 1441 1442 **5.3. Examples from published research**

1443 The multitude of factors described above suggests that the specific effects of biomechanical  
1444 force on EV uptake are deeply situation-dependent. Numerous studies relating cyclic stretch to  
1445 protein or synthetic nanoparticle uptake have been decidedly inconclusive, with uptake  
1446 increasing (Doryab et al., 2021; Doryab et al., 2020; Hu and Liu, 2015; Huh et al., 2010; Rouse  
1447 et al., 2008; Yu, W. et al., 2021), decreasing (Freese et al., 2014; Tsai et al., 2022), or  
1448 remaining unchanged (Freese et al., 2017; Schmitz et al., 2019) depending on the nature and  
1449 concentration of the proteins/nanoparticles, the type of implicated target cells, and the  
1450 characteristics of the cyclic stretch. The synthesis of existing literature relating protein and  
1451 synthetic nanoparticle uptake under shear is just as inconclusive (Godoy-Gallardo et al., 2015);  
1452 shear has been regularly found to both promote (Han et al., 2015; He, Z. et al., 2018; Lawler et  
1453 al., 2009; Raghavan et al., 2014; Samuel et al., 2012) and inhibit (Bhowmick et al., 2012; Chen,  
1454 Y.Y. et al., 2020; Lin et al., 2010; Nguyen et al., 2009) uptake of proteins and nanoparticles. In  
1455 at least one case involving endothelial cells, lower shear magnitude promoted protein  
1456 endocytosis (relative to static conditions) and higher such magnitude *inhibited* it (Ueda et al.,  
1457 2004). Increases in protein/nanoparticle uptake induced by shear exposure may also be  
1458 reversed following the cessation of stress (Raghavan et al., 2014), a phenomenon similarly  
1459 observed for tension induced by cyclic stretch (Hu and Liu, 2015).

1460 The only EV-specific research on EV delivery under tension and/or compression involves the  
1461 adhesion of platelet microparticles to vascular smooth muscle cells, which is increased under  
1462 supraphysiological levels (15%) of cyclic stretch relative to physiological levels (5%) of cyclic  
1463 stretch (Chen, Y. et al., 2020). We have also found two studies examining EV binding and/or  
1464 uptake under conditions of shear stress, both of which concern VECs (Gomez et al., 2020; Qin  
1465 et al., 2022). Specifically, both adhesion of neutrophil-derived EVs (Gomez et al., 2020) and  
1466 uptake of erythrocyte-derived EVs (Qin et al., 2022) were found to increase under conditions of  
1467 low and/or oscillatory (i.e., atheroprone) shear. Such flow promotes an increase in oxidative  
1468 stress (Qin et al., 2022), which in turn serves to up-regulate various surface receptors—such as  
1469 VCAM-1, ICAM-1, and E-selectin—on the target cells (Chappell et al., 1998). In particular,  
1470 ICAM-1 likely serves to bind with CD18 present on neutrophil EVs (Gomez et al., 2020).  
1471 Expression of VCAM-1 and ICAM-1 on VEC EVs was likewise up-regulated under oscillatory  
1472 shear (Chung et al., 2022), demonstrating that EV characteristics—including those modulated  
1473 by flow—may also impact EV uptake, though a discussion of such characteristics is better  
1474 suited to the previous section of this review. Still, one other example of note involves exosomes  
1475 derived from MSCs and passively loaded with siRNA via simple co-incubation (1 h at 37°C).  
1476 When produced in agitated microcarrier cultures, these exosomes were significantly more likely  
1477 to be taken up by target neurons (Haraszti et al., 2018). Similar phenomena have been  
1478 described in other publications (Huang et al., 2022; Vechetti et al., 2021; Wang, Y. et al., 2020;  
1479 Xie et al., 2020). Proteins enriched in EVs produced under biomechanical force may promote  
1480 EV binding to target cell ligands, facilitate endocytosis, or simplify intracellular processing. In  
1481 general, EV characteristics, discussed in detail previously, go hand-in-hand with cellular  
1482 characteristics in determining the frequency and nature of EV uptake, though a lack of EV-  
1483 specific research renders the impact of mechanical stress on EV uptake an area ripe for future  
1484 study. Regarding EV delivery specifically, the only conclusion currently available is that non-  
1485 physiological (i.e., pathological) levels of mechanical stress increase EV uptake, though such a  
1486 finding incorporates only three studies and two cell types (Chen, Y. et al., 2020; Gomez et al.,  
1487 2020; Qin et al., 2022).

1490 **6. Do biomechanical forces affect and complicate EV isolation and purification?**

1491 The role of biomechanical forces in impacting EV characteristics and biological efficacy does not  
1492 cease at harvest. Most EV collection and isolation methods involve some form of biomechanical  
1493 stress applied to EVs. The extent of the effects on EVs will largely depend on the nature of the  
1494 surrounding medium and the properties of the cell/EV type(s) in question. Both theoretical and  
1495 experimental work *in vivo* has demonstrated an increase in EV counts resulting from the shear  
1496 of needle-based sampling on red blood cells (Stukelj et al., 2017). Ultracentrifugation, a  
1497 standard lab-scale isolation technique, has likewise been shown to deform and even fragment  
1498 existing EVs, creating significant new, distinct EV populations as a result (Božič et al., 2020;  
1499 Stukelj et al., 2017; Sustar et al., 2011). Cells and EVs experience very high levels of shear due  
1500 to friction with tube walls during centrifugation and ultracentrifugation, a phenomenon  
1501 exacerbated by the higher viscosities observed at low temperatures (Božič et al., 2020; Stukelj  
1502 et al., 2017; Sustar et al., 2011). In fact, current work suggests that the *majority* of EVs isolated  
1503 from blood using common protocols may be generated during harvest and centrifugation via  
1504 shear-induced stimulation of cells and fragmentation of EVs (Stukelj et al., 2017; Sustar et al.,  
1505 2011). At very high speeds (100,000 g) and for long centrifugation times (8 h), cargo may even  
1506 leak through EV membranes (Božič et al., 2020). Although the impact of biomechanical force  
1507 applied during “dead-end” ultrafiltration has not been evaluated in the context of EV production,  
1508 the involvement of significant shear stress—intensified by membrane fouling—nonetheless  
1509 gives cause for concern (Gagnon et al., 2020; Li et al., 2019). Tangential flow filtration, a  
1510 uniquely scalable isolation method with relatively high EV yields (Busatto et al., 2018; Kim et al.,  
1511 2021; McNamara et al., 2018), also involves significant biomechanical stresses (Vickroy et al.,  
1512 2007; Wang, S. et al., 2017), though the impact of such stresses on EV properties and  
1513 biological efficacy have not been investigated. Indeed, among current scalable EV isolation  
1514 techniques, only EV precipitation (e.g., with polyethylene glycol) and chromatography appear to  
1515 avoid significant mechanical stressors that could damage cell/EV membranes or alter EV  
1516 quantity and quality (Gagnon et al., 2020; Li et al., 2019; Staubach et al., 2021). It should be  
1517 noted that much of the aforementioned research (Božič et al., 2020; Stukelj et al., 2017; Sustar  
1518 et al., 2011) has been conducted exclusively on blood samples and the EVs therein; future work  
1519 must expand the scope of the findings to different cell types. In the studies above, as in many,  
1520 “shear” may be used as an umbrella term under which non-shear forces are unwittingly  
1521 included, but not mentioned. Contributions of extensional flow to the overall mechanical force  
1522 exerted by needle-based sampling may be particularly important, due to rapid contraction of the  
1523 flow field (Foster et al., 2021). Likewise, during ultracentrifugation, hefty compressive forces on  
1524 EV pellets are likely partly determinative of EV quantities and properties.

1525 Excess debris resulting from biomechanical forces during EV generation and isolation may also  
1526 pose a significant issue for EV sample purity. Several studies have suggested that cellular  
1527 debris levels are correlated with increased mechanical stresses during EV preparation, though  
1528 whether this debris release is intentional or not on the part of the parent cells is unclear (Piffoux  
1529 et al., 2017). The risk of co-isolating debris and EVs is therefore a significant concern, especially  
1530 for more forceful, extrusion-based production methods (Piffoux et al., 2017). In agitated  
1531 bioreactors, the presence of debris in EV samples has not yet been evaluated, except in the  
1532 context of protein contamination, where data conflict (de Almeida Fuzeta et al., 2020; Haraszti  
1533 et al., 2018).

1535 **7. Considerations for the scale-up of EV production**

1536 Given the high EV doses required for clinical applications (Gupta et al., 2021), scaled EV  
1537 production will almost certainly require mechanical agitation to attain clinical relevance (Colao et  
1538 al., 2018; Gobin et al., 2021; Grangier et al., 2021; Paganini et al., 2019; Staubach et al., 2021).  
1539 As EV technology remains in its infancy from a commercial perspective, however, few scale-up

1541 studies have been published. Production schemes employing Good Manufacturing Practices  
1542 (GMPs) have been developed at the lab scale, but either rely entirely on static culture or fail to  
1543 consider the role of mechanical agitation as a significant driver of EV quantity and quality  
1544 (Andriolo et al., 2018; Gobin et al., 2021; Mendt et al., 2018; Watson et al., 2018). To date, lab-  
1545 scale research into EV production in stirred/aerated tank bioreactors has been limited.  
1546

### 1547 **7.1. EV production in stirred/aerated tank bioreactors**

1548 Thanks to a tremendous accumulation of empirical knowledge regarding design and scale-up  
1549 (Chalmers and Ma, 2015), stirred/aerated tank bioreactors are likely the most practical and  
1550 preferred option for industrial-scale EV manufacturing. For suspension cells or adherent cells  
1551 bound to microcarriers, culture in these tanks offers large-scale production capacity and a  
1552 relatively homogenous culture environment with respect to nutrient, oxygen, and pH gradients  
1553 (Tsai et al., 2020). However, these reactors are in fact quite heterogeneous where mechanical  
1554 stress distribution is concerned. Turbulence predominates, meaning Kolmogorov eddies induce  
1555 constant, random variation in flow (Papoutsakis, 1991). Where microcarriers are present, these  
1556 eddies—even large eddies produced under relatively mild stirring or sparging—and microcarrier  
1557 collisions combine to induce significant cell damage (Cherry and Papoutsakis, 1988; Cherry and  
1558 Papoutsakis, 1989; Chisti, 2001; Croughan et al., 1987; Papoutsakis, 1991). For smaller  
1559 suspension cells, however, cell damage is most often the result of biomechanical stress  
1560 imposed by bubble breakup at the bulk gas-liquid interface (Chisti, 2001; Kunas and  
1561 Papoutsakis, 1990; Papoutsakis, 1991). For a given bioreactor, it seems likely that the  
1562 phenomena governing cell damage will also have the most significant impact on EV biology,  
1563 though this hypothesis remains to be investigated. Importantly, however, we expect that even  
1564 mild, sublethal mechanical stressors will influence EV biology to some degree, given the extent  
1565 to which such stressors have been shown to modify cellular metabolism, intracellular protein  
1566 and nucleic acid levels, cell cycle phase distribution, specific productivity, and mAb  
1567 glycosylation, even as cells remain “undamaged” with respect to viability and proliferative  
1568 capacity (Chalmers and Ma, 2015; Chisti, 2001; Papoutsakis, 1991). Even microcarrier  
1569 curvature—which dictates the shape of cells’ projected area—may impact EV production, with  
1570 cells adhered to smaller microcarriers experiencing greater mechanical force (Tsai et al., 2020).  
1571

1572 To date, lab-scale EV production in stirred/aerated tanks has been demonstrated for both  
1573 suspension cells—notably, CHO (Keysberg et al., 2021), THP-1, HeLa, and Raji cells (Grangier  
1574 et al., 2020)—and microcarrier-bound adherent cells, including human HUVECs (Gazeau et al.,  
1575 2020) and MSCs (Adlerz et al., 2019; de Almeida Fuzeta et al., 2020; Gazeau et al., 2020;  
1576 Haraszti et al., 2018; Jarmalavičiūtė et al., 2015) and murine MSCs (Berger et al., 2021;  
1577 Gazeau et al., 2020; Pinto et al., 2021). Relative to static cultures, EV yield in these production  
1578 schemes has increased by as much as 20-fold (for a 48 h culture of microcarrier-bound MSCs)  
1579 (Haraszti et al., 2018) and as little as 3-fold (for a 48 h culture of microcarrier-bound MSCs  
1580 agitated with a gentle “Vertical-Wheel” impeller) (de Almeida Fuzeta et al., 2020). Bioreactor-  
1581 derived EVs also possessed consistently distinct proteomic profiles, though their relative purity  
1582 varied between studies (de Almeida Fuzeta et al., 2020; Haraszti et al., 2018). In two instances,  
1583 bioreactor-derived EVs demonstrated desirable bioactivity (with respect to target cells) not  
1584 observed in EVs from static cultures (Haraszti et al., 2018; Jarmalavičiūtė et al., 2015). Similar  
1585 results have been observed in other types of bioreactors that impose biomechanical force. For  
1586 instance, a seesaw-motion bioreactor yielded a nearly 2-fold increase in daily EV production  
1587 from natural killer cells without impacting EV morphology, structure, or bioactivity (though  
1588 differences in protein cargo were noted) (Wu et al., 2022). Various flow-perfusion bioreactors  
1589 have also demonstrated dramatically increased EV yields for a variety of cell types, even after  
1590 controlling for the architecture of cell scaffolds (Guo et al., 2021; Patel et al., 2019). It remains  
1591 difficult to fully attribute the aforementioned instances of differential EV biology to mechanical

1592 stress, as growing cells on microcarriers or other various scaffolds can independently alter—and  
1593 often improve—various EV production metrics, even in static conditions (Cha et al., 2018; Kim  
1594 et al., 2018; Patel et al., 2019; Yang et al., 2020; Zhang et al., 2017). Still, the innumerable lab-  
1595 scale studies cited throughout this review attest to the crucial contributions of culture agitation to  
1596 EV quantity and quality.

## 1598 **7.2. Mixing characteristics for scalable EV production**

1599 Some research into microcarrier-based EV production has begun using the Kolmogorov eddy  
1600 length scale as a characteristic value with which to describe, compare, and scale  
1601 stirred/aerated-tank cultures (Berger et al., 2021; Gazeau et al., 2020; Pinto et al., 2021). EV  
1602 production by HUVECs and human/murine MSCs seeded on ~200  $\mu\text{m}$  microcarriers was found  
1603 to accelerate markedly for eddy length scales below 50  $\mu\text{m}$ , with the most substantial increases  
1604 beginning consistently in the 30–40  $\mu\text{m}$  range (Gazeau et al., 2020). Recently, this technique  
1605 has also been applied to suspension cells: EV production by monocytic cell line THP-1  
1606 underwent a 10-fold increase after 72 h of agitation with an eddy length scale less than 30  $\mu\text{m}$   
1607 (Grangier et al., 2020). No product quality differential was noted, though testing was not  
1608 comprehensive in this regard. Given the lack of a full paper in this instance, it remains unclear  
1609 how researchers accounted for the significant stress imposed by bubble entrainment and  
1610 breakup, which is far more impactful than eddies for suspension cells in a stirred/aerated tank  
1611 (Kunas and Papoutsakis, 1990; Papoutsakis, 1991).

1612 In most of the aforementioned publications, the role of mechanical agitation, while noted, has  
1613 not been rigorously documented or optimized. Rather, most studies simply confirm that  
1614 biomechanical force broadly has boosted EV yields relative to static cultures, with no mention of  
1615 the impact of particular subcategories of stress (e.g., shear, tension, or compression). Of  
1616 paramount importance for industrial- and clinical-scale EV production, then, is the establishment  
1617 of rigorous correlations—applicable even in turbulence—between mechanical agitation and the  
1618 quality and quantity of the resulting EVs. As noted, the Kolmogorov eddy length scale is gaining  
1619 attention as a characteristic parameter with which to define EV production across various cell  
1620 types and reactor geometries (Berger et al., 2021; Gazeau et al., 2020; Grangier et al., 2020).  
1621 Many other possible such quantities—including average or maximum shear rate (Chisti, 2001;  
1622 Garcia-Briones and Chalmers, 1994), impeller speed (Chisti, 2001; Garcia-Briones and  
1623 Chalmers, 1994), integrated shear factor (Chisti, 2001; Croughan et al., 1987; Garcia-Briones  
1624 and Chalmers, 1994), turbulent collision severity (Cherry and Papoutsakis, 1989), frequency of  
1625 bubble production or rupture (Czermak et al., 2009; Garcia-Briones and Chalmers, 1994), and  
1626 mean energy dissipation rate (mathematically dependent on the Kolmogorov eddy length scale)  
1627 (Chalmers and Ma, 2015; Czermak et al., 2009; Garcia-Briones and Chalmers, 1994) remain  
1628 unexplored. More complex parameters have also been proposed (Garcia-Briones and  
1629 Chalmers, 1994). Employing many of these quantities could be problematic, however. For  
1630 instance, mean energy dissipation rate does not always scale with shear stress, possibly  
1631 explaining why shear effects on cells are less pronounced in industrial-scale operations  
1632 (Czermak et al., 2009; Henzler and Kauling, 1993; Nienow, 2006). Use of the Kolmogorov eddy  
1633 length scale also breaks down at scales of production beyond ~1 to 2 L, given the uncertainty in  
1634 estimating the mean energy dissipation rate (Garcia-Briones and Chalmers, 1994; Gregoriades  
1635 et al., 2000). Values that depend on reactor geometry—and not intrinsic characteristics of the  
1636 flow—are likewise ineffective, a conclusion that implicates impeller speed and the integrated  
1637 shear factor (Garcia-Briones and Chalmers, 1994). All the proposed parameters are  
1638 independent of cell type, which we have highlighted previously as a crucial variable in EV  
1639 production. Any chosen parameter must also describe the impact of transient mechanical stress  
1640 application; after all, cells in most bioreactors are not exposed to “average” forces, but local,  
1641 temporary extremes, which may differently impact EV biology (Garcia-Briones and Chalmers,  
1642

1643 1994; Gregoriades et al., 2000; Holme et al., 1997; Roka-Moia et al., 2021; Sakariassen et al.,  
1644 1998). Currently, and with all this in mind, it appears unlikely that any common characteristic  
1645 value will be sufficient to account for the effect of mechanical stress on cellular phenotype  
1646 across all bioreactor geometries and/or cell types (Freiberger et al., 2022). Thus, any broad  
1647 correlation of EV quantity/quality with generalized flow characteristics may be doomed to the  
1648 realm of academic curiosity. Absent precise scale-up on a reactor-by-reactor basis, tailored to  
1649 each individual cell type of interest, computational fluid dynamics will surely be required for  
1650 industrial EV production (Freiberger et al., 2022; Gregoriades et al., 2000).

### 1652 **7.3. Shear sensitivity and EV product quality**

1653 Complicating the situation is the concept of “shear sensitivity,” in which previous exposure to  
1654 shear, culture age, and changes in pH can all modulate the cellular response to mechanical  
1655 stress (Petersen et al., 1988)—and with it, EV biogenesis and uptake. The nature of the factors  
1656 informing shear sensitivity suggests that process control for EV manufacturing must account for  
1657 time-dependent variation in the impact of agitation (illustrated previously in **Figure 5**). The  
1658 ramifications of shear protectants such as Pluronic F-68—commonplace in industry but  
1659 unexplored in the context of EV production—are another topic requiring investigation (Chalmers  
1660 and Ma, 2015; Chisti, 2001; Thomas, 1993). Specifically, the reduced plasma membrane fluidity  
1661 induced by many shear protectants (Czermak et al., 2009) may interfere with the exocytosis,  
1662 membrane blebbing, and endocytosis required for exosome release, microparticle release, and  
1663 EV uptake, respectively.

## 1664 **8. Future directions**

1665 The intersection of biomechanical stress and EV biology offers multiple avenues for continued  
1666 exploration. In this context, numerous parent cell varieties—including leukocytes and  
1667 erythrocytes—remain almost entirely unexplored, while in other cases, either exosomes (e.g.,  
1668 from MSCs, fibroblasts, and tumors) or microparticles (e.g., from platelets) have been examined  
1669 exclusively, without regard for the other EV subtype. Detailed investigation into said subtypes is  
1670 particularly important given the degree to which mechanical stress may differently mediate their  
1671 loading and release, a phenomenon most apparent in VECs. Additionally, despite basic  
1672 characterization of EV cargo loading under mechanical stress, the cellular mechanisms  
1673 implicated in said loading are almost entirely unexplored. The impact of mechanical stress on  
1674 EV uptake is likewise poorly understood, with most of the relevant existing literature failing to  
1675 fully differentiate between EV collision with, adhesion to, and internalization by the target cell(s).  
1676 In this respect, internalization via membrane fusion is in particular need of study. Nevertheless,  
1677 the massive, ongoing exchange of EVs *in vitro* and *in vivo* can rapidly and continually alter  
1678 cellular phenotypes, a phenomenon we suggest is substantially influenced by mechanical  
1679 stress. In sum, although the eventual relevance of this research involves EV production in  
1680 scalable, complex bioreactors, there remains an urgent need for fundamental research into the  
1681 distinct impacts of isolated shear/tensile/compressive forces on EV biology.

1682 EV glycosylation is now recognized as a key factor influencing EV biogenesis, cargo loading,  
1683 uptake, and bioactivity (Harada et al., 2021; Macedo-da-Silva et al., 2021; Martins et al., 2021;  
1684 Williams et al., 2018). While no published data have yet linked biomechanical force on parent  
1685 cells to differential glycosylation in EVs, such force is a known mediator of glycosylation in a  
1686 variety of cell types, including platelets (Nowak et al., 2012) and CHO cells (Senger and Karim,  
1687 2003). Indeed, EV isolation method has already been linked to differential EV protein  
1688 glycosylation, though the mechanisms underlying this phenomenon are unclear (Freitas et al.,  
1689 2019). With this in mind, we hypothesize that the impact of biomechanical stress on EV protein  
1690 glycosylation is substantial and just as deserving of future study as stress-induced variation in

1693 protein and miRNA cargo. Heterogeneous glycosylation in EV samples—whether a result of  
1694 biomechanical force or other factors—will hinder clinical implementation of EV technology.  
1695

1696 We also note a significant dearth of research into the impacts of biomechanical forces on EVs  
1697 from genetically engineered cells. Although Pironti et al. observed increased loading (into EVs)  
1698 of overexpressed AT1R cargo following the application of high osmotic stress to HEK293T cells  
1699 (Pironti et al., 2015), whether such a phenomenon would be similarly observed for other  
1700 overexpressed biomolecules or in other cells is unclear. Genetic engineering that specifically  
1701 targets EV biogenesis, cargo loading, and uptake pathways is particularly intriguing: such  
1702 methods may provide a path to modulate the impact of biomechanical force on EV biology and  
1703 thereby remedy some of the quality control issues inherent in EV biomanufacturing, though no  
1704 specific research yet supports this hypothesis.  
1705

1706 As fundamental research continues to expand our basic knowledge, it is increasingly desirable  
1707 to transfer our findings to the complex flows in laboratory and industrial-scale bioreactors, where  
1708 individual forces cannot be easily isolated outside of computational fluid dynamics. EV quantity  
1709 and quality must be correlated with reactor-independent flow characteristics on a cell-by-cell  
1710 basis. At the same time, the impact of common media additives—such as shear protectants—  
1711 and processing steps—such as EV isolation—on EV biology must be rigorously monitored.  
1712 Notably, we suggest that any quality control efforts for EV production must additionally account  
1713 for the time-dependent nature of cellular responses to mechanical stress (illustrated previously  
1714 in **Figure 5**). That is, as cultures grow and age and EV exchange proceeds, cells may become  
1715 more or less sensitive to stress and respond by altering their EV output, creating a time-  
1716 dependent differential in EV product quality. With respect to EVs, however, research on these  
1717 topics is almost nonexistent. Nevertheless, as the field of EV research expands and breaches  
1718 the gates of clinical relevance, we ignore the impacts of mechanical stress on EV biology at our  
1719 own peril.  
1720

## 1721 **Funding**

1722 This work was supported by the US National Science Foundation (grant number CBET-  
1723 1804741) and by a GAANN Fellowship (WT) funded by the US Department of Education (grant  
1724 number P200A210065).  
1725

## 1726 **CRedit authorship contribution statement**

1727 **Will Thompson**: conceptualization, writing - original draft, writing - review & editing. **Eleftherios**  
1728 **Terry Papoutsakis**: conceptualization, funding acquisition, writing - review & editing,  
1729 supervision.  
1730

## 1731 **Declaration of competing interest**

1732 The authors declare no conflicts of interest.  
1733

## 1734 **Data availability**

1735 No data were produced for the preparation of this manuscript.  
1736  
1737  
1738  
1739  
1740

## 1741 **References**

1743 Abid Hussein, M.N., Boing, A.N., Sturk, A., Hau, C.M., Nieuwland, R., 2007. Inhibition of  
1744 microparticle release triggers endothelial cell apoptosis and detachment. *Thromb Haemost*  
1745 98(5), 1096-1107.

1746 Adlerz, K., Trempel, M., Wang, D., Kirian, R.D., Rowley, J.A., Ahsan, T., 2019. Comparison of  
1747 msc-evs manufactured in 2D versus scalable 3D bioreactor systems. *Cyotherapy* 21(5), S58.

1748 Akerman, A.W., Blanding, W.M., Stroud, R.E., Nadeau, E.K., Mukherjee, R., Ruddy, J.M., Zile,  
1749 M.R., Ikonomidis, J.S., Jones, J.A., 2019. Elevated Wall Tension Leads to Reduced miR-133a  
1750 in the Thoracic Aorta by Exosome Release. *J Am Heart Assoc* 8(1), e010332.

1751 Ambattu, L.A., Ramesan, S., Dekiwadia, C., Hanssen, E., Li, H., Yeo, L.Y., 2020. High  
1752 frequency acoustic cell stimulation promotes exosome generation regulated by a calcium-  
1753 dependent mechanism. *Commun Biol* 3(1), 553.

1754 Anand, S., Samuel, M., Kumar, S., Mathivanan, S., 2019. Ticket to a bubble ride: Cargo sorting  
1755 into exosomes and extracellular vesicles. *BBA - Proteins and Proteomics*.

1756 Andrews, A.M., Lutton, E.M., Merkel, S.F., Razmpour, R., Ramirez, S.H., 2016. Mechanical  
1757 Injury Induces Brain Endothelial-Derived Microvesicle Release: Implications for Cerebral  
1758 Vascular Injury during Traumatic Brain Injury. *Front Cell Neurosci* 10, 43.

1759 Andriolo, G., Provasi, E., Lo Cicero, V., Brambilla, A., Soncin, S., Torre, T., Milano, G., Biemmi,  
1760 V., Vassalli, G., Turchetto, L., Barile, L., Radrizzani, M., 2018. Exosomes From Human Cardiac  
1761 Progenitor Cells for Therapeutic Applications: Development of a GMP-Grade Manufacturing  
1762 Method. *Front Physiol* 9, 1169.

1763 Apodaca, G., 2002. Modulation of membrane traffic by mechanical stimuli. *American Journal of  
1764 Physiology-Renal Physiology* 282(2), F179-F190.

1765 Baietti, M.F., Zhang, Z., Mortier, E., Melchior, A., Degeest, G., Geeraerts, A., Ivarsson, Y.,  
1766 Depoortere, F., Coomans, C., Vermeiren, E., Zimmermann, P., David, G., 2012. Syndecan-  
1767 syntenin-ALIX regulates the biogenesis of exosomes. *Nat Cell Biol* 14(7), 677-685.

1768 Ballermann, B.J., Dardik, A., Eng, E., Liu, A., 1998. Shear stress and the endothelium. *Kidney  
1769 International* 54, S100-S108.

1770 Becker, A., Thakur, B.K., Weiss, J.M., Kim, H.S., Peinado, H., Lyden, D., 2016. Extracellular  
1771 Vesicles in Cancer: Cell-to-Cell Mediators of Metastasis. *Cancer Cell* 30(6), 836-848.

1772 Belliveau, J., Papoutsakis, E.T., 2022. Extracellular vesicles facilitate large-scale dynamic  
1773 exchange of proteins and RNA among cultured Chinese hamster ovary and human cells.  
1774 *Biotechnol Bioeng*.

1775 Berger, A., Araujo-Filho, I., Piffoux, M., Nicolas-Boluda, A., Grangier, A., Boucenna, I., Real,  
1776 C.C., Marques, F.L.N., de Paula Faria, D., do Rego, A.C.M., Broudin, C., Gazeau, F., Wilhelm,  
1777 C., Clement, O., Cellier, C., Buchpigel, C.A., Rahmi, G., Silva, A.K.A., 2021. Local  
1778 administration of stem cell-derived extracellular vesicles in a thermoresponsive hydrogel  
1779 promotes a pro-healing effect in a rat model of colo-cutaneous post-surgical fistula. *Nanoscale*  
1780 13(1), 218-232.

1781 Bhowmick, T., Berk, E., Cui, X., Muzykantov, V.R., Muro, S., 2012. Effect of flow on endothelial  
1782 endocytosis of nanocarriers targeted to ICAM-1. *J Control Release* 157(3), 485-492.

1783 Blum, A.J., Templeman, N., Li, H., Wang, X., Bollyky, P.L., Keswani, S.G., Balaji, S., 2018.  
1784 Mechanical tension regulates exosome production by fibroblasts to influence heterogeneity in  
1785 cutaneous scarring. *Journal of Investigative Dermatology* 138.

1786 Boehning, D., Patterson, R.L., Sedaghat, L., Glebova, N.O., Kurosaki, T., Snyder, S.H., 2003.  
1787 Cytochrome c binds to inositol (1,4,5) trisphosphate receptors, amplifying calcium-dependent  
1788 apoptosis. *Nat Cell Biol* 5(12), 1051-1061.

1789 Boulanger, C.M., Amabile, N., Guerin, A.P., Pannier, B., Leroyer, A.S., Mallat, C.N., Tedgui, A.,  
1790 London, G.M., 2007. In vivo shear stress determines circulating levels of endothelial  
1791 microparticles in end-stage renal disease. *Hypertension* 49(4), 902-908.

1792 Božić, D., Hočevar, M., Kononenko, V., Jeran, M., Štibler, U., Fiume, I., Pajnič, M., Pađen, L.,  
1793 Kogej, K., Drobne, D., Iglič, A., Pocsfalvi, G., Kralj-Iglič, V., 2020. Pursuing mechanisms of  
1794 extracellular vesicle formation. Effects of sample processing, *Advances in Biomembranes and*  
1795 *Lipid Self-Assembly*. Elsevier Inc., pp. 113-155.

1796 Burger, D., Thibodeau, J.F., Holterman, C.E., Burns, K.D., Touyz, R.M., Kennedy, C.R., 2014.  
1797 Urinary podocyte microparticles identify prealbuminuric diabetic glomerular injury. *J Am Soc*  
1798 *Nephrol* 25(7), 1401-1407.

1799 Busatto, S., Vilanilam, G., Ticer, T., Lin, W.L., Dickson, D.W., Shapiro, S., Bergese, P.,  
1800 Wolfram, J., 2018. Tangential Flow Filtration for Highly Efficient Concentration of Extracellular  
1801 Vesicles from Large Volumes of Fluid. *Cells* 7(12).

1802 Cantaluppi, V., Gatti, S., Medica, D., Figliolini, F., Bruno, S., Deregibus, M.C., Sordi, A.,  
1803 Biancone, L., Tetta, C., Camussi, G., 2012. Microvesicles derived from endothelial progenitor  
1804 cells protect the kidney from ischemia-reperfusion injury by microRNA-dependent  
1805 reprogramming of resident renal cells. *Kidney Int* 82(4), 412-427.

1806 Cha, J.M., Shin, E.K., Sung, J.H., Moon, G.J., Kim, E.H., Cho, Y.H., Park, H.D., Bae, H., Kim,  
1807 J., Bang, O.Y., 2018. Efficient scalable production of therapeutic microvesicles derived from  
1808 human mesenchymal stem cells. *Sci Rep* 8(1), 1171.

1809 Chaar, V., Romana, M., Tripette, J., Broquere, C., Huisse, M.G., Hue, O., Hardy-Dessources,  
1810 M.D., Connes, P., 2011. Effect of strenuous physical exercise on circulating cell-derived  
1811 microparticles. *Clin Hemorheol Microcirc* 47(1), 15-25.

1812 Chalmers, J.J., Ma, N., 2015. Chapter 6 - Hydrodynamic Damage to Animal Cells, in: Al-Rubeai,  
1813 M. (Ed.) *Animal Cell Culture*. Springer International Publishing, Switzerland, pp. 169-183.

1814 Chang, S.-F., Chang, C.A., Lee, D.-Y., Lee, P.-L., Yeh, Y.-M., Yeh, C.-R., Cheng, C.-K., Chien,  
1815 S., Chiu, J.-J., 2008. Tumor cell cycle arrest induced by shear stress: Roles of integrins and  
1816 Smad. *Proceedings of the National Academy of Sciences of the United States of America*  
1817 105(10), 3927-3932.

1818 Chappell, D.C., Varner, S.E., Nerem, R.M., Medford, R.M., Alexander, R.W., 1998. Oscillatory  
1819 Shear Stress Stimulates Adhesion Molecule Expression in Cultured Human Endothelium.  
1820 Circulation Research 82(5), 532-539.

1821 Chen, Y., Bao, H., Yan, J., Xiao, Q., Qi, Y., 2020. Cyclic Stretch Induces Adhesion of VSMCs  
1822 with Platelet-Derived Microparticles and the Role in Autophagy. Journal of Medical  
1823 Biomechanics 35(1), 49-56.

1824 Chen, Y., Zhao, Y., Yin, Y., Jia, X., Mao, L., 2021. Mechanism of cargo sorting into small  
1825 extracellular vesicles. Bioengineered 12(1), 8186-8201.

1826 Chen, Y.W., Chen, J.K., Wang, J.S., 2010. Strenuous exercise promotes shear-induced  
1827 thrombin generation by increasing the shedding of procoagulant microparticles from platelets.  
1828 Thromb Haemost 104(2), 293-301.

1829 Chen, Y.Y., Syed, A.M., MacMillan, P., Rocheleau, J.V., Chan, W.C.W., 2020. Flow Rate  
1830 Affects Nanoparticle Uptake into Endothelial Cells. Advanced Materials 32(24), 1906274.

1831 Cherry, R.S., Kwon, K.-Y., 1990. Transient shear stresses on a suspension cell in turbulence.  
1832 Biotechnology and Bioengineering 36(6), 563-571.

1833 Cherry, R.S., Papoutsakis, E.T., 1988. Physical mechanisms of cell damage in microcarrier cell  
1834 culture bioreactors. Biotechnology and Bioengineering 32(8), 1001-1014.

1835 Cherry, R.S., Papoutsakis, E.T., 1989. Growth and death rates of bovine embryonic kidney cells  
1836 in turbulent microcarrier bioreactors. Bioprocess Engineering 4, 81-89.

1837 Chisti, Y., 2001. Hydrodynamic Damage to Animal Cells. Critical Reviews in Biotechnology  
1838 21(2), 67-110.

1839 Chung, J., Kim, K.H., Yu, N., An, S.H., Lee, S., Kwon, K., 2022. Fluid Shear Stress Regulates  
1840 the Landscape of microRNAs in Endothelial Cell-Derived Small Extracellular Vesicles and  
1841 Modulates the Function of Endothelial Cells. Int J Mol Sci 23(3).

1842 Colao, I.L., Corteling, R., Bracewell, D., Wall, I., 2018. Manufacturing Exosomes: A Promising  
1843 Therapeutic Platform. Trends Mol Med 24(3), 242-256.

1844 Corrado, C., Barreca, M.M., Zichittella, C., Alessandro, R., Conigliaro, A., 2021. Molecular  
1845 Mediators of RNA Loading into Extracellular Vesicles. Cells 10(12).

1846 Croughan, M.S., Hamel, J.-F., Wang, D.I.C., 1987. Hydrodynamic effects on animal cells grown  
1847 in microcarrier cultures. Biotechnology and Bioengineering 29(1), 130-141.

1848 Czermak, P., Pörtner, R., Brix, A., 2009. Chapter 4 - Special Engineering Aspects, Cell and  
1849 Tissue Reaction Engineering. Springer-Verlag, Berlin Heidelberg, pp. 83-172.

1850 de Almeida Fuzeta, M., Bernardes, N., Oliveira, F.D., Costa, A.C., Fernandes-Platzgummer, A.,  
1851 Farinha, J.P., Rodrigues, C.A.V., Jung, S., Tseng, R.J., Milligan, W., Lee, B., Castanho, M.,  
1852 Gaspar, D., Cabral, J.M.S., da Silva, C.L., 2020. Scalable Production of Human Mesenchymal  
1853 Stromal Cell-Derived Extracellular Vesicles Under Serum-/Xeno-Free Conditions in a  
1854 Microcarrier-Based Bioreactor Culture System. Front Cell Dev Biol 8, 553444.

1855 Deng, L., Blanco, F.J., Stevens, H., Lu, R., Caudrillier, A., McBride, M., McClure, J.D., Grant, J.,  
1856 Thomas, M., Frid, M., Stenmark, K., White, K., Seto, A.G., Morrell, N.W., Bradshaw, A.C.,  
1857 MacLean, M.R., Baker, A.H., 2015. MicroRNA-143 Activation Regulates Smooth Muscle and  
1858 Endothelial Cell Crosstalk in Pulmonary Arterial Hypertension. *Circ Res* 117(10), 870-883.

1859 Deregibus, M.C., Cantaluppi, V., Calogero, R., Lo Iacono, M., Tetta, C., Biancone, L., Bruno, S.,  
1860 Bussolati, B., Camussi, G., 2007. Endothelial progenitor cell derived microvesicles activate an  
1861 angiogenic program in endothelial cells by a horizontal transfer of mRNA. *Blood* 110(7), 2440-  
1862 2448.

1863 Diehl, P., Aleker, M., Helbing, T., Sossong, V., Beyersdorf, F., Olschewski, M., Bode, C., Moser,  
1864 M., 2010. Enhanced microparticles in ventricular assist device patients predict platelet,  
1865 leukocyte and endothelial cell activation. *Interact Cardiovasc Thorac Surg* 11(2), 133-137.

1866 Dinarelli, S., Longo, G., Francioso, A., Mosca, L., Girasole, M., 2022. Mechano-Transduction  
1867 Boosts the Aging Effects in Human Erythrocytes Submitted to Mechanical Stimulation. *Int J Mol  
1868 Sci* 23(17).

1869 Doryab, A., Taskin, M.B., Stahlhut, P., Schroppel, A., Orak, S., Voss, C., Ahluwalia, A.,  
1870 Rehberg, M., Hilgendorff, A., Stoger, T., Groll, J., Schmid, O., 2021. A Bioinspired in vitro Lung  
1871 Model to Study Particokinetics of Nano-/Microparticles Under Cyclic Stretch and Air-Liquid  
1872 Interface Conditions. *Front Bioeng Biotechnol* 9, 616830.

1873 Doryab, A., Taskin, M.B., Stahlhut, P., Schröppel, A., Wagner, D.E., Groll, J., Schmid, O., 2020.  
1874 A Biomimetic, Copolymeric Membrane for Cell-Stretch Experiments with Pulmonary Epithelial  
1875 Cells at the Air-Liquid Interface. *Advanced Functional Materials* 31(10).

1876 Elosegui-Artola, A., Andreu, I., Beedle, A.E.M., Lezamiz, A., Uroz, M., Kosmalska, A.J., Oria, R.,  
1877 Kechagia, J.Z., Rico-Lastres, P., Le Roux, A.L., Shanahan, C.M., Trepat, X., Navajas, D.,  
1878 Garcia-Manyes, S., Roca-Cusachs, P., 2017. Force Triggers YAP Nuclear Entry by Regulating  
1879 Transport across Nuclear Pores. *Cell* 171(6), 1397-1410 e1314.

1880 Escobar, C., Kao, C.Y., Das, S., Papoutsakis, E.T., 2020. Human megakaryocytic microparticles  
1881 induce de novo platelet biogenesis in a wild-type murine model. *Blood Adv* 4(5), 804-814.

1882 Fabbiano, F., Corsi, J., Gurrieri, E., Trevisan, C., Notarangelo, M., D'Agostino, V.G., 2020. RNA  
1883 packaging into extracellular vesicles: An orchestra of RNA-binding proteins? *J Extracell Vesicles*  
1884 10(2), e12043.

1885 Faghih, M.M., Sharp, M.K., 2018. Characterization of erythrocyte membrane tension for  
1886 hemolysis prediction in complex flows. *Biomech Model Mechanobiol* 17(3), 827-842.

1887 Feng, S., Chen, J.W., Shu, X.Y., Aihemaiti, M., Quan, J.W., Lu, L., Zhang, R.Y., Yang, C.D.,  
1888 Wang, X.Q., 2022. Endothelial microparticles: A mechanosensitive regulator of vascular  
1889 homeostasis and injury under shear stress. *Front Cell Dev Biol* 10, 980112.

1890 Feng, T., Fang, F., Zhang, C., Li, T., He, J., Shen, Y., Yu, H., Liu, X., 2022. Fluid Shear Stress-  
1891 Induced Exosomes from Liver Cancer Cells Promote Activation of Cancer-Associated  
1892 Fibroblasts via IGF2-PI3K Axis. *Front Biosci (Landmark Ed)* 27(3), 104.

1893 Fielding, A.B., Royle, S.J., 2013. Mitotic inhibition of clathrin-mediated endocytosis. *Cell Mol Life*  
1894 *Sci* 70(18), 3423-3433.

1895 Flaumenhaft, R., Dilks, J.R., Richardson, J., Alden, E., Patel-Hett, S.R., Battinelli, E., Klement,  
1896 G.L., Sola-Visner, M., Italiano, J.E., Jr., 2009. Megakaryocyte-derived microparticles: direct  
1897 visualization and distinction from platelet-derived microparticles. *Blood* 113(5), 1112-1121.

1898 Foster, K.M., Papavassiliou, D.V., O'Rear, E.A., 2021. Elongational Stresses and Cells. *Cells*  
1899 10(9).

1900 Freese, C., Anspach, L., Deller, R.C., Richards, S.J., Gibson, M.I., Kirkpatrick, C.J., Unger,  
1901 R.E., 2017. Gold nanoparticle interactions with endothelial cells cultured under physiological  
1902 conditions. *Biomaterials Science* 5(4), 707-717.

1903 Freese, C., Schreiner, D., Anspach, L., Bantz, C., Maskos, M., Unger, R.E., Kirkpatrick, C.J.,  
1904 2014. In vitro investigation of silica nanoparticle uptake into human endothelial cells under  
1905 physiological cyclic stretch. *Part Fibre Toxicol* 11, 68.

1906 Freiberger, F., Budde, J., Ateş, E., Schlüter, M., Pörtner, R., Möller, J., 2022. New Insights from  
1907 Locally Resolved Hydrodynamics in Stirred Cell Culture Reactors. *Processes* 10(1).

1908 Freitas, D., Balmana, M., Pocas, J., Campos, D., Osorio, H., Konstantinidi, A., Vakhrushev,  
1909 S.Y., Magalhaes, A., Reis, C.A., 2019. Different isolation approaches lead to diverse  
1910 glycosylated extracellular vesicle populations. *J Extracell Vesicles* 8(1), 1621131.

1911 Gagnon, P., Vrabec, K., Lojpur, T., Strancar, A., 2020. Setting a Cornerstone for Platform  
1912 Purification of Exosomes, *BioProcess International*.

1913 Garcia-Briones, M.A., Chalmers, J.J., 1994. Flow parameters associated with hydrodynamic cell  
1914 injury. *Biotechnology and Bioengineering* 44.

1915 Gazeau, F., Silva, A.K.A., Merten, O.-w., Wilhelm, C., Piffoux, M., 2020. FLUID SYSTEM FOR  
1916 PRODUCING EXTRACELLULAR VESICLES AND ASSOCIATED METHOD. UNIVERSITE  
1917 PARIS DIDEROT PARIS 7  
1918 CENTRE NATIONAL DE LA RECHERCHE SCIENTIFIQUE (CNRS)  
1919 GENETHON, USA.

1920 Gobin, J., Muradia, G., Mehic, J., Westwood, C., Couvrette, L., Stalker, A., Bigelow, S.,  
1921 Luebbert, C.C., Bissonnette, F.S., Johnston, M.J.W., Sauve, S., Tam, R.Y., Wang, L., Rosu-  
1922 Myles, M., Lavoie, J.R., 2021. Hollow-fiber bioreactor production of extracellular vesicles from  
1923 human bone marrow mesenchymal stromal cells yields nanovesicles that mirrors the immuno-  
1924 modulatory antigenic signature of the producer cell. *Stem Cell Res Ther* 12(1), 127.

1925 Godoy-Gallardo, M., Ek, P.K., Jansman, M.M., Wohl, B.M., Hosta-Rigau, L., 2015. Interaction  
1926 between drug delivery vehicles and cells under the effect of shear stress. *Biomicrofluidics* 9(5),  
1927 052605.

1928 Gomez, I., Ward, B., Souilhol, C., Recarti, C., Ariaans, M., Johnston, J., Burnett, A., Mahmoud,  
1929 M., Luong, L.A., West, L., Long, M., Parry, S., Woods, R., Hulston, C., Benedikter, B., Niespolo,  
1930 C., Bazaz, R., Francis, S., Kiss-Toth, E., van Zandvoort, M., Schober, A., Hellewell, P., Evans,

1931 P.C., Ridger, V., 2020. Neutrophil microvesicles drive atherosclerosis by delivering miR-155 to  
1932 atheroprone endothelium. *Nat Commun* 11(1), 214.

1933 Goto, S., Tamura, N., Li, M., Handa, M., Ikeda, Y., Handa, S., Ruggeri, Z.M., 2003. Different  
1934 effects of various anti-GPIIb-IIIa agents on shear-induced platelet activation and expression of  
1935 procoagulant activity. *Journal of Thrombosis and Haemostasis* 1(9), 2022-2030.

1936 Grangier, A., Branchu, J., Volatron, J., Piffoux, M., Gazeau, F., Wilhelm, C., Silva, A.K.A., 2021.  
1937 Technological advances towards extracellular vesicles mass production. *Advanced Drug  
1938 Delivery Reviews* 176, 113843.

1939 Grangier, A., Wilhelm, C., Gazeau, F., Silva, A., 2020. High yield and scalable EV production  
1940 from suspension cells triggered by turbulence in a bioreactor. *Cyotherapy* 22(5, Supplement),  
1941 S50.

1942 Gregoriades, N., Clay, J., Ma, N., Koelling, K., Chalmers, J.J., 2000. Cell damage of  
1943 microcarrier cultures as a function of local energy dissipation created by a rapid extensional  
1944 flow. *Biotechnology and Bioengineering* 69(2), 171-182.

1945 Groot, M., Lee, H., 2020. Sorting Mechanisms for MicroRNAs into Extracellular Vesicles and  
1946 Their Associated Diseases. *Cells* 9(4).

1947 Guo, S., Debbi, L., Zohar, B., Samuel, R., Arzi, R.S., Fried, A.I., Carmon, T., Shevach, D.,  
1948 Redenski, I., Schlachet, I., Sosnik, A., Levenberg, S., 2021. Stimulating Extracellular Vesicles  
1949 Production from Engineered Tissues by Mechanical Forces. *Nano Lett* 21(6), 2497-2504.

1950 Gupta, D., Zickler, A.M., El Andaloussi, S., 2021. Dosing extracellular vesicles. *Adv Drug Deliv  
1951 Rev* 178, 113961.

1952 Haga, J.H., Slack, S.M., Jennings, L.K., 2003. Comparison of shear stress-induced platelet  
1953 microparticle formation and phosphatidylserine expression in presence of alphallbbeta3  
1954 antagonists. *J Cardiovasc Pharmacol* 41(3), 363-371.

1955 Han, J., Shuvaev, V.V., Davies, P.F., Eckmann, D.M., Muro, S., Muzykantov, V.R., 2015. Flow  
1956 shear stress differentially regulates endothelial uptake of nanocarriers targeted to distinct  
1957 epitopes of PECAM-1. *J Control Release* 210, 39-47.

1958 Han, J., Zern, B.J., Shuvaev, V.V., Davies, P.F., Muro, S., Muzykantov, V., 2012. Acute and  
1959 Chronic Shear Stress Differently Regulate Endothelial Internalization of Nanocarriers Targeted  
1960 to Platelet-Endothelial Cell Adhesion Molecule-1. *ACS Nano* 6(10), 8824-8836.

1961 Hao, R., Hu, S., Zhang, H., Chen, X., Yu, Z., Ren, J., Guo, H., Yang, H., 2023. Mechanical  
1962 stimulation on a microfluidic device to highly enhance small extracellular vesicle secretion of  
1963 mesenchymal stem cells. *Mater Today Bio* 18, 100527.

1964 Harada, Y., Ohkawa, Y., Maeda, K., Kizuka, Y., Taniguchi, N., 2021. Extracellular Vesicles and  
1965 Glycosylation, in: Lauc, G., Trbojević-Akmačić, I. (Eds.), *The Role of Glycosylation in Health and  
1966 Disease*. Springer International Publishing, Cham, pp. 137-149.

1967 Haraszti, R.A., Miller, R., Stoppato, M., Sere, Y.Y., Coles, A., Didiot, M.C., Wollacott, R., Sapp,  
1968 E., Dubuke, M.L., Li, X., Shaffer, S.A., DiFiglia, M., Wang, Y., Aronin, N., Khvorova, A., 2018.

1969 Exosomes Produced from 3D Cultures of MSCs by Tangential Flow Filtration Show Higher Yield  
1970 and Improved Activity. *Mol Ther* 26(12), 2838-2847.

1971 He, S., Wu, C., Xiao, J., Li, D., Sun, Z., Li, M., 2018. Endothelial extracellular vesicles modulate  
1972 the macrophage phenotype: Potential implications in atherosclerosis. *Scand J Immunol* 87(4),  
1973 e12648.

1974 He, Y., Macarak, E.J., Korostoff, J.M., Howard, P.S., 2004. Compression and Tension:  
1975 Differential Effects on Matrix Accumulation by Periodontal Ligament Fibroblasts In Vitro.  
1976 *Connective Tissue Research* 45(1), 28-39.

1977 He, Z., Zhang, W., Mao, S., Li, N., Li, H., Lin, J.M., 2018. Shear Stress-Enhanced Internalization  
1978 of Cell Membrane Proteins Indicated by a Hairpin-Type DNA Probe. *Anal Chem* 90(9), 5540-  
1979 5545.

1980 Headland, S.E., Jones, H.R., D'Sa, A.S., Perretti, M., Norling, L.V., 2014. Cutting-edge analysis  
1981 of extracellular microparticles using ImageStream(X) imaging flow cytometry. *Sci Rep* 4, 5237.

1982 Henzler, H.J., Kauling, D.J., 1993. Oxygenation of cell cultures. *Bioprocess Engineering* 9(2),  
1983 61-75.

1984 Hergenreider, E., Heydt, S., Treguer, K., Boettger, T., Horrevoets, A.J., Zeiher, A.M., Scheffer,  
1985 M.P., Frangakis, A.S., Yin, X., Mayr, M., Braun, T., Urbich, C., Boon, R.A., Dimmeler, S., 2012.  
1986 Atheroprotective communication between endothelial cells and smooth muscle cells through  
1987 miRNAs. *Nat Cell Biol* 14(3), 249-256.

1988 Herrmann, I.K., Wood, M.J.A., Fuhrmann, G., 2021. Extracellular vesicles as a next-generation  
1989 drug delivery platform. *Nat Nanotechnol* 16(7), 748-759.

1990 Hill, C., Dellar, E.R., Baena-Lopez, L.A., 2022. Caspases help to spread the message via  
1991 extracellular vesicles. *FEBS J.*

1992 Holme, P.A., Ørvim, U., Hamers, M.J.A.G., Solum, N.O., Brosstad, F.R., Barstad, R.M.,  
1993 Sakariassen, K.S., 1997. Shear-Induced Platelet Activation and Platelet Microparticle Formation  
1994 at Blood Flow Conditions as in Arteries With a Severe Stenosis. *Arteriosclerosis, Thrombosis,*  
1995 and *Vascular Biology* 17(4), 646-653.

1996 Hopkin, K., 2016. Core Concept: Extracellular vesicles garner interest from academia and  
1997 biotech. *Proc Natl Acad Sci U S A* 113(33), 9126-9128.

1998 Hu, J., Liu, Y., 2015. Cyclic Strain Enhances Cellular Uptake of Nanoparticles. *Journal of*  
1999 *Nanomaterials* 2015, 1-8.

2000 Hu, Y., Tao, R., Wang, L., Chen, L., Lin, Z., Panayi, A.C., Xue, H., Li, H., Xiong, L., Liu, G.,  
2001 2021. Exosomes Derived from Bone Mesenchymal Stem Cells Alleviate Compression-Induced  
2002 Nucleus Pulposus Cell Apoptosis by Inhibiting Oxidative Stress. *Oxid Med Cell Longev* 2021,  
2003 2310025.

2004 Huang, H.M., Han, C.S., Cui, S.J., Zhou, Y.K., Xin, T.Y., Zhang, T., Zhu, S.B., Zhou, Y.H.,  
2005 Yang, R.L., 2022. Mechanical force-promoted osteoclastic differentiation via periodontal  
2006 ligament stem cell exosomal protein ANXA3. *Stem Cell Reports* 17(8), 1842-1858.

2007 Huh, D., Matthews, B.D., Mammoto, A., Montoya-Zavala, M., Hsin, H.Y., Ingber, D.E., 2010.

2008 Reconstituting organ-level lung functions on a chip. *Science* 328(5986), 1662-1668.

2009 Jae, N., McEwan, D.G., Manavski, Y., Boon, R.A., Dimmeler, S., 2015. Rab7a and Rab27b

2010 control secretion of endothelial microRNA through extracellular vesicles. *FEBS Lett* 589(20 Pt

2011 B), 3182-3188.

2012 Jarmalavičiūtė, A., Tunaitis, V., Pivoraitė, U., Venalis, A., Pivoriūnas, A., 2015. Exosomes from

2013 dental pulp stem cells rescue human dopaminergic neurons from 6-hydroxy-dopamine-induced

2014 apoptosis. *Cyotherapy* 17(7), 932-939.

2015 Jenkins, N.T., Padilla, J., Boyle, L.J., Credeur, D.P., Laughlin, M.H., Fadel, P.J., 2013.

2016 Disturbed blood flow acutely induces activation and apoptosis of the human vascular

2017 endothelium. *Hypertension* 61(3), 615-621.

2018 Jia, L.X., Zhang, W.M., Li, T.T., Liu, Y., Piao, C.M., Ma, Y.C., Lu, Y., Wang, Y., Liu, T.T., Qi,

2019 Y.F., Du, J., 2017. ER stress dependent microparticles derived from smooth muscle cells

2020 promote endothelial dysfunction during thoracic aortic aneurysm and dissection. *Clin Sci (Lond)*

2021 131(12), 1287-1299.

2022 Jiang, J., Woulfe, D.S., Papoutsakis, E.T., 2014. Shear enhances thrombopoiesis and formation

2023 of microparticles that induce megakaryocytic differentiation of stem cells. *Blood* 124(13), 2094-

2024 2103.

2025 Jimenez, A.J., Maiuri, P., Lafaurie-Janvore, J., Divoux, S., Piel, M., Perez, F., 2014. ESCRT

2026 machinery is required for plasma membrane repair. *Science* 343(6174), 1247136.

2027 Jo, W., Jeong, D., Kim, J., Cho, S., Jang, S.C., Han, C., Kang, J.Y., Gho, Y.S., Park, J., 2014.

2028 Microfluidic fabrication of cell-derived nanovesicles as endogenous RNA carriers. *Lab on a Chip*

2029 14(7), 1261-1269.

2030 Jo, W., Kim, J., Yoon, J., Jeong, D., Cho, S., Jeong, H., Yoon, Y.J., Kim, S.C., Gho, Y.S., Park,

2031 J., 2014. Large-scale generation of cell-derived nanovesicles. *Nanoscale* 6(20), 12056-12064.

2032 Junt, T., Schulze, H., Chen, Z., Massberg, S., Goerge, T., Krueger, A., Wagner, D.D., Graf, T.,

2033 Italiano, J.E., Jr., Shivedasani, R.A., von Andrian, U.H., 2007. Dynamic visualization of

2034 thrombopoiesis within bone marrow. *Science* 317(5845), 1767-1770.

2035 Kaksonen, M., Roux, A., 2018. Mechanisms of clathrin-mediated endocytosis. *Nat Rev Mol Cell*

2036 *Biol* 19(5), 313-326.

2037 Kang, H., Bae, Y.-h., Kwon, Y., Kim, S., Park, J., 2022. Extracellular Vesicles Generated Using

2038 Bioreactors and their Therapeutic Effect on the Acute Kidney Injury Model. *Advanced*

2039 *Healthcare Materials* 11(4), 2101606.

2040 Kao, C.-Y., Jiang, J., Thompson, W., Papoutsakis, E.T., 2022. miR-486-5p and miR-22-3p

2041 Enable Megakaryocytic Differentiation of Hematopoietic Stem and Progenitor Cells without

2042 Thrombopoietin. *International Journal of Molecular Sciences* 23(10).

2043 Kao, C.Y., Papoutsakis, E.T., 2019. Extracellular vesicles: exosomes, microparticles, their parts,  
2044 and their targets to enable their biomanufacturing and clinical applications. *Curr Opin Biotechnol*  
2045 60, 89-98.

2046 Karami, D., Srivastava, A., Ramesh, R., Sikavitsas, V.I., 2022. Investigating Cancerous  
2047 Exosomes' Effects on CD8+ T-Cell IL-2 Production in a 3D Unidirectional Flow Bioreactor Using  
2048 3D Printed, RGD-Functionalized PLLA Scaffolds. *J Funct Biomater* 13(1).

2049 Keysberg, C., Hertel, O., Schelletter, L., Busche, T., Sochart, C., Kalinowski, J., Hoffrogge, R.,  
2050 Otte, K., Noll, T., 2021. Exploring the molecular content of CHO exosomes during  
2051 bioprocessing. *Appl Microbiol Biotechnol* 105(9), 3673-3689.

2052 Kim, J.S., Kim, B., Lee, H., Thakkar, S., Babbitt, D.M., Eguchi, S., Brown, M.D., Park, J.Y.,  
2053 2015. Shear stress-induced mitochondrial biogenesis decreases the release of microparticles  
2054 from endothelial cells. *Am J Physiol Heart Circ Physiol* 309(3), H425-433.

2055 Kim, K., Park, J., Jung, J.H., Lee, R., Park, J.H., Yuk, J.M., Hwang, H., Yeon, J.H., 2021. Cyclic  
2056 tangential flow filtration system for isolation of extracellular vesicles. *APL Bioeng* 5(1), 016103.

2057 Kim, M.H., Wu, W.H., Choi, J.H., Kim, J.H., Hong, S.H., Jun, J.H., Ko, Y., Lee, J.H., 2018.  
2058 Conditioned medium from the three-dimensional culture of human umbilical cord perivascular  
2059 cells accelerate the migration and proliferation of human keratinocyte and fibroblast. *J Biomater  
2060 Sci Polym Ed* 29(7-9), 1066-1080.

2061 Koomullil, R., Tehrani, B., Goliwas, K., Wang, Y., Ponnazhagan, S., Berry, J., Deshane, J.,  
2062 2021. Computational Simulation of Exosome Transport in Tumor Microenvironment. *Front Med  
2063 (Lausanne)* 8, 643793.

2064 Kordelas, L., Rebmann, V., Ludwig, A.K., Radtke, S., Ruesing, J., Doeppner, T.R., Epple, M.,  
2065 Horn, P.A., Beelen, D.W., Giebel, B., 2014. MSC-derived exosomes: a novel tool to treat  
2066 therapy-refractory graft-versus-host disease. *Leukemia* 28(4), 970-973.

2067 Kunas, K.T., Papoutsakis, E.T., 1990. Damage mechanisms of suspended animal cells in  
2068 agitated bioreactors with and without bubble entrainment. *Biotechnology and Bioengineering*  
2069 36(5), 476-483.

2070 Lakhotia, S., Bauer, K.D., Papoutsakis, E.T., 1992. Damaging agitation intensities increase DNA  
2071 synthesis rate and alter cell-cycle phase distributions of CHO cells. *Biotechnology and  
2072 Bioengineering* 40(8), 978-990.

2073 Lawler, K., O'Sullivan, G., Long, A., Kenny, D., 2009. Shear stress induces internalization of E-  
2074 cadherin and invasiveness in metastatic oesophageal cancer cells by a Src-dependent pathway.  
2075 *Cancer Sci* 100(6), 1082-1087.

2076 Lazaro-Ibanez, E., Neuvonen, M., Takatalo, M., Thanigai Arasu, U., Capasso, C., Cerullo, V.,  
2077 Rhim, J.S., Rilla, K., Yliperttula, M., Siljander, P.R., 2017. Metastatic state of parent cells  
2078 influences the uptake and functionality of prostate cancer cell-derived extracellular vesicles. *J  
2079 Extracell Vesicles* 6(1), 1354645.

2080 Le Roux, A.L., Quiroga, X., Walani, N., Arroyo, M., Roca-Cusachs, P., 2019. The plasma  
2081 membrane as a mechanochemical transducer. *Philos Trans R Soc Lond B Biol Sci* 374(1779),  
2082 20180221.

2083 Lee, J.H., Yoon, J.Y., Lee, J.H., Lee, H.H., Knowles, J.C., Kim, H.W., 2021. Emerging  
2084 biogenesis technologies of extracellular vesicles for tissue regenerative therapeutics. *J Tissue*  
2085 *Eng* 12, 20417314211019015.

2086 Lee, Y.H., Lai, C.W., Cheng, Y.C., 2018. Fluid Shear Stress Induces Cell Cycle Arrest in Human  
2087 Urinary Bladder Transitional Cell Carcinoma Through Bone Morphogenetic Protein Receptor-  
2088 Smad1/5 Pathway. *Cell Mol Bioeng* 11(3), 185-195.

2089 Lenzini, S., Debnath, K., Joshi, J.C., Wong, S.W., Srivastava, K., Geng, X., Cho, I.S., Song, A.,  
2090 Bargi, R., Lee, J.C., Mo, G.C.H., Mehta, D., Shin, J.W., 2021. Cell-Matrix Interactions Regulate  
2091 Functional Extracellular Vesicle Secretion from Mesenchymal Stromal Cells. *ACS Nano* 15(11),  
2092 17439-17452.

2093 Letsiou, E., Sammani, S., Zhang, W., Zhou, T., Quijada, H., Moreno-Vinasco, L., Dudek, S.M.,  
2094 Garcia, J.G., 2015. Pathologic mechanical stress and endotoxin exposure increases lung  
2095 endothelial microparticle shedding. *Am J Respir Cell Mol Biol* 52(2), 193-204.

2096 Leytin, V., Allen, D.J., Mykhaylov, S., Mis, L., Lyubimov, E.V., Garvey, B., Freedman, J., 2004.  
2097 Pathologic high shear stress induces apoptosis events in human platelets. *Biochem Biophys*  
2098 *Res Commun* 320(2), 303-310.

2099 Li, B., Ding, T., Chen, H., Li, C., Chen, B., Xu, X., Huang, P., Hu, F., Guo, L., 2023. CircStrn3  
2100 targeting microRNA-9-5p is involved in the regulation of cartilage degeneration and subchondral  
2101 bone remodelling in osteoarthritis. *Bone Joint Res* 12(1), 33-45.

2102 Li, L., Wen, J., Li, H., He, Y., Cui, X., Zhang, X., Guan, X., Li, Z., Cheng, M., 2023. Exosomal  
2103 circ-1199 derived from EPCs exposed to oscillating shear stress acts as a sponge of let-7g-5p  
2104 to promote endothelial-mesenchymal transition of EPCs by increasing HMGA2 expression. *Life*  
2105 *Sci* 312, 121223.

2106 Li, S., Chen, D.Q., Ji, L., Sun, S., Jin, Z., Jin, Z.L., Sun, H.W., Zeng, H., Zhang, W.J., Lu, D.S.,  
2107 Luo, P., Zhao, A.N., Luo, J., Zou, Q.M., Li, H.B., 2020. Development of Different Methods for  
2108 Preparing *Acinetobacter baumannii* Outer Membrane Vesicles Vaccine: Impact of Preparation  
2109 Method on Protective Efficacy. *Front Immunol* 11, 1069.

2110 Li, X., Corbett, A.L., Taatizadeh, E., Tasnim, N., Little, J.P., Garnis, C., Daugaard, M., Guns, E.,  
2111 Hoorfar, M., Li, I.T.S., 2019. Challenges and opportunities in exosome research-Perspectives  
2112 from biology, engineering, and cancer therapy. *APL Bioeng* 3(1), 011503.

2113 Li, X., Wang, Y., Cai, Z., Zhou, Q., Li, L., Fu, P., 2021. Exosomes from human umbilical cord  
2114 mesenchymal stem cells inhibit ROS production and cell apoptosis in human articular  
2115 chondrocytes via the miR-100-5p/NOX4 axis. *Cell Biol Int* 45(10), 2096-2106.

2116 Lin, A., Sabnis, A., Kona, S., Nattama, S., Patel, H., Dong, J.F., Nguyen, K.T., 2010. Shear-  
2117 regulated uptake of nanoparticles by endothelial cells and development of endothelial-targeting  
2118 nanoparticles. *J Biomed Mater Res A* 93(3), 833-842.

2119 Lin, K., Hsu, P.-P., Chen Benjamin, P., Yuan, S., Usami, S., Shyy John, Y.J., Li, Y.-S., Chien,  
2120 S., 2000. Molecular mechanism of endothelial growth arrest by laminar shear stress.  
2121 Proceedings of the National Academy of Sciences 97(17), 9385-9389.

2122 Liu, Q., Wang, R., Hou, S., He, F., Ma, Y., Ye, T., Yu, S., Chen, H., Wang, H., Zhang, M., 2022.  
2123 Chondrocyte-derived exosomes promote cartilage calcification in temporomandibular joint  
2124 osteoarthritis. Arthritis Res Ther 24(1), 44.

2125 Liu, Z., Jin, Q., Yan, T., Wo, Y., Liu, H., Wang, Y., 2022. Exosome-mediated transduction of  
2126 mechanical force regulates prostate cancer migration via microRNA. Biochem Biophys Rep 31,  
2127 101299.

2128 Luff, S.A., Kao, C.Y., Papoutsakis, E.T., 2018. Role of p53 and transcription-independent p53-  
2129 induced apoptosis in shear-stimulated megakaryocytic maturation, particle generation, and  
2130 platelet biogenesis. PLoS One 13(9), e0203991.

2131 Lv, P.Y., Gao, P.F., Tian, G.J., Yang, Y.Y., Mo, F.F., Wang, Z.H., Sun, L., Kuang, M.J., Wang,  
2132 Y.L., 2020. Osteocyte-derived exosomes induced by mechanical strain promote human  
2133 periodontal ligament stem cell proliferation and osteogenic differentiation via the miR-181b-  
2134 5p/PTEN/AKT signaling pathway. Stem Cell Res Ther 11(1), 295.

2135 Macedo-da-Silva, J., Santiago, V.F., Rosa-Fernandes, L., Marinho, C.R.F., Palmisano, G.,  
2136 2021. Protein glycosylation in extracellular vesicles: Structural characterization and biological  
2137 functions. Molecular Immunology 135, 226-246.

2138 Martins, A.M., Ramos, C.C., Freitas, D., Reis, C.A., 2021. Glycosylation of Cancer Extracellular  
2139 Vesicles: Capture Strategies, Functional Roles and Potential Clinical Applications. Cells 10(1).

2140 Maruyama, K., Kadono, T., Morishita, E., 2012. Plasma levels of platelet-derived microparticles  
2141 are increased after anaerobic exercise in healthy subjects. J Atheroscler Thromb 19(6), 585-  
2142 587.

2143 Mathieu, M., Martin-Jaular, L., Lavieu, G., Thery, C., 2019. Specificities of secretion and uptake  
2144 of exosomes and other extracellular vesicles for cell-to-cell communication. Nat Cell Biol 21(1),  
2145 9-17.

2146 McNamara, R.P., Caro-Vegas, C.P., Costantini, L.M., Landis, J.T., Griffith, J.D., Damania, B.A.,  
2147 Dittmer, D.P., 2018. Large-scale, cross-flow based isolation of highly pure and endocytosis-  
2148 competent extracellular vesicles. J Extracell Vesicles 7(1), 1541396.

2149 Mendt, M., Kamerkar, S., Sugimoto, H., McAndrews, K.M., Wu, C.C., Gagea, M., Yang, S.,  
2150 Blanko, E.V.R., Peng, Q., Ma, X., Marszalek, J.R., Maitra, A., Yee, C., Rezvani, K., Shpall, E.,  
2151 LeBleu, V.S., Kalluri, R., 2018. Generation and testing of clinical-grade exosomes for pancreatic  
2152 cancer. JCI Insight 3(8).

2153 Meyer, A.D., Rishmawi, A.R., Kamucheka, R., Lafleur, C., Batchinsky, A.I., Mackman, N., Cap,  
2154 A.P., 2020. Effect of blood flow on platelets, leukocytes, and extracellular vesicles in thrombosis  
2155 of simulated neonatal extracorporeal circulation. J Thromb Haemost 18(2), 399-410.

2156 Michaels, J.D., Mallik, A.K., Papoutsakis, E.T., 1996. Sparging and agitation-induced injury of  
2157 cultured animals cells: Do cell-to-bubble interactions in the bulk liquid injure cells?  
2158 Biotechnology and Bioengineering 51(4), 399-409.

2159 Min Lim, K., Kim, S., Yeom, J., Choi, Y., Lee, Y., An, J., Gil, M., Abdal Dayem, A., Kim, K.,  
2160 Kang, G.H., Kim, A., Hong, K., Kim, K., Cho, S.G., 2022. Advanced 3D dynamic culture system  
2161 with transforming growth factor-beta3 enhances production of potent extracellular vesicles with  
2162 modified protein cargoes via upregulation of TGF-beta signaling. J Adv Res.

2163 Mir, B., Goettsch, C., 2020. Extracellular Vesicles as Delivery Vehicles of Specific Cellular  
2164 Cargo. Cells 9(7).

2165 Mitchel, J.A., Antoniak, S., Lee, J.H., Kim, S.H., McGill, M., Kasahara, D.I., Randell, S.H., Israel,  
2166 E., Shore, S.A., Mackman, N., Park, J.A., 2016. IL-13 Augments Compressive Stress-Induced  
2167 Tissue Factor Expression in Human Airway Epithelial Cells. Am J Respir Cell Mol Biol 54(4),  
2168 524-531.

2169 Miyazaki, Y., Nomura, S., Miyake, T., Kagawa, H., Kitada, C., Taniguchi, H., Komiya, Y.,  
2170 Fujimura, Y., Ikeda, Y., Fukuura, S., 1996. High shear stress can initiate both platelet  
2171 aggregation and shedding of procoagulant containing microparticles. Blood 88(9), 3456-3464.

2172 Mo, M., Zhou, Y., Li, S., Wu, Y., 2018. Three-Dimensional Culture Reduces Cell Size By  
2173 Increasing Vesicle Excretion. Stem Cells 36(2), 286-292.

2174 Morrell, A.E., Brown, G.N., Robinson, S.T., Sattler, R.L., Baik, A.D., Zhen, G., Cao, X.,  
2175 Bonewald, L.F., Jin, W., Kam, L.C., Guo, X.E., 2018. Mechanically induced Ca(2+) oscillations  
2176 in osteocytes release extracellular vesicles and enhance bone formation. Bone Res 6, 6.

2177 Mullen, M., Williams, K., LaRocca, T., Duke, V., Hambright, W.S., Ravuri, S.K., Bahney, C.S.,  
2178 Ehrhart, N., Huard, J., 2022. Mechanical strain drives exosome production, function, and miRNA  
2179 cargo in C2C12 muscle progenitor cells. J Orthop Res.

2180 Mwase, C., Phung, T.N., O'Sullivan, M.J., Mitchel, J.A., De Marzio, M., Kilic, A., Weiss, S.T.,  
2181 Fredberg, J.J., Park, J.A., 2022. Mechanical Compression of Human Airway Epithelial Cells  
2182 Induces Release of Extracellular Vesicles Containing Tenascin C. Cells 11(2).

2183 Najrana, T., Mahadeo, A., Abu-Eid, R., Kreienberg, E., Schulte, V., Uzun, A., Schorl, C.,  
2184 Goldberg, L., Quesenberry, P., Sanchez-Esteban, J., 2020. Mechanical stretch regulates the  
2185 expression of specific miRNA in extracellular vesicles released from lung epithelial cells. J Cell  
2186 Physiol 235(11), 8210-8223.

2187 Navasiolava, N.M., Dignat-George, F., Sabatier, F., Larina, I.M., Demiot, C., Forrat, J.-O.,  
2188 Gauquelin-Koch, G., Kozlovskaya, I.B., Custaud, M.-A., 2010. Enforced physical inactivity  
2189 increases endothelial microparticle levels in healthy volunteers. American Journal of Physiology-  
2190 Heart and Circulatory Physiology 299(2), H248-H256.

2191 Nguyen, K.T., Shukla, K.P., Moctezuma, M., Braden, A.R., Zhou, J., Hu, Z., Tang, L., 2009.  
2192 Studies of the cellular uptake of hydrogel nanospheres and microspheres by phagocytes,  
2193 vascular endothelial cells, and smooth muscle cells. J Biomed Mater Res A 88(4), 1022-1030.

2194 Nienow, A.W., 2006. Reactor engineering in large scale animal cell culture. *Cytotechnology*  
2195 50(1-3), 9-33.

2196 Nomura, S., Nakamura, T., Cone, J., Tandon, N.N., Kambayashi, J., 2000. Cytometric analysis  
2197 of high shear-induced platelet microparticles and effect of cytokines on microparticle generation.  
2198 *Cytometry* 40(3), 173-181.

2199 Nowak, A.A., Canis, K., Riddell, A., Laffan, M.A., McKinnon, T.A., 2012. O-linked glycosylation  
2200 of von Willebrand factor modulates the interaction with platelet receptor glycoprotein Ib under  
2201 static and shear stress conditions. *Blood* 120(1), 214-222.

2202 Paganini, C., Capasso Palmiero, U., Pocsfalvi, G., Touzet, N., Bongiovanni, A., Arosio, P.,  
2203 2019. Scalable Production and Isolation of Extracellular Vesicles: Available Sources and  
2204 Lessons from Current Industrial Bioprocesses. *Biotechnol J*, e1800528.

2205 Papaioannou, T.G., Stefanidis, C., 2005. Vascular wall shear stress: basic principles and  
2206 methods. *Hellenic J Cardiol* 46(1), 9-15.

2207 Papoutsakis, E.T., 1991. Fluid-mechanical damage of animal cells in bioreactors. *Trends in  
2208 biotechnology* 9 12, 427-437.

2209 Park, J.A., Sharif, A.S., Tschumperlin, D.J., Lau, L., Limbrey, R., Howarth, P., Drazen, J.M.,  
2210 2012. Tissue factor-bearing exosome secretion from human mechanically stimulated bronchial  
2211 epithelial cells in vitro and in vivo. *J Allergy Clin Immunol* 130(6), 1375-1383.

2212 Paszek, M.J., Zahir, N., Johnson, K.R., Lakins, J.N., Rozenberg, G.I., Gefen, A., Reinhart-King,  
2213 C.A., Margulies, S.S., Dembo, M., Boettiger, D., Hammer, D.A., Weaver, V.M., 2005. Tensional  
2214 homeostasis and the malignant phenotype. *Cancer Cell* 8(3), 241-254.

2215 Patel, D.B., Luthers, C.R., Lerman, M.J., Fisher, J.P., Jay, S.M., 2019. Enhanced extracellular  
2216 vesicle production and ethanol-mediated vascularization bioactivity via a 3D-printed scaffold-  
2217 perfusion bioreactor system. *Acta Biomater* 95, 236-244.

2218 Patel, D.B., Santoro, M., Born, L.J., Fisher, J.P., Jay, S.M., 2018. Towards rationally designed  
2219 biomanufacturing of therapeutic extracellular vesicles: impact of the bioproduction  
2220 microenvironment. *Biotechnol Adv* 36(8), 2051-2059.

2221 Patwardhan, S., Mahadik, P., Shetty, O., Sen, S., 2021. ECM stiffness-tuned exosomes drive  
2222 breast cancer motility through thrombospondin-1. *Biomaterials* 279, 121185.

2223 Petersen, J.F., McIntire, L.V., Papoutsakis, E.T., 1988. Shear sensitivity of cultured hybridoma  
2224 cells (CRL-8018) depends on mode of growth, culture age and metabolite concentration.  
2225 *Journal of Biotechnology* 7(3), 229-246.

2226 Petry, F., Salzig, D., 2021. Impact of Bioreactor Geometry on Mesenchymal Stem Cell  
2227 Production in Stirred-Tank Bioreactors. *Chemie Ingenieur Technik* 93(10), 1537-1554.

2228 Piffoux, M., Silva, A.K.A., Lugagne, J.B., Hersen, P., Wilhelm, C., Gazeau, F., 2017.  
2229 Extracellular Vesicle Production Loaded with Nanoparticles and Drugs in a Trade-off between  
2230 Loading, Yield and Purity: Towards a Personalized Drug Delivery System. *Adv Biosyst* 1(5),  
2231 e1700044.

2232 Pinto, A., Marangon, I., Mereaux, J., Nicolas-Boluda, A., Lavieu, G., Wilhelm, C., Sarda-Mantel,  
2233 L., Silva, A.K.A., Pocard, M., Gazeau, F., 2021. Immune Reprogramming Precision  
2234 Photodynamic Therapy of Peritoneal Metastasis by Scalable Stem-Cell-Derived Extracellular  
2235 Vesicles. *ACS Nano* 15(2), 3251-3263.

2236 Pironti, G., Strachan, R.T., Abraham, D., Mon-Wei Yu, S., Chen, M., Chen, W., Hanada, K.,  
2237 Mao, L., Watson, L.J., Rockman, H.A., 2015. Circulating Exosomes Induced by Cardiac  
2238 Pressure Overload Contain Functional Angiotensin II Type 1 Receptors. *Circulation* 131(24),  
2239 2120-2130.

2240 Pontiggia, L., Steiner, B., Ulrichs, H., Deckmyn, H., Forestier, M., Beer, J.H., 2006. Platelet  
2241 microparticle formation and thrombin generation under high shear are effectively suppressed by  
2242 a monoclonal antibody against GPIba. *Thromb Haemost* 96(12), 774-780.

2243 Qin, X., Zhang, K., Qiu, J., Wang, N., Qu, K., Cui, Y., Huang, J., Luo, L., Zhong, Y., Tian, T.,  
2244 Wu, W., Wang, Y., Wang, G., 2022. Uptake of oxidative stress-mediated extracellular vesicles  
2245 by vascular endothelial cells under low magnitude shear stress. *Bioact Mater* 9, 397-410.

2246 Raghavan, V., Rbaibi, Y., Pastor-Soler, N.M., Carattino, M.D., Weisz, O.A., 2014. Shear stress-  
2247 dependent regulation of apical endocytosis in renal proximal tubule cells mediated by primary  
2248 cilia. *Proc Natl Acad Sci U S A* 111(23), 8506-8511.

2249 Ramesan, S., Rezk, A.R., Dekiwadia, C., Cortez-Jugo, C., Yeo, L.Y., 2018. Acoustically-  
2250 mediated intracellular delivery. *Nanoscale* 10(27), 13165-13178.

2251 Ramkhelawon, B., Lehoux, S., Tedgui, A., Boulanger, C.M., 2008. Abstract 1910: Shear Stress  
2252 Modulates Endothelial Microparticles Shedding. *Circulation* 118(suppl\_18), S\_403-S\_403.

2253 Raposo, G., Stoorvogel, W., 2013. Extracellular vesicles: exosomes, microvesicles, and friends.  
2254 *J Cell Biol* 200(4), 373-383.

2255 Ratajczak, J., Wysoczynski, M., Hayek, F., Janowska-Wieczorek, A., Ratajczak, M.Z., 2006.  
2256 Membrane-derived microvesicles: important and underappreciated mediators of cell-to-cell  
2257 communication. *Leukemia* 20(9), 1487-1495.

2258 Ratajczak, M.Z., Ratajczak, J., 2020. Extracellular microvesicles/exosomes: discovery, disbelief,  
2259 acceptance, and the future? *Leukemia* 34(12), 3126-3135.

2260 Rautou, P.E., Vion, A.C., Amabile, N., Chironi, G., Simon, A., Tedgui, A., Boulanger, C.M.,  
2261 2011. Microparticles, vascular function, and atherothrombosis. *Circ Res* 109(5), 593-606.

2262 Reininger, A.J., Heijnen, H.F., Schumann, H., Specht, H.M., Schramm, W., Ruggeri, Z.M., 2006.  
2263 Mechanism of platelet adhesion to von Willebrand factor and microparticle formation under high  
2264 shear stress. *Blood* 107(9), 3537-3545.

2265 Rigamonti, A.E., Bollati, V., Pergoli, L., Iodice, S., De Col, A., Tamini, S., Cicolini, S., Tringali,  
2266 G., De Micheli, R., Cella, S.G., Sartorio, A., 2020. Effects of an acute bout of exercise on  
2267 circulating extracellular vesicles: tissue-, sex-, and BMI-related differences. *Int J Obes (Lond)*  
2268 44(5), 1108-1118.

2269 Roka-Moia, Y., Miller-Gutierrez, S., Palomares, D.E., Italiano, J.E., Sheriff, J., Bluestein, D.,  
2270 Slepian, M.J., 2021. Platelet Dysfunction During Mechanical Circulatory Support: Elevated  
2271 Shear Stress Promotes Downregulation of alphallbbeta3 and GPIb via Microparticle Shedding  
2272 Decreasing Platelet Aggregability. *Arterioscler Thromb Vasc Biol* 41(4), 1319-1336.

2273 Rouse, J.G., Haslauer, C.M., Loba, E.G., Monteiro-Riviere, N.A., 2008. Cyclic tensile strain  
2274 increases interactions between human epidermal keratinocytes and quantum dot nanoparticles.  
2275 *Toxicol In Vitro* 22(2), 491-497.

2276 Sakariassen, K.S., Holme, P.A., Orvim, U., Barstad, R.M., Solum, N.O., Brosstad, F.R., 1998.  
2277 Shear-induced platelet activation and platelet microparticle formation in native human blood.  
2278 *Thromb Res* 92(6 Suppl 2), S33-41.

2279 Samuel, S.P., Jain, N., O'Dowd, F., Paul, T., Kashanin, D., Gerard, V.A., Gun'ko, Y.K., Prina-  
2280 Mello, A., Volkov, Y., 2012. Multifactorial determinants that govern nanoparticle uptake by  
2281 human endothelial cells under flow. *Int J Nanomedicine* 7, 2943-2956.

2282 Scheffer, L.L., Sreetama, S.C., Sharma, N., Medikayala, S., Brown, K.J., Defour, A., Jaiswal,  
2283 J.K., 2014. Mechanism of Ca(2)(+)-triggered ESCRT assembly and regulation of cell membrane  
2284 repair. *Nat Commun* 5, 5646.

2285 Schmitz, C., Welck, J., Tavernaro, I., Grinberg, M., Rahnenfuhrer, J., Kiemer, A.K., van Thriel,  
2286 C., Hengstler, J.G., Kraegeloh, A., 2019. Mechanical strain mimicking breathing amplifies  
2287 alterations in gene expression induced by SiO<sub>2</sub> NPs in lung epithelial cells. *Nanotoxicology*  
2288 13(9), 1227-1243.

2289 Senger, R.S., Karim, M.N., 2003. Effect of shear stress on intrinsic CHO culture state and  
2290 glycosylation of recombinant tissue-type plasminogen activator protein. *Biotechnol Prog* 19(4),  
2291 1199-1209.

2292 Sengupta, V., Sengupta, S., Lazo, A., Woods, P., Nolan, A., Bremer, N., 2020. Exosomes  
2293 Derived from Bone Marrow Mesenchymal Stem Cells as Treatment for Severe COVID-19. *Stem  
2294 Cells Dev* 29(12), 747-754.

2295 Shah, N., Morsi, Y., Manasseh, R., 2014. From mechanical stimulation to biological pathways in  
2296 the regulation of stem cell fate. *Cell Biochem Funct* 32(4), 309-325.

2297 Shai, E., Rosa, I., Parguina, A.F., Motahedeh, S., Varon, D., Garcia, A., 2012. Comparative  
2298 analysis of platelet-derived microparticles reveals differences in their amount and proteome  
2299 depending on the platelet stimulus. *J Proteomics* 76 Spec No., 287-296.

2300 Shi, Y., Shao, J., Zhang, Z., Zhang, J., Lu, H., 2022. Effect of condylar chondrocyte exosomes  
2301 on condylar cartilage osteogenesis in rats under tensile stress. *Front Bioeng Biotechnol* 10,  
2302 1061855.

2303 Silva, T.O.C., Sales, A.R.K., Araujo, G.S.M., Fonseca, G.W.P., Braga, P.G.S., Faria, D., Rocha,  
2304 H.N.M., Rocha, N.G., Lima, M.F., Mady, C., Negrao, C.E., Alves, M., 2021. Disturbed Blood  
2305 Flow Acutely Increases Endothelial Microparticles and Decreases Flow Mediated Dilation in  
2306 Patients With Heart Failure With Reduced Ejection Fraction. *Front Physiol* 12, 629674.

2307 Sinha, B., Koster, D., Ruez, R., Gonnord, P., Bastiani, M., Abankwa, D., Stan, R.V., Butler-  
2308 Browne, G., Vedie, B., Johannes, L., Morone, N., Parton, R.G., Raposo, G., Sens, P., Lamaze,  
2309 C., Nassoy, P., 2011. Cells respond to mechanical stress by rapid disassembly of caveolae. *Cell*  
2310 144(3), 402-413.

2311 Smith, R.A., Hartley, R.C., Cocheme, H.M., Murphy, M.P., 2012. Mitochondrial pharmacology.  
2312 *Trends Pharmacol Sci* 33(6), 341-352.

2313 Sosdorf, M., Otto, G.P., Claus, R.A., Gabriel, H.H., Losche, W., 2010. Release of pro-  
2314 coagulant microparticles after moderate endurance exercise. *Platelets* 21(5), 389-391.

2315 Sosdorf, M., Otto, G.P., Claus, R.A., Gabriel, H.H., Losche, W., 2011. Cell-derived  
2316 microparticles promote coagulation after moderate exercise. *Med Sci Sports Exerc* 43(7), 1169-  
2317 1176.

2318 Stampfuss, J.J., Censarek, P., Fischer, J.W., Schror, K., Weber, A.A., 2006. Rapid release of  
2319 active tissue factor from human arterial smooth muscle cells under flow conditions. *Arterioscler*  
2320 *Thromb Vasc Biol* 26(5), e34-37.

2321 Staubach, S., Bauer, F.N., Tertel, T., Borger, V., Stambouli, O., Salzig, D., Giebel, B., 2021.  
2322 Scaled preparation of extracellular vesicles from conditioned media. *Adv Drug Deliv Rev* 177,  
2323 113940.

2324 Stone, A.P., Nikols, E., Freire, D., Machlus, K.R., 2022. The pathobiology of platelet and  
2325 megakaryocyte extracellular vesicles: A (c)lot has changed. *J Thromb Haemost* 20(7), 1550-  
2326 1558.

2327 Stukelj, R., Schara, K., Bedina-Zavec, A., Sustar, V., Pajnic, M., Paden, L., Krek, J.L., Kralj-Iglic,  
2328 V., Mrvar-Brecko, A., Jansa, R., 2017. Effect of shear stress in the flow through the sampling  
2329 needle on concentration of nanovesicles isolated from blood. *Eur J Pharm Sci* 98, 17-29.

2330 Stylianopoulos, T., Martin, J.D., Snuderl, M., Mpekris, F., Jain, S.R., Jain, R.K., 2013.  
2331 Coevolution of solid stress and interstitial fluid pressure in tumors during progression:  
2332 implications for vascular collapse. *Cancer Res* 73(13), 3833-3841.

2333 Sun, W., Han, D., Awad, M.A., Leibowitz, J.L., Griffith, B.P., Wu, Z.J., 2022. Role of thrombin to  
2334 non-physiological shear stress induced platelet activation and function alternation. *Thrombosis*  
2335 *Research* 219, 141-149.

2336 Sustar, V., Bedina-Zavec, A., Stukelj, R., Frank, M., Bobojevic, G., Jansa, R., Ogorevc, E.,  
2337 Kruljc, P., Mam, K., Simunic, B., Mancek-Keber, M., Jerala, R., Rozman, B., Veranic, P.,  
2338 Hagerstrand, H., Kralj-Iglic, V., 2011. Nanoparticles isolated from blood: a reflection of  
2339 vesiculability of blood cells during the isolation process. *Int J Nanomedicine* 6, 2737-2748.

2340 Takafuji, Y., Tatsumi, K., Kawao, N., Okada, K., Muratani, M., Kaji, H., 2021. Effects of fluid flow  
2341 shear stress to mouse muscle cells on the bone actions of muscle cell-derived extracellular  
2342 vesicless. *PLoS One* 16(5), e0250741.

2343 Tang, C., Hou, Y.X., Shi, P.X., Zhu, C.H., Lu, X., Wang, X.L., Que, L.L., Zhu, G.Q., Liu, L.,  
2344 Chen, Q., Li, C.F., Xu, Y., Li, J.T., Li, Y.H., 2023. Cardiomyocyte-specific Peli1 contributes to

2345 the pressure overload-induced cardiac fibrosis through miR-494-3p-dependent exosomal  
2346 communication. *FASEB J* 37(1), e22699.

2347 Tang, R., Mei, S., Xu, Q., Feng, J., Zhou, Y., Xing, S., He, Z., Gao, Y., 2022. ASK1-ER stress  
2348 pathway-mediated fibrotic-EV release contributes to the interaction of alveolar epithelial cells  
2349 and lung fibroblasts to promote mechanical ventilation-induced pulmonary fibrosis. *Exp Mol Med*  
2350 54(12), 2162-2174.

2351 Thery, C., Witwer, K.W., Aikawa, E., Alcaraz, M.J., Anderson, J.D., Andriantsitohaina, R.,  
2352 Antoniou, A., Arab, T., Archer, F., Atkin-Smith, G.K., Ayre, D.C., Bach, J.M., Bachurski, D.,  
2353 Baharvand, H., Balaj, L., Baldacchino, S., Bauer, N.N., Baxter, A.A., Bebawy, M., Beckham, C.,  
2354 Bedina Zavec, A., Benmoussa, A., Berardi, A.C., Bergese, P., Bielska, E., Blenkiron, C., Bobis-  
2355 Wozowicz, S., Boilard, E., Boireau, W., Bongiovanni, A., Borras, F.E., Bosch, S., Boulanger,  
2356 C.M., Breakefield, X., Breglio, A.M., Brennan, M.A., Brigstock, D.R., Brisson, A., Broekman,  
2357 M.L., Bromberg, J.F., Bryl-Gorecka, P., Buch, S., Buck, A.H., Burger, D., Busatto, S.,  
2358 Buschmann, D., Bussolati, B., Buzas, E.I., Byrd, J.B., Camussi, G., Carter, D.R., Caruso, S.,  
2359 Chamley, L.W., Chang, Y.T., Chen, C., Chen, S., Cheng, L., Chin, A.R., Clayton, A., Clerici,  
2360 S.P., Cocks, A., Cocucci, E., Coffey, R.J., Cordeiro-da-Silva, A., Couch, Y., Coumans, F.A.,  
2361 Coyle, B., Crescitelli, R., Criado, M.F., D'Souza-Schorey, C., Das, S., Datta Chaudhuri, A., de  
2362 Candia, P., De Santana, E.F., De Wever, O., Del Portillo, H.A., Demaret, T., Deville, S., Devitt,  
2363 A., Dhondt, B., Di Vizio, D., Dieterich, L.C., Dolo, V., Dominguez Rubio, A.P., Dominici, M.,  
2364 Dourado, M.R., Driedonks, T.A., Duarte, F.V., Duncan, H.M., Eichenberger, R.M., Ekstrom, K.,  
2365 El Andaloussi, S., Elie-Caille, C., Erdbrugger, U., Falcon-Perez, J.M., Fatima, F., Fish, J.E.,  
2366 Flores-Bellver, M., Forsonits, A., Frelet-Barrand, A., Fricke, F., Fuhrmann, G., Gabrielsson, S.,  
2367 Gamez-Valero, A., Gardiner, C., Gartner, K., Gaudin, R., Gho, Y.S., Giebel, B., Gilbert, C.,  
2368 Gimona, M., Giusti, I., Goberdhan, D.C., Gorgens, A., Gorski, S.M., Greening, D.W., Gross,  
2369 J.C., Gualerzi, A., Gupta, G.N., Gustafson, D., Handberg, A., Haraszti, R.A., Harrison, P.,  
2370 Hegyesi, H., Hendrix, A., Hill, A.F., Hochberg, F.H., Hoffmann, K.F., Holder, B., Holthofer, H.,  
2371 Hosseinkhani, B., Hu, G., Huang, Y., Huber, V., Hunt, S., Ibrahim, A.G., Ikezu, T., Inal, J.M.,  
2372 Isin, M., Ivanova, A., Jackson, H.K., Jacobsen, S., Jay, S.M., Jayachandran, M., Jenster, G.,  
2373 Jiang, L., Johnson, S.M., Jones, J.C., Jong, A., Jovanovic-Talisman, T., Jung, S., Kalluri, R.,  
2374 Kano, S.I., Kaur, S., Kawamura, Y., Keller, E.T., Khamari, D., Khomyakova, E., Khvorova, A.,  
2375 Kierulf, P., Kim, K.P., Kislinger, T., Klingeborn, M., Klinke, D.J., 2nd, Kornek, M., Kosanovic,  
2376 M.M., Kovacs, A.F., Kramer-Albers, E.M., Krasemann, S., Krause, M., Kurochkin, I.V., Kusuma,  
2377 G.D., Kuypers, S., Laitinen, S., Langevin, S.M., Languino, L.R., Lannigan, J., Lasser, C.,  
2378 Laurent, L.C., Lavieu, G., Lazaro-Ibanez, E., Le Lay, S., Lee, M.S., Lee, Y.X.F., Lemos, D.S.,  
2379 Lenassi, M., Leszczynska, A., Li, I.T., Liao, K., Libregts, S.F., Ligeti, E., Lim, R., Lim, S.K., Line,  
2380 A., Linnemannstons, K., Llorente, A., Lombard, C.A., Lorenowicz, M.J., Lorincz, A.M., Lotvall, J.,  
2381 Lovett, J., Lowry, M.C., Loyer, X., Lu, Q., Lukomska, B., Lunavat, T.R., Maas, S.L., Malhi, H.,  
2382 Marcilla, A., Mariani, J., Mariscal, J., Martens-Uzunova, E.S., Martin-Jaular, L., Martinez, M.C.,  
2383 Martins, V.R., Mathieu, M., Mathivanan, S., Maugeri, M., McGinnis, L.K., McVey, M.J., Meckes,  
2384 D.G., Jr., Meehan, K.L., Mertens, I., Minciachchi, V.R., Moller, A., Moller Jorgensen, M., Morales-  
2385 Kastresana, A., Morhayim, J., Mullier, F., Muraca, M., Musante, L., Mussack, V., Muth, D.C.,  
2386 Myburgh, K.H., Najrana, T., Nawaz, M., Nazarenko, I., Nejsum, P., Neri, C., Neri, T., Nieuwland,  
2387 R., Nimrichter, L., Nolan, J.P., Nolte-'t Hoen, E.N., Noren Hooten, N., O'Driscoll, L., O'Grady, T.,  
2388 O'Loghlen, A., Ochiya, T., Olivier, M., Ortiz, A., Ortiz, L.A., Osteikoetxea, X., Ostergaard, O.,  
2389 Ostrowski, M., Park, J., Pegtel, D.M., Peinado, H., Perut, F., Pfaffl, M.W., Phinney, D.G.,  
2390 Pieters, B.C., Pink, R.C., Pisetsky, D.S., Pogge von Strandmann, E., Polakovicova, I., Poon,  
2391 I.K., Powell, B.H., Prada, I., Pulliam, L., Quesenberry, P., Radeghieri, A., Raffai, R.L.,  
2392 Raimondo, S., Rak, J., Ramirez, M.I., Raposo, G., Rayyan, M.S., Regev-Rudzki, N., Ricklefs,  
2393 F.L., Robbins, P.D., Roberts, D.D., Rodrigues, S.C., Rohde, E., Rome, S., Rouschop, K.M.,

2394 Rughetti, A., Russell, A.E., Saa, P., Sahoo, S., Salas-Huenuleo, E., Sanchez, C., Saugstad,  
2395 J.A., Saul, M.J., Schiffelers, R.M., Schneider, R., Schoyen, T.H., Scott, A., Shahaj, E., Sharma,  
2396 S., Shatnyeva, O., Shekari, F., Shelke, G.V., Shetty, A.K., Shiba, K., Siljander, P.R., Silva, A.M.,  
2397 Skowronek, A., Snyder, O.L., 2nd, Soares, R.P., Sodar, B.W., Soekmadji, C., Sotillo, J., Stahl,  
2398 P.D., Stoorvogel, W., Stott, S.L., Strasser, E.F., Swift, S., Tahara, H., Tewari, M., Timms, K.,  
2399 Tiwari, S., Tixeira, R., Tkach, M., Toh, W.S., Tomasini, R., Torrecilhas, A.C., Tosar, J.P.,  
2400 Toxavidis, V., Urbanelli, L., Vader, P., van Balkom, B.W., van der Grein, S.G., Van Deun, J., van  
2401 Herwijnen, M.J., Van Keuren-Jensen, K., van Niel, G., van Royen, M.E., van Wijnen, A.J.,  
2402 Vasconcelos, M.H., Vechetti, I.J., Jr., Veit, T.D., Vella, L.J., Velot, E., Verweij, F.J., Vestad, B.,  
2403 Vinas, J.L., Visnovitz, T., Vukman, K.V., Wahlgren, J., Watson, D.C., Wauben, M.H., Weaver,  
2404 A., Webber, J.P., Weber, V., Wehman, A.M., Weiss, D.J., Welsh, J.A., Wendt, S., Wheelock,  
2405 A.M., Wiener, Z., Witte, L., Wolfram, J., Xagorari, A., Xander, P., Xu, J., Yan, X., Yanez-Mo, M.,  
2406 Yin, H., Yuana, Y., Zappulli, V., Zarubova, J., Zekas, V., Zhang, J.Y., Zhao, Z., Zheng, L.,  
2407 Zheutlin, A.R., Zickler, A.M., Zimmermann, P., Zivkovic, A.M., Zocco, D., Zuba-Surma, E.K.,  
2408 2018. Minimal information for studies of extracellular vesicles 2018 (MISEV2018): a position  
2409 statement of the International Society for Extracellular Vesicles and update of the MISEV2014  
2410 guidelines. *J Extracell Vesicles* 7(1), 1535750.

2411 Thomas, C.R., 1993. Chapter 6 - Shear effects on cells in bioreactors, in: Shamlou, P.A. (Ed.)  
2412 Processing of Solid–Liquid Suspensions. Butterworth-Heinemann, pp. 158-191.

2413 Trajkovic, K., Hsu, C., Chiantia, S., Rajendran, L., Wenzel, D., Wieland, F., Schwille, P.,  
2414 Brugger, B., Simons, M., 2008. Ceramide Triggers Budding of Exosome Vesicles into  
2415 Multivesicular Endosomes. *Science* 319(5867), 1244-1247.

2416 Tremblay, J.C., Thom, S.R., Yang, M., Ainslie, P.N., 2017. Oscillatory shear stress, flow-  
2417 mediated dilatation, and circulating microparticles at sea level and high altitude. *Atherosclerosis*  
2418 256, 115-122.

2419 Tsai, A.C., Jeske, R., Chen, X., Yuan, X., Li, Y., 2020. Influence of Microenvironment on  
2420 Mesenchymal Stem Cell Therapeutic Potency: From Planar Culture to Microcarriers. *Front  
2421 Bioeng Biotechnol* 8, 640.

2422 Tsai, C.L., Huang, C.Y., Lu, Y.C., Pai, L.M., Horak, D., Ma, Y.H., 2022. Cyclic Strain Mitigates  
2423 Nanoparticle Internalization by Vascular Smooth Muscle Cells. *Int J Nanomedicine* 17, 969-981.

2424 Ueda, A., Shimomura, M., Ikeda, M., Yamaguchi, R., Tanishita, K., 2004. Effect of glycocalyx on  
2425 shear-dependent albumin uptake in endothelial cells. *Am J Physiol Heart Circ Physiol* 287(5),  
2426 H2287-2294.

2427 van Niel, G., D'Angelo, G., Raposo, G., 2018. Shedding light on the cell biology of extracellular  
2428 vesicles. *Nature Reviews: Molecular Cell Biology* 19, 213-228.

2429 Vangapandu, H., Robertson, M., Colchado, D., Templeman, N., Li, H., Ning, Y., Blum, A.,  
2430 Bollyky, P., Keswani, S., Coarfa, C., Balaji, S., 2019. MECHANICAL TENSION INFLUENCES  
2431 THE REGULATORY LANDSCAPE OF MSC-DERIVED EXOSOMES DURING WOUND  
2432 HEALING, WOUND REPAIR AND REGENERATION. pp. A2-A3.

2433 Vechetti, I.J., Jr., Peck, B.D., Wen, Y., Walton, R.G., Valentino, T.R., Alimov, A.P., Dungan,  
2434 C.M., Van Pelt, D.W., von Walden, F., Alkner, B., Peterson, C.A., McCarthy, J.J., 2021.

2435 Mechanical overload-induced muscle-derived extracellular vesicles promote adipose tissue  
2436 lipolysis. *FASEB J* 35(6), e21644.

2437 Vickroy, B., Lorenz, K., Kelly, W., 2007. Modeling Shear Damage to Suspended CHO Cells  
2438 during Cross-Flow Filtration. *Biotechnology Progress* 23(1), 194-199.

2439 Villasante, A., Marturano-Kruik, A., Ambati, S.R., Liu, Z., Godier-Furnemont, A., Parsa, H., Lee,  
2440 B.W., Moore, M.A., Vunjak-Novakovic, G., 2016. Recapitulating the Size and Cargo of Tumor  
2441 Exosomes in a Tissue-Engineered Model. *Theranostics* 6(8), 1119-1130.

2442 Vining, K.H., Mooney, D.J., 2017. Mechanical forces direct stem cell behaviour in development  
2443 and regeneration. *Nat Rev Mol Cell Biol* 18(12), 728-742.

2444 Vion, A.C., Birukova, A.A., Boulanger, C.M., Birukov, K.G., 2013a. Mechanical forces stimulate  
2445 endothelial microparticle generation via caspase-dependent apoptosis-independent mechanism.  
2446 *Pulm Circ* 3(1), 95-99.

2447 Vion, A.C., Ramkhelawon, B., Loyer, X., Chironi, G., Devue, C., Loirand, G., Tedgui, A., Lehoux,  
2448 S., Boulanger, C.M., 2013b. Shear stress regulates endothelial microparticle release. *Circ Res*  
2449 112(10), 1323-1333.

2450 Wada, S., Kanzaki, H., Narimiya, T., Nakamura, Y., 2017. Novel device for application of  
2451 continuous mechanical tensile strain to mammalian cells. *Biol Open* 6(4), 518-524.

2452 Wan, Y., Xia, Y.Q., Zheng, S.Y., 2022. Extruded small extracellular vesicles: splinters of  
2453 circulating tumour cells may promote cancer metastasis? *Br J Cancer* 127(7), 1180-1183.

2454 Wang, J., Nikonorova, I.A., Gu, A., Sternberg, P.W., Barr, M.M., 2020. Release and targeting of  
2455 polycystin-2-carrying ciliary extracellular vesicles. *Curr Biol* 30(13), R755-R756.

2456 Wang, J.H., Li, B., 2010. Mechanics rules cell biology. *Sports Med Arthrosc Rehabil Ther  
2457 Technol* 2, 16.

2458 Wang, K., Wei, Y., Liu, W., Liu, L., Guo, Z., Fan, C., Wang, L., Hu, J., Li, B., 2019. Mechanical  
2459 Stress-Dependent Autophagy Component Release via Extracellular Nanovesicles in Tumor  
2460 Cells. *ACS Nano* 13(4), 4589-4602.

2461 Wang, L., Bao, H., Wang, K.X., Zhang, P., Yao, Q.P., Chen, X.H., Huang, K., Qi, Y.X., Jiang,  
2462 Z.L., 2017. Secreted miR-27a Induced by Cyclic Stretch Modulates the Proliferation of  
2463 Endothelial Cells in Hypertension via GRK6. *Sci Rep* 7, 41058.

2464 Wang, S., Godfrey, S., Ravikrishnan, J., Lin, H., Vogel, J., Coffman, J., 2017. Shear  
2465 contributions to cell culture performance and product recovery in ATF and TFF perfusion  
2466 systems. *J Biotechnol* 246, 52-60.

2467 Wang, Y., Goliwas, K.F., Severino, P.E., Hough, K.P., Van Vessem, D., Wang, H., Tousif, S.,  
2468 Koomullil, R.P., Frost, A.R., Ponnazhagan, S., Berry, J.L., Deshane, J.S., 2020. Mechanical  
2469 strain induces phenotypic changes in breast cancer cells and promotes immunosuppression in  
2470 the tumor microenvironment. *Lab Invest* 100(12), 1503-1516.

2471 Wang, Y., Jia, L., Zheng, Y., Li, W., 2018. Bone remodeling induced by mechanical forces is  
2472 regulated by miRNAs. *Biosci Rep* 38(4).

2473 Wang, Y., Xie, W., Feng, Y., Xu, Z., He, Y., Xiong, Y., Chen, L., Li, X., Liu, J., Liu, G., Wu, Q.,  
2474 Wang, Y., Xie, W., Feng, Y., Xu, Z., He, Y., Xiong, Y., Chen, L., Li, X., Liu, J., Liu, G., Wu, Q.,  
2475 2022. Epithelial-derived exosomes promote M2 macrophage polarization via Notch2/SOCS1  
2476 during mechanical ventilation. *Int J Mol Med* 50(1), 96.

2477 Wang, Y.U.E., Zheng, Y., Li, W., 2021. Exosomes derived from osteoclasts under compression  
2478 stress inhibit osteoblast differentiation. *Biocell* 45(2), 427-444.

2479 Wang, Z., Maruyama, K., Sakisaka, Y., Suzuki, S., Tada, H., Suto, M., Saito, M., Yamada, S.,  
2480 Nemoto, E., 2019. Cyclic Stretch Force Induces Periodontal Ligament Cells to Secrete  
2481 Exosomes That Suppress IL-1beta Production Through the Inhibition of the NF-kappaB  
2482 Signaling Pathway in Macrophages. *Front Immunol* 10, 1310.

2483 Watson, D.C., Yung, B.C., Bergamaschi, C., Chowdhury, B., Bear, J., Stellas, D., Morales-  
2484 Kastresana, A., Jones, J.C., Felber, B.K., Chen, X., Pavlakis, G.N., 2018. Scalable, cGMP-  
2485 compatible purification of extracellular vesicles carrying bioactive human heterodimeric IL-  
2486 15/lactadherin complexes. *J Extracell Vesicles* 7(1), 1442088.

2487 Weber, A., Liu, S.S., Cardone, L., Rellecke, P., Sixt, S.U., Lichtenberg, A., Akhyari, P., 2020.  
2488 The Course of Circulating Small Extracellular Vesicles in Patients Undergoing Surgical Aortic  
2489 Valve Replacement. *Biomed Res Int* 2020, 6381396.

2490 Wen, Y., Fu, Q., Soliwoda, A., Zhang, S., Zheng, M., Mao, W., Wan, Y., 2022. Cell-derived  
2491 nanovesicles prepared by membrane extrusion are good substitutes for natural extracellular  
2492 vesicles. *Extracell Vesicle* 1.

2493 Wiklander, O.P.B., Brennan, M.A., Lotvall, J., Breakefield, X.O., El Andaloussi, S., 2019.  
2494 Advances in therapeutic applications of extracellular vesicles. *Sci Transl Med* 11(492).

2495 Wilhelm, E.N., Gonzalez-Alonso, J., Chiesa, S.T., Trangmar, S.J., Kalsi, K.K., Rakobowchuk,  
2496 M., 2017. Whole-body heat stress and exercise stimulate the appearance of platelet  
2497 microvesicles in plasma with limited influence of vascular shear stress. *Physiol Rep* 5(21).

2498 Wilhelm, E.N., Gonzalez-Alonso, J., Parris, C., Rakobowchuk, M., 2016. Exercise intensity  
2499 modulates the appearance of circulating microvesicles with proangiogenic potential upon  
2500 endothelial cells. *Am J Physiol Heart Circ Physiol* 311(5), H1297-H1310.

2501 Williams, C., Royo, F., Aizpurua-Olaizola, O., Pazos, R., Boons, G.J., Reichardt, N.C., Falcon-  
2502 Perez, J.M., 2018. Glycosylation of extracellular vesicles: current knowledge, tools and clinical  
2503 perspectives. *J Extracell Vesicles* 7(1), 1442985.

2504 Wittkowske, C., Reilly, G.C., Lacroix, D., Perrault, C.M., 2016. In Vitro Bone Cell Models: Impact  
2505 of Fluid Shear Stress on Bone Formation. *Frontiers in Bioengineering and Biotechnology* 4.

2506 Wu, B., Liu, D.A., Guan, L., Myint, P.K., Chin, L., Dang, H., Xu, Y., Ren, J., Li, T., Yu, Z.,  
2507 Jabban, S., Mills, G.B., Nukpezah, J., Chen, Y.H., Furth, E.E., Gimotty, P.A., Wells, R.G.,  
2508 Weaver, V.M., Radhakrishnan, R., Wang, X.W., Guo, W., 2023. Stiff matrix induces exosome  
2509 secretion to promote tumour growth. *Nat Cell Biol* 25(3), 415-424.

2510 Wu, J., Wu, D., Wu, G., Bei, H.P., Li, Z., Xu, H., Wang, Y., Wu, D., Liu, H., Shi, S., Zhao, C., Xu,  
2511 Y., He, Y., Li, J., Wang, C., Zhao, X., Wang, S., 2022. Scale-out production of extracellular  
2512 vesicles derived from natural killer cells via mechanical stimulation in a seesaw-motion  
2513 bioreactor for cancer therapy. *Biofabrication* 14(4).

2514 Wu, X., Liu, Z., Hu, L., Gu, W., Zhu, L., 2018. Exosomes derived from endothelial progenitor  
2515 cells ameliorate acute lung injury by transferring miR-126. *Exp Cell Res* 370(1), 13-23.

2516 Xia, B., Gao, J., Li, S., Huang, L., Zhu, L., Ma, T., Zhao, L., Yang, Y., Luo, K., Shi, X., Mei, L.,  
2517 Zhang, H., Zheng, Y., Lu, L., Luo, Z., Huang, J., 2020. Mechanical stimulation of Schwann cells  
2518 promote peripheral nerve regeneration via extracellular vesicle-mediated transfer of microRNA  
2519 23b-3p. *Theranostics* 10(20), 8974-8995.

2520 Xiao, F., Zuo, B., Tao, B., Wang, C., Li, Y., Peng, J., Shen, C., Cui, Y., Zhu, J., Chen, X., 2021.  
2521 Exosomes derived from cyclic mechanical stretch-exposed bone marrow mesenchymal stem  
2522 cells inhibit RANKL-induced osteoclastogenesis through the NF- $\kappa$ B signaling pathway. *Ann  
2523 Transl Med* 9(9), 798.

2524 Xiao, W., Pahlavanneshan, M., Eun, C.-Y., Zhang, X., DeKalb, C., Mahgoub, B., Knaneh-  
2525 Monem, H., Shah, S., Sohrabi, A., Seidlits, S.K., Hill, R., 2022. Matrix stiffness mediates  
2526 pancreatic cancer chemoresistance through induction of exosome hypersecretion in a cancer  
2527 associated fibroblasts-tumor organoid biomimetic model. *Matrix Biology Plus* 14.

2528 Xie, F., Wen, G., Sun, W., Jiang, K., Chen, T., Chen, S., Wen, J., 2020. Mechanical stress  
2529 promotes angiogenesis through fibroblast exosomes. *Biochem Biophys Res Commun* 533(3),  
2530 346-353.

2531 Yamamoto, K., Ando, J., 2015. Vascular endothelial cell membranes differentiate between  
2532 stretch and shear stress through transitions in their lipid phases. *Am J Physiol Heart Circ  
2533 Physiol* 309(7), H1178-1185.

2534 Yamamoto, K., Furuya, K., Nakamura, M., Kobatake, E., Sokabe, M., Ando, J., 2011.  
2535 Visualization of flow-induced ATP release and triggering of Ca<sup>2+</sup> waves at caveolae in vascular  
2536 endothelial cells. *J Cell Sci* 124(Pt 20), 3477-3483.

2537 Yamamoto, K., Imamura, H., Ando, J., 2018. Shear stress augments mitochondrial ATP  
2538 generation that triggers ATP release and Ca(2+) signaling in vascular endothelial cells. *Am J  
2539 Physiol Heart Circ Physiol* 315(5), H1477-H1485.

2540 Yang, L., Zhai, Y., Hao, Y., Zhu, Z., Cheng, G., 2020. The Regulatory Functionality of  
2541 Exosomes Derived from hUMSCs in 3D Culture for Alzheimer's Disease Therapy. *Small* 16(3),  
2542 1906273.

2543 Yu, H.-S., Kim, J.-J., Kim, H.-W., Lewis, M.P., Wall, I., 2016. Impact of mechanical stretch on  
2544 the cell behaviors of bone and surrounding tissues. *Journal of Tissue Engineering* 7.

2545 Yu, Q., Wang, D., Wen, X., Tang, X., Qi, D., He, J., Zhao, Y., Deng, W., Zhu, T., 2020. Adipose-  
2546 derived exosomes protect the pulmonary endothelial barrier in ventilator-induced lung injury by  
2547 inhibiting the TRPV4/Ca(2+) signaling pathway. *Am J Physiol Lung Cell Mol Physiol* 318(4),  
2548 L723-L741.

2549 Yu, W., Chen, C., Kou, X., Sui, B., Yu, T., Liu, D., Wang, R., Wang, J., Shi, S., 2021.  
2550 Mechanical force-driven TNFalpha endocytosis governs stem cell homeostasis. *Bone Res* 8(1),  
2551 44.

2552 Yu, W., Su, X., Li, M., Wan, W., Li, A., Zhou, H., Xu, F., 2021. Three-dimensional mechanical  
2553 microenvironment enhanced osteogenic activity of mesenchymal stem cells-derived exosomes.  
2554 *Chemical Engineering Journal* 417.

2555 Yuan, J., Liu, H., Gao, W., Zhang, L., Ye, Y., Yuan, L., Ding, Z., Wu, J., Kang, L., Zhang, X.,  
2556 Wang, X., Zhang, G., Gong, H., Sun, A., Yang, X., Chen, R., Cui, Z., Ge, J., Zou, Y., 2018.  
2557 MicroRNA-378 suppresses myocardial fibrosis through a paracrine mechanism at the early  
2558 stage of cardiac hypertrophy following mechanical stress. *Theranostics* 8(9), 2565-2582.

2559 Zhang, Y., Chopp, M., Zhang, Z.G., Katakowski, M., Xin, H., Qu, C., Ali, M., Mahmood, A.,  
2560 Xiong, Y., 2017. Systemic administration of cell-free exosomes generated by human bone  
2561 marrow derived mesenchymal stem cells cultured under 2D and 3D conditions improves  
2562 functional recovery in rats after traumatic brain injury. *Neurochemistry International* 111, 69-81.

2563 Zhang, Y., Zhang, T., Zhang, Z., Su, J., Wu, X., Chen, L., Ge, X., Wang, X., Jiang, N., 2022.  
2564 Periodontal ligament cells derived small extracellular vesicles are involved in orthodontic tooth  
2565 movement. *Eur J Orthod* 44(6), 690-697.

2566 Zhao, M., Ma, Q., Zhao, Z., Guan, X., Bai, Y., 2021. Periodontal ligament fibroblast-derived  
2567 exosomes induced by compressive force promote macrophage M1 polarization via Yes-  
2568 associated protein. *Arch Oral Biol* 132, 105263.

2569 Zhou, Y., Li, P., Goodwin, A.J., Cook, J.A., Halushka, P.V., Chang, E., Fan, H., 2018.  
2570 Exosomes from Endothelial Progenitor Cells Improve the Outcome of a Murine Model of Sepsis.  
2571 *Mol Ther* 26(5), 1375-1384.

2572 Zhuang, F., Bao, H., Shi, Q., Li, J., Jiang, Z.L., Wang, Y., Qi, Y.X., 2020a. Endothelial  
2573 microparticles induced by cyclic stretch activate Src and modulate cell apoptosis. *FASEB J*  
2574 34(10), 13586-13596.

2575 Zhuang, F., Shi, Q., Wang, W.B., Bao, H., Yan, J., Gao, S., Liu, Z., Jiang, Z.L., Qi, Y.X., 2020b.  
2576 Endothelial microvesicles induced by physiological cyclic stretch inhibit ICAM1-Dependent  
2577 leukocyte adhesion. *Exp Cell Res* 386(1), 111710.

2578 Zwaal, R.F.A., Schroit, A.J., 1997. Pathophysiologic Implications of Membrane Phospholipid  
2579 Asymmetry in Blood Cells. *Blood* 89(4), 1121-1132.  
2580  
2581  
2582  
2583  
2584  
2585  
2586  
2587  
2588  
2589  
2590

2591 **Figures:**

2592  
2593 **Figure 1. The biology of extracellular vesicles.** Exosomes (small EVs, generally 30-100 nm)  
2594 are formed when intraluminal vesicles produced via the inward budding of multivesicular body  
2595 (MVB) membranes are released into the extracellular space following MVB exocytosis.  
2596 Microparticles (large EVs, generally 100-1,000 nm) form as a result of the direct outward  
2597 budding of the plasma membrane. In both EV types, cargo is selectively loaded. EVs bind with  
2598 target cells and are taken up via either membrane fusion or endocytosis.  
2599

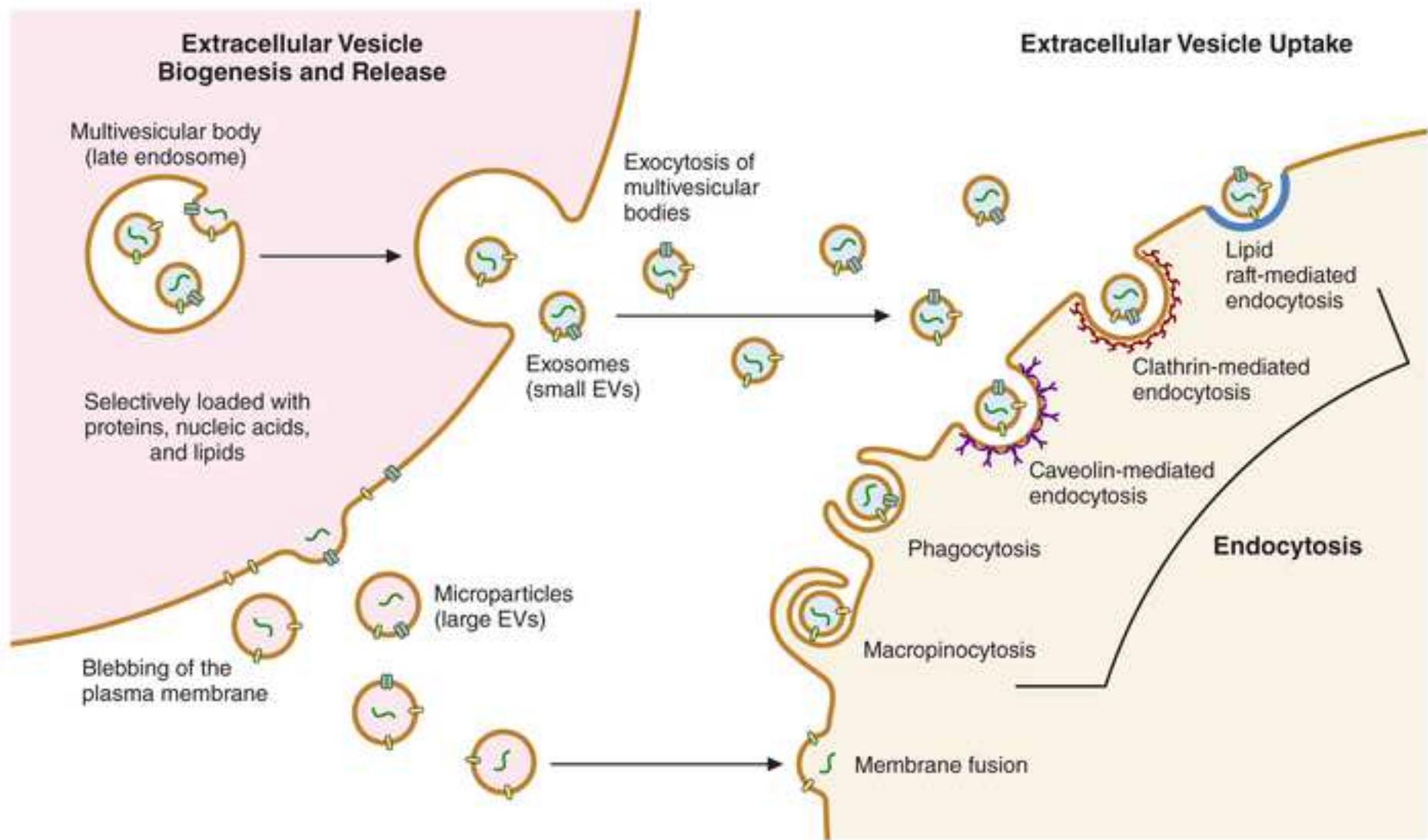
2600 **Figure 2. Basic biomechanical forces, their applications, and their manifestations in**  
2601 **bioreactors.** Cells and EVs experience biomechanical forces as shear, tension, compression,  
2602 or some combination thereof. Lab-scale application of each individual type of force can involve a  
2603 variety of techniques and equipment. In most bioreactors, the individual effects of these forces  
2604 combine to create complex biomechanical stimulation.  
2605

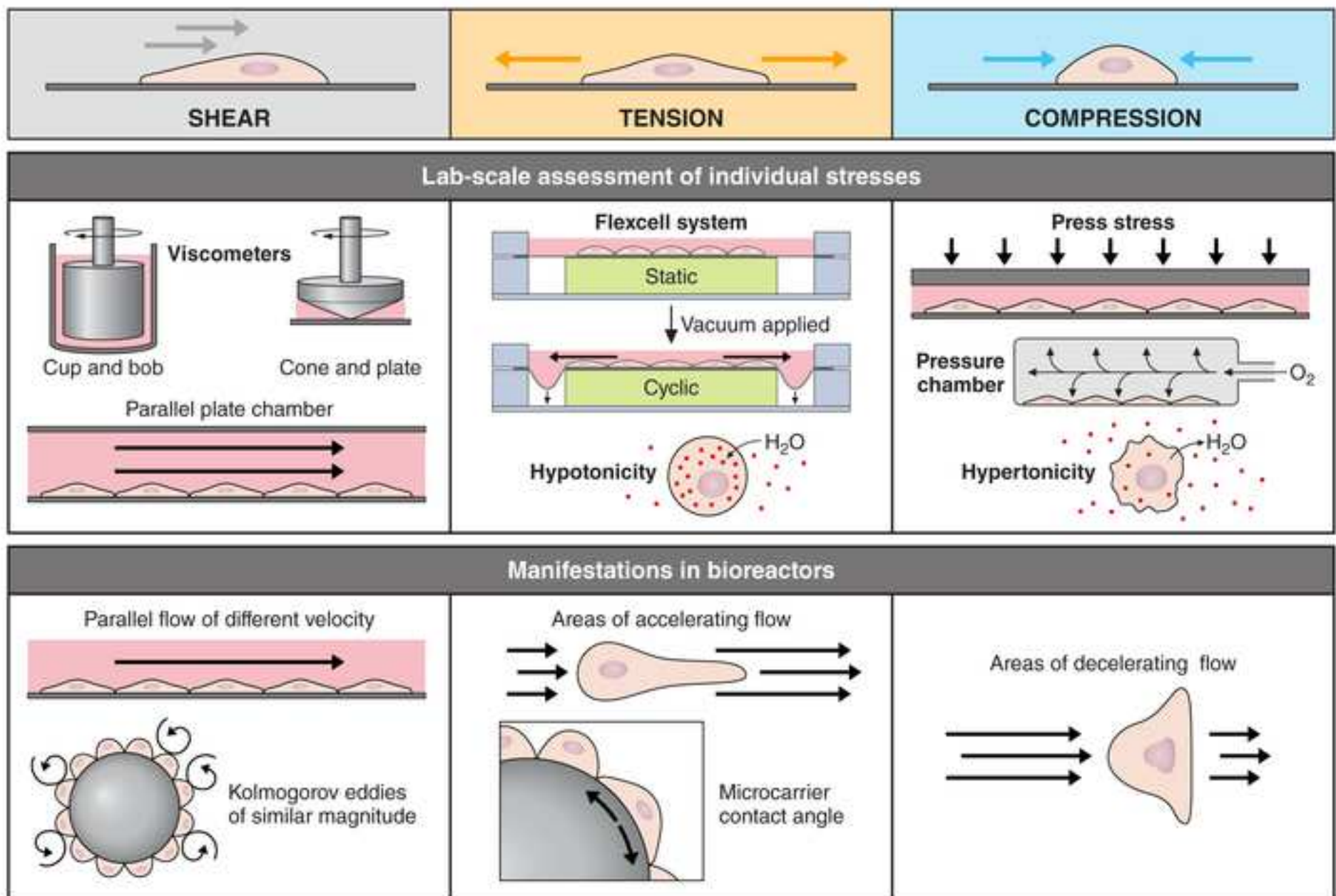
2606 **Figure 3. Mechanisms for the impact of biomechanical force on EV biogenesis.**  
2607 Mechanisms for EV biogenesis under biomechanical stress are numerous. Non-apoptotic  
2608 caspase action—initiated by several pathways and mediated by mitochondrial dysfunction—is  
2609 one mechanism of note. Alternatively, influxes in intracellular  $\text{Ca}^{2+}$  levels may activate PKC  
2610 and/or calpain, promote PS externalization, and trigger actomyosin contractions on the plasma  
2611 membrane. Additional EV release can occur during ESCRT-mediated repair of  $\text{Ca}^{2+}$  membrane  
2612 channels. Mitochondrial dysfunction may further exacerbate the flood of  $\text{Ca}^{2+}$  via the binding of  
2613 cytochrome c to the ER and/or release of extracellular ATP. Various integrin signaling pathways  
2614 can independently mediate EV biogenesis via PKC, ERK, or RhoA/ROCK activity. In some  
2615 cases, stress-induced nuclear import of YAP may result in transcriptional regulation of EV  
2616 biogenesis. Shear can directly sever protrusions on the plasma membrane (as in the case of  
2617 platelet EVs), while tension and compression may upregulate MVB exocytosis and plasma  
2618 membrane blebbing, respectively.  
2619

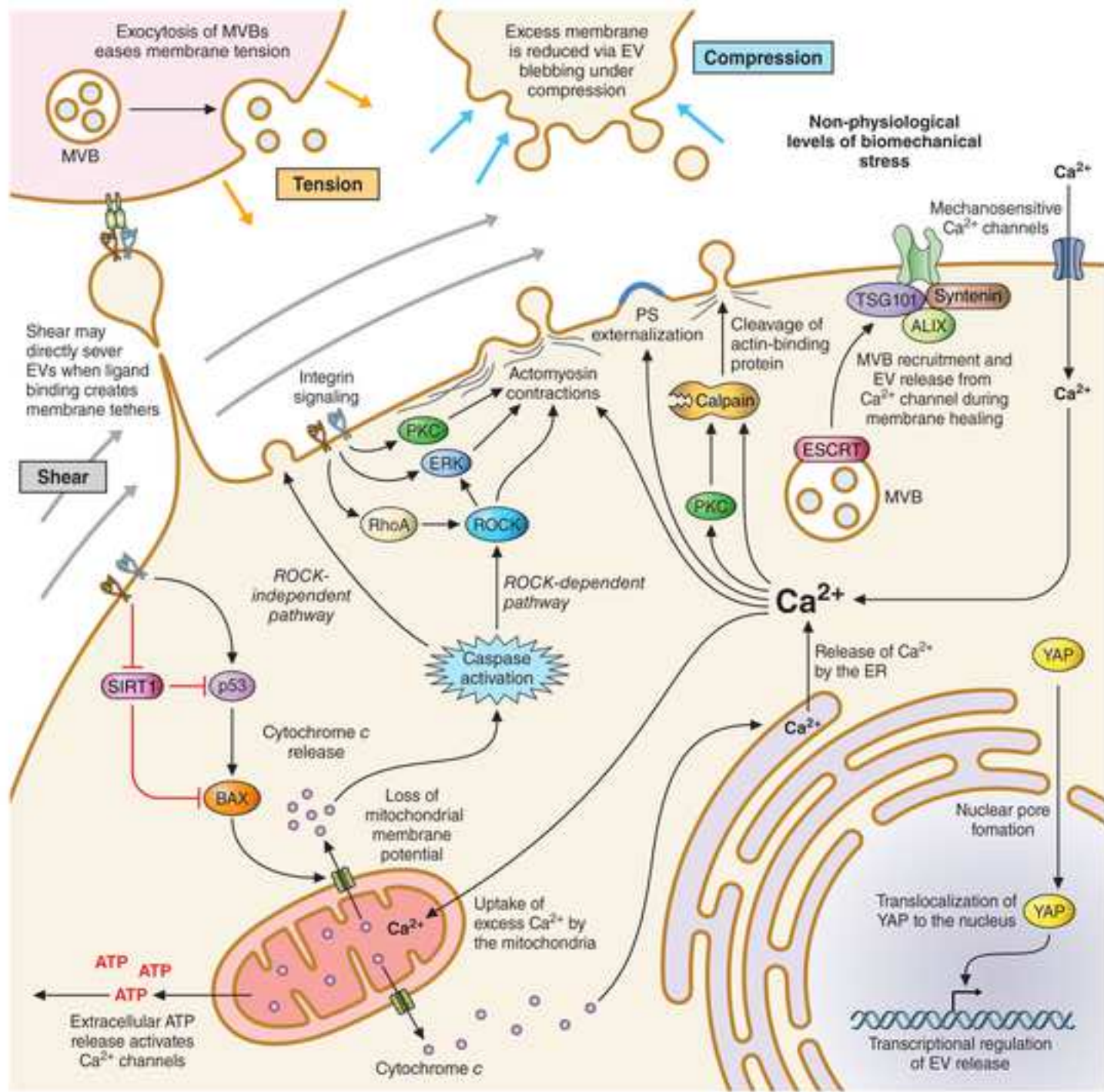
2620 **Figure 4. EV cargo loading *in vivo* for selected cases of aberrant biomechanical stress.**  
2621 Most instances of biomechanical stress *in vivo* affect multiple cell types at once. EV cargo  
2622 loading is subsequently altered in each cell type, resulting in several diverse responses to the  
2623 original stimuli that influence an overall phenotype.  
2624

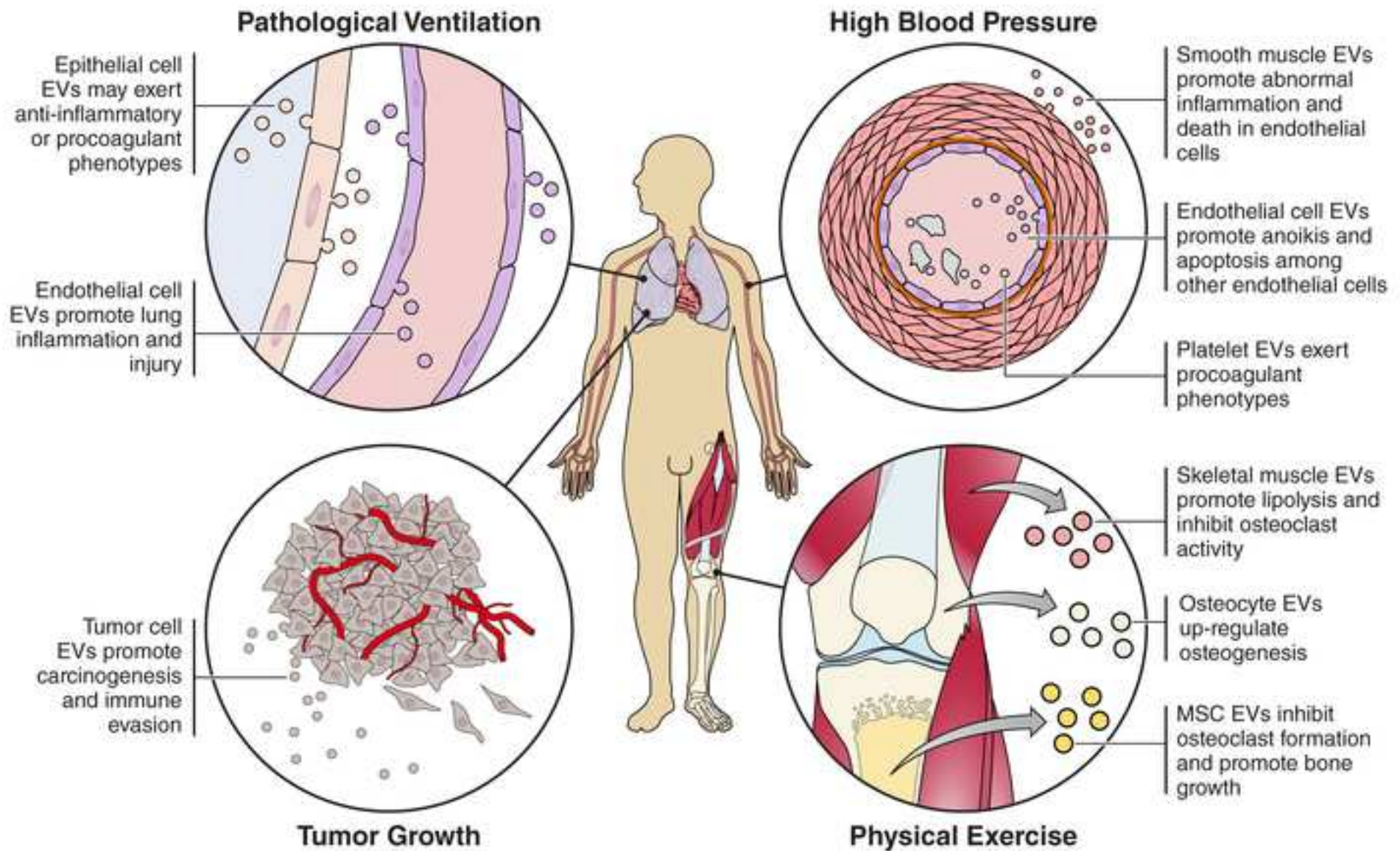
2625 **Figure 5. EV sample quality is transient and varies with biomechanical stress.** As levels of  
2626 cellular sensitivity to stress vary with time, the characteristics of released EVs will fluctuate.  
2627 Subsequent uptake of these EVs by nearby cells may further mediate cell and EV phenotypes,  
2628 complicating EV quality control during bioprocessing.  
2629

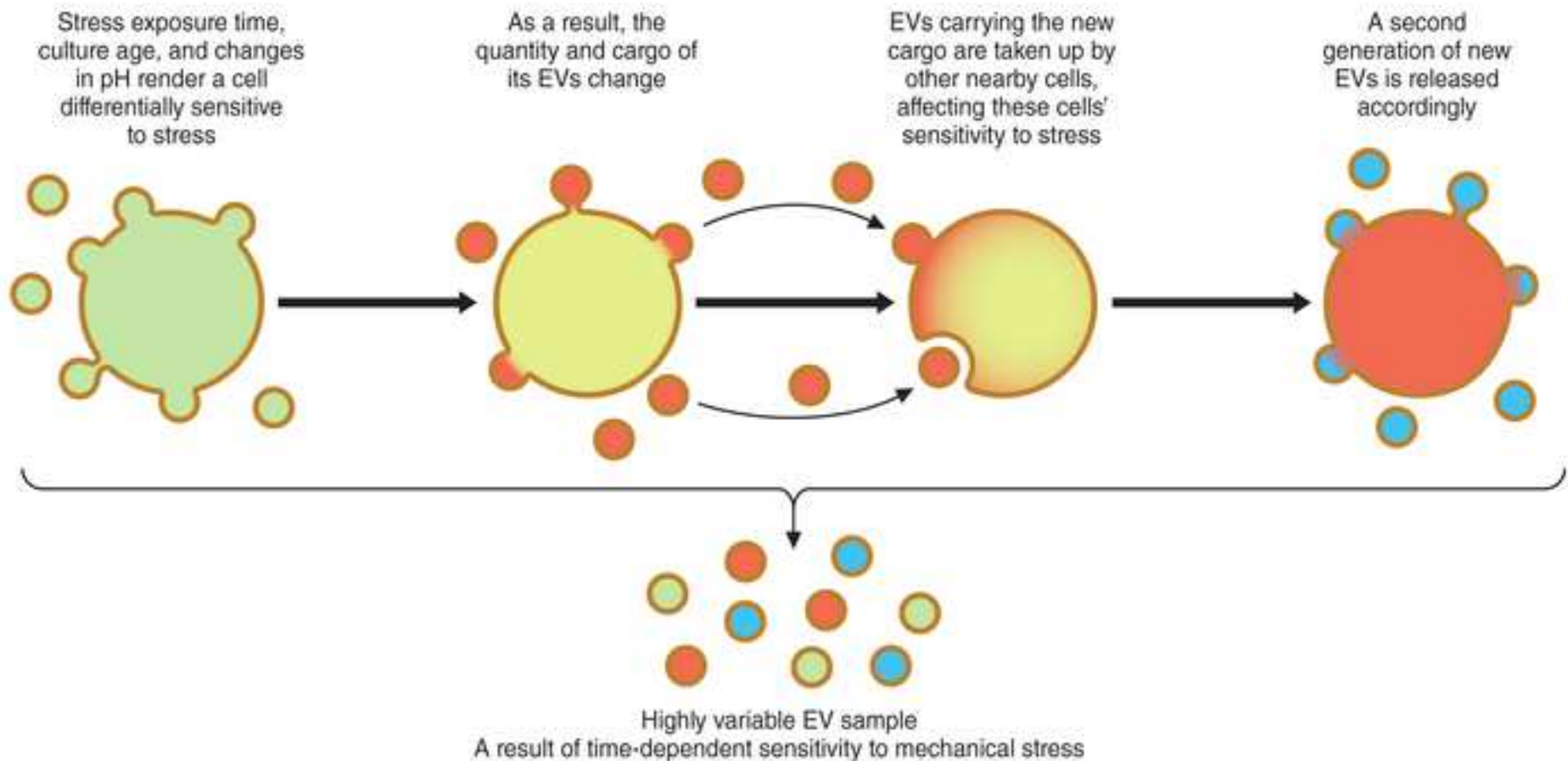
2630 **Figure 6. The impact of biomechanical force on EV uptake by target cells.** EV uptake by  
2631 target cells occurs in three steps: (I) cell-EV collision, (II) cell-EV adhesion, and (III) EV  
2632 internalization/uptake. Biomechanical forces will influence all three steps, with particularly  
2633 notable influence on endocytosis (or the lack thereof). For the variety of reasons identified,  
2634 endocytosis appears to be upregulated by compression, downregulated by tension, and variably  
2635 regulated by shear.

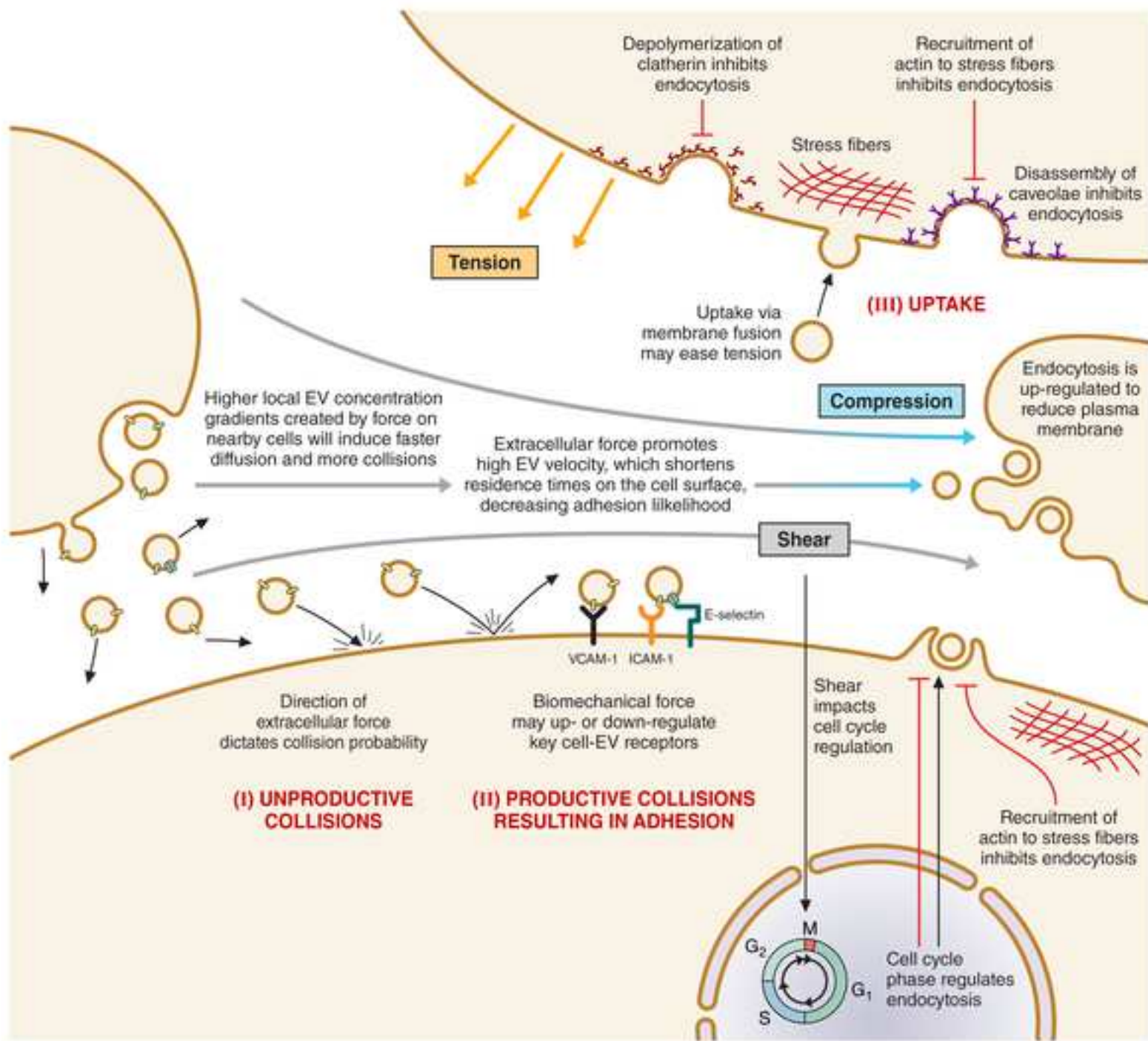












1    **CRediT authorship contribution statement**

2    **Will Thompson**: conceptualization, writing - original draft, writing - review & editing. **Eleftherios**  
3    **Terry Papoutsakis**: conceptualization, funding acquisition, writing - review & editing,  
4    supervision.